



In-Ditch Validation Methodology for Determination of Defect Sizing

Domenico Bellistri, Harvey Haines, Lars Hörchens,
Jasper Schouten, Jeff Vinyard, and Wouter Westerveld
April 04, 2018



Intentionally blank

Phase II Report

on

**IN-DITCH VALIDATION METHODOLOGY FOR DETERMINATION OF DEFECT
SIZING**

to

PHMSA

DTPH56-13-T-000008

April 04, 2018

Prepared by

**Domenico Bellistri, Harvey Haines, Lars Hörchens, Jasper Schouten, Jeff Vinyard,
and Wouter Westerveld**

**Applus RTD
11801 South Sam Houston Parkway West
Houston, TX 77031**

DISCLAIMER

This document presents findings and/or recommendations based on engineering services performed by employees of ApplusRTD USA, Inc. The work addressed herein has been performed according to the authors' knowledge, information, and belief in accordance with commonly accepted procedures consistent with applicable standards of practice, and is not a guaranty or warranty, either expressed or implied.

The analysis and conclusions provided in this report are for the sole use and benefit of the Client. No information or representations contained herein are for the use or benefit of any party other than the party contracting with ApplusRTD USA, Inc. The scope of use of the information presented herein is limited to the facts as presented and examined, as outlined within the body of this document. No additional representations are made as to matters not specifically addressed within this report. Any additional facts or circumstances in existence but not described or considered within this report may change the analysis, outcomes and representations made in this report.

TABLE OF CONTENTS

Acknowledgements.....	v
Executive Summary.....	vi
Section 1 Introduction.....	8
Basic description of the IWEX measurement system	9
Generation of the IWEX image	11
Inclusion of skip paths	12
Section 2 Summary and Conclusion	13
Section 3 Enhancement of the Current Data Acquisition IWEX Algorithm.....	15
Parameter study to find which parameters influence the IWEX image the most.....	15
Deviations from the cylindrical pipe model	20
Results.....	29
Discussion	35
Wedge calibration	37
Scan setup calibration.....	38
Development of a Written Procedure	40
Conclusions	40
Section 4 Development of an Automated Defect Detection, Identification, and Sizing Module	41
Develop 3D & 2D GUI to display the IWEX data	41
Develop SQL storage of the feature data	45
Develop module to Merge 1-inch wide scans into a continuous data set by calculating the offsets (and overlap) to be able to render it as a continuous image.....	48
Develop module for Automatic and Manual Detection of features	50
Develop module for Automatic and Manual Classification of features and calculation of severity using equations from KAPA. Cracks maybe in colonies and require interaction rules.....	51
Design and develop a module for on-site reporting for Implementation of field application software.	52
Develop module for Matching of data to other data sources MT, PA, ToFD, and possibly ILI data... ..	53
Develop module modifications for Automatic and Manual Detection of features using Immersion Data	54
Testing of Automated Sizing and Report Features	54
Conclusions.....	54
Section 5 Development of an Inversion Algorithm	55
Develop Inversion scheme	55
Validation of the inversion method	58
Development of a finite-element method to model free-surfaces and cracks.....	60
Progress in Ultrasonic Full Wave-field Inversion for UT inspection	62
Modelling of the source type	64
Ghost events in measured data	65
Wavelet extraction and calibration of frequency components	65

Evaluate the performance of the inversion method and compare to IWEX images.....	66
Section 6 Develop Immersion Probe Algorithms for Improved Alignment and Sizing	70
Introduction.....	70
Transducer design (1): frequency, pitch, inter-element spacing	71
Theory	71
Experiments: frequency, pitch	74
Design of inter-element spacing (element size).....	78
Transducer design (2): element width, curvature (lateral focus).....	78
Algorithm improvements.....	78
Immersion IWEX travel-time computation	79
Filter to reduce long-wave artefacts	80
Exclude beam-paths with transmission or reflection in wrong direction.....	83
Exclude beam-paths that skipped at invalid points of the extracted ID interface	85
Results	89
Test cases	89
Transducers and validation of the new transducer design.....	90
Results.....	90
Automated calibration and pipe surface detection for immersion.....	94
Development of software for full-matrix-capture recording of seam scans.....	97
FMC scanning of lab samples	109
Development of software for full-matrix-capture recording of seam scans.....	119
Development of software for viewing and interpreting immersion IWEX scan files	120
Delivery of immersion probes.....	120
Modification of the linear scanner probe holder for water wedge measurements of seam-welds.	123
FMC scanning of lab samples	124

Appendix A IWEX RTD™ Written Procedure – Revision 0

ACKNOWLEDGEMENTS

In addition to the Pipeline and Hazardous Materials Administration the authors would like to thank Enbridge Pipeline and TransCanada Pipeline for directly cofounding this work. In addition, we wish to thank the many pipeline companies and organizations that contributed cofounding and samples for the study including Enbridge, TransCanada, Marathon, Koch and others.

EXECUTIVE SUMMARY

Four major activities were completed during Phase II of the project. Automated calibration was improved to facilitate data acquisition and image production in the field. IWEX processor software was improved to facilitating detection, classification and sizing of image data once obtained from field scans. Immersion IWEX was developed to obtain well aligned images on pipe that deviates from an ideal cylinder, a condition that occurs more often than expected near the seam weld. And Inversion R&D progressed to the point of producing the highest resolution images to date for a FMC dataset obtained in a lab setting.

Current plastic wedge IWEX data acquisition interpretation has been improved to the point it is capable of inspecting ERW seams and SCC in the field on a routine basis. A tool for calibrating the wedges and setup on the pipe was developed which allows the tool to setup and scan pipe in a few minutes rather than the trial and error process that was used at the end of Phase I which could take the better part of a day. The limitation of the current software is it assumes a cylindrical pipe geometry with some limited variability.

Software for interpreting IWEX image data has been improved adding some automation, which has facilitated detection of features during the inspection. Because of the robustness of IWEX data acquisition, a large number of features is often acquired which shows more detail about flaws in the pipe, this results in a common problem that interpreting IWEX data can take more time than acquiring to data, especially if the number of indications is large. The automation helps to reduce interpretation time in the field.

Because several pipes examined during testing in Phase 1 showed deviations from ideal cylinders, Immersion IWEX was developed. The development progressed in Phase 2 to the point that measurements can be taken on pipe with flexible wedges and processed into an image. Results on 2 different pipe samples, with known deviations in the seam from an ideal cylindrical pipe, showed much better alignment and focusing of images. The immersion system has been adapted with water wedges for scanning on whole pipe. Although we feel this type of processing will be needed for these pipes with deviations from a cylinder, in-ditch field work is not yet practical because of the time needed for full matrix capture (FMC) data acquisition (~2 hours) and adaptive IWEX processing of the FMC data (overnight). Improvements in processing speed are possible, but further development is needed to accelerate FMC acquisition and adaptive image processing.

Inversion, another method of producing images was continued during Phase II. Inversion progressed to the point it was tested on FMC data acquired on a sample with side-drilled holes. Images, obtained using inversion, were compared to current IWEX images processed from the same dataset. Results showed the resolution obtained using inversion is significantly higher

than for current IWEX imaging techniques – however, the iterative scheme was much much slower because of the extensive computational effort needed to produce an image. The computation time is too long and impractical for implementation in the field. Continued research and development will be needed for practical use in the lab, let alone the field.

The results of the project showed that UT imaging using IWEX imaging is a significant improvement over current Phased Array technology showing much more detail such as stacked flaws and remaining ligaments of embedded flaws. In addition, imaging with FMC data has significant upside potential in the future through continued improvement of adaptive processing and full inversion of the FMC data.

In-Ditch Validation Methodology for Determination of Defect Sizing

Domenico Bellistri, Harvey Haines, Lars Hörchens, Jasper Schouten, Jeff Vinyard, and Wouter Westerveld

SECTION 1 INTRODUCTION

This report describes improvements to the IWEX measurement system as carried out in Phase II of the project. The report describes four portions of the work carried out in the project:

- Improvements and limitations to the current IWEX data acquisition – Section 3
- Improvements for interpreting the data involving automatic detection, interpretation and sizing – Section 4
- Inversion processing of full matrix capture data, the ultimate image processing system for UT imaging – Section 5
- Immersion acquisition and processing to handle deviations of the pipe shape from a perfect cylinder – Section 6

The goal of Phase II was to improve the sizing accuracy of the system by accounting for measurement errors caused by small variations in several parameters (Section 3) and improving the interpretation software used to interpret the images (Section 4). Inversion (Section 5) was considered a research topic to look at the ultimate image processing of the data for the best quality images. During the project, we learned it was not possible to compensate for all of the variabilities caused by how the plastic wedge ride on the steel pipe. As a result, resources were diverted from planned activities to pursue immersion which uses flexible water wedges to couple the ultrasound to the pipe and advanced processing to map the outer and inner pipe surfaces (Section 6).

The project obtained good results using immersion; however, the processing speed needs to be accelerated to make it a viable technique for field use. Immersion data acquisition with adaptive IWEX processing can be thought of as a compromise between the simplicity of plastic wedge IWEX and the complete solution of inversion.

Current plastic wedge IWEX acquires the full matrix capture (FMC) data and processes it in real time using the IWEX processing technique which assumes both outer and inner cylindrical pipe

surfaces. An image is produced in real time and the raw FMC data is discarded to facilitate real time processing of the data. This technique works well if the pipe is perfectly cylindrical.

Immersion replaces the rigid plastic wedges with a set of flexible water wedges which ride along the pipe and conform to the surface. Importantly they allow for conforming to small deviations in the pipe surface which we've observed in some pipes, especially near the ERW seam. These deviations are imperceptible to pipe integrity, but affect the ultrasonic wave path just enough to require compensation for a true image of anomalies in the pipe. The acquired FMC data is output to disk and must currently be processed overnight to produce an image for a typical inspection of a seam for about 1 meter in length. Typically the FMC data is 100 times larger than the resulting image data. We believe this technique has the best chance of meeting industry needs and should be developed further so it can be used in the field for validation of ILI data and other needs. Optimization of the data acquisition and processing routines is needed to obtain results in a realistic time frame for routine field use.

Inversion was found to produce the best images. The processing routine works on the same FMC input data, but because the processing is time consuming, only individual 2-D sections have been processed to date. Inversion uses all of the data, longitudinal waves, shear waves, and conversions from one mode to another. This technique was the best at discriminating objects that were closely spaced. The research shows one test where two side drilled holes 1/2 mm in diameter 1 mm apart were imaged and discriminated using 2 MHz UT probes.

Basic description of the IWEX measurement system

Although the IWEX system was described in the Phase I report it is repeated here as background material for the reader.

IWEX, being an acronym for "**I**nverse **W**ave field **E**xtrapolation", is an ultrasonic inspection technology for acoustical imaging. For pipe weld inspection, it relies on the usage of array transducers, which are positioned on wedges to the left and right of the weld. Instead of generating ultrasonic beams as commonly done with Phased Arrays, IWEX uses each array element consecutively as a source, while receiving with all array elements. Signals are picked up by all array elements from reflected or diffracted waves from the material boundaries or flaws in or near the weld. The dataset obtained this way contains a large number of A-scans, each of which corresponds to a different source-receiver combination. This type of data acquisition is usually referred to as 'full matrix capture' or FMC.



Figure 1-1. Laboratory test setup for IWEX on seam welds

In contrast to conventional ultrasonic approaches, the data is not used 'as is' in an A-scan representation, but processed to generate a two-dimensional image. This image corresponds to a virtual cross-section of the material representing the real dimensions of the object inspected. It provides an easily interpretable visual representation that resembles a metallographic section obtained from destructive testing.

The figure below shows an IWEX image of a 16-inch diameter ERW seam weld with a wall thickness of 6.35 mm (0.250-in) (left side) and the corresponding metallographic section (right side).

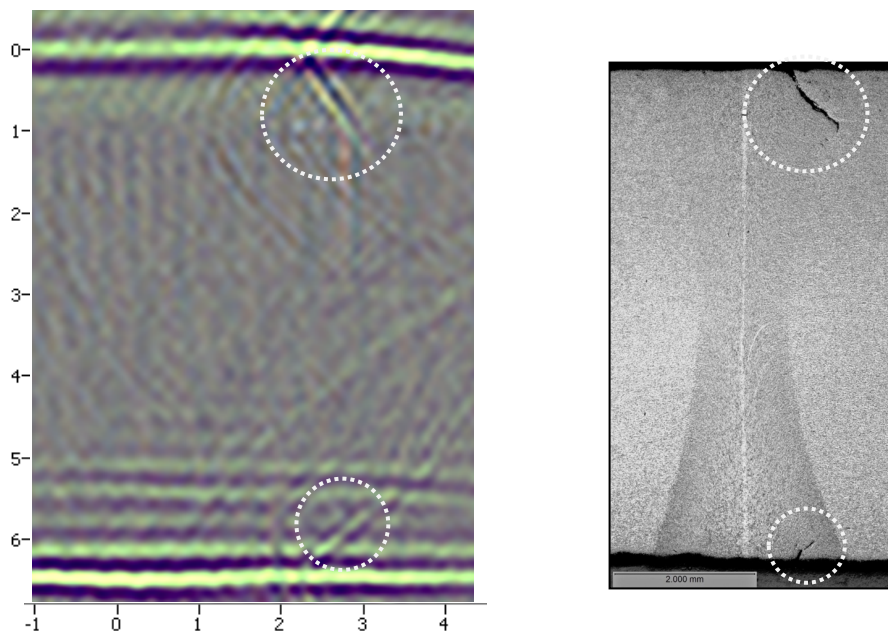


Figure 1-2. IWEX image (left) and corresponding macro photograph (right) of an ERW seam weld with a wall thickness of 6.35 mm (0.250 in)

Since 2010, a dedicated, hardware-based IWEX system for the inspection of girth welds has been developed. The adaptation for seam weld inspection started in 2012.

Generation of the IWEX image

The general approach of acoustical imaging has been used in the context of seismic exploration and medical acoustics for several decades. It is only within the last decade that the basic technology has been adopted and refined to be applicable for non-destructive inspection.

The figure below shows the three principal paths (blue) from an element at the center of the array to a point in the region of interest (green rectangle) for a seam weld setup.

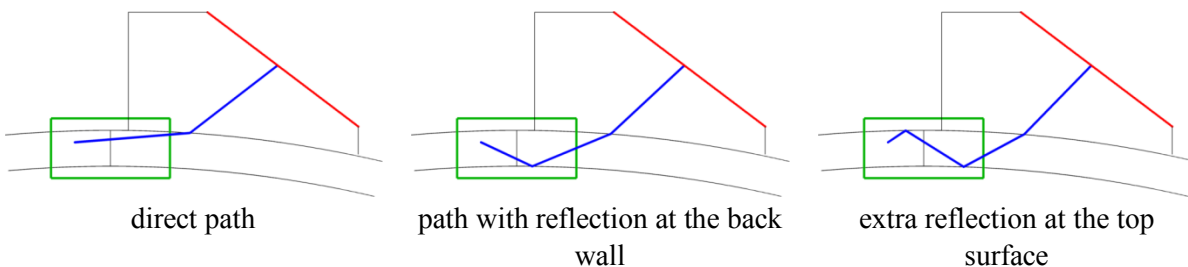


Figure 1-3. Principal paths from an array element to an image point that are taken into account in the image formation process with IWEX.

A numerical procedure was developed to calculate the ray path taken from a certain array element to a certain point in the area of interest and the respective travel time for each of these three cases. To this end, an iterative method is used to find the path with the shortest travel time.

In phased array applications, the different sound paths are generated physically by firing different array elements with appropriate delays to generate and steer ultrasonic beams thereby focusing at points in the region of interest. This approach is inherently limited by the time required for the sound to propagate through the sample. This means that sound waves can be focused only at a limited number of points within a given period of time.

For IWEX inspection, signals of all possible source-receiver combinations of the array elements are measured. It is only after the measurement that different delay laws are applied to focus at all points of a pixel grid in the defined region of interest. This focusing operation is carried out in hardware processing by a field-programmable gate array (FPGA), which generates the IWEX images before sending them to a computer for further processing and evaluation.

In order to form the images, the travel times from all array elements to all points in the image have to be calculated and made available to the hardware. During the inspection, this

information is used to look up samples in the recorded A-scans and add their contribution to the respective points in the image.

Inclusion of skip paths

One of the major advantages of IWEX is the simultaneous usage of different acoustical paths for generating the image. By combining the three principal paths described above, several modes for interrogating the weld volume can be formed. The modes currently used in the IWEX system are shown in Figure 1-4. Note that the modes correspond to different directions of acoustical illumination and reception. In the measurement software, the images obtained by using the different paths are presented in a single overlay image. By combining these different directions for inspection, defects of arbitrary orientation can be detected. Thereby, the overall chance of missing a defect is minimized.

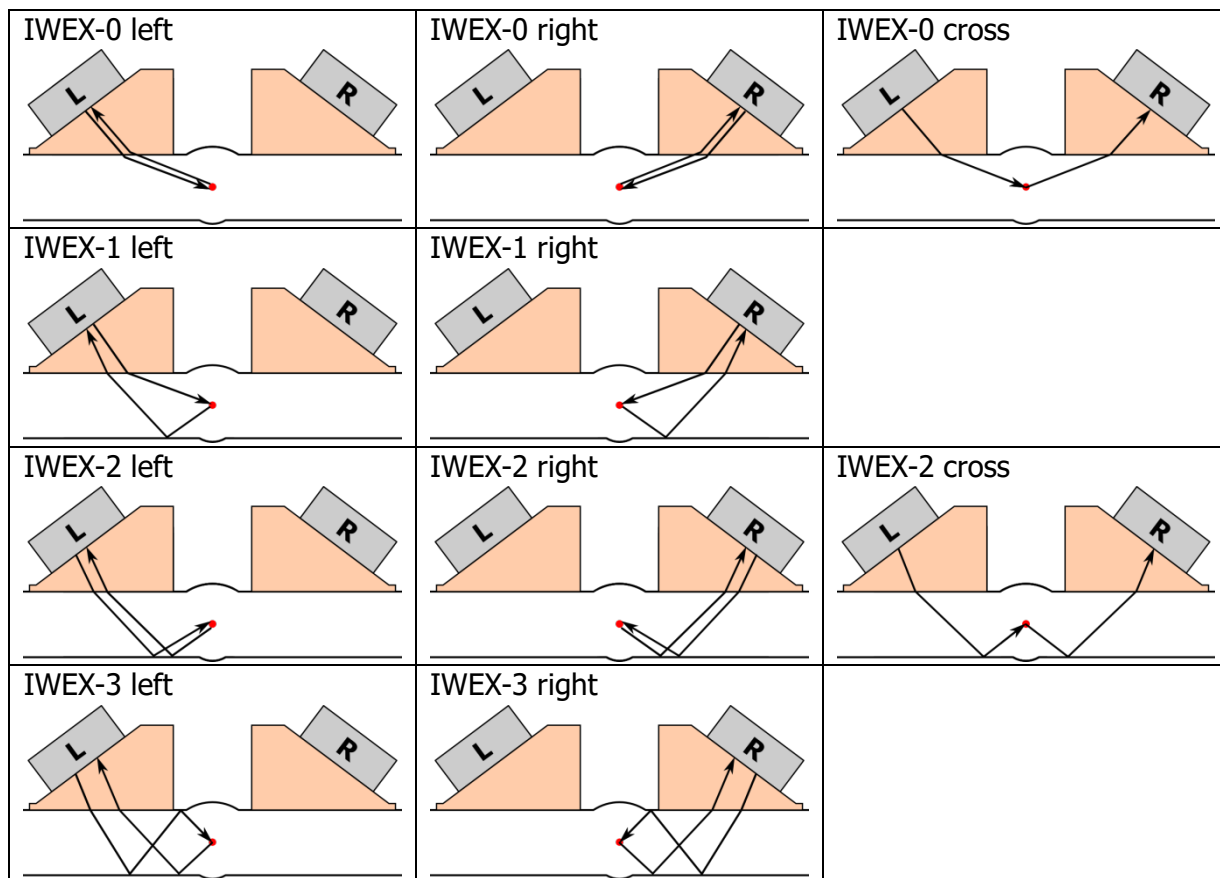


Figure 1-4. Different combined paths between two array elements that are taken into account in the image formation process with IWEX

SECTION 2

SUMMARY AND CONCLUSION

Current plastic wedge IWEX data acquisition has been improved. A tool for calibrating the wedges and setup on the pipe was developed assuming a cylindrical pipe with some limited variability. The existing calibration routine for the wedges was improved in terms of robustness and simplicity for the user. The calibration tool was extended to provide means for calibrating the seam weld setup on the pipe sample to determine wall thickness and relative alignment of the wedges. The coupling condition can be checked by measuring the thickness of the water layer below the wedges and assessing the strength of the reflections received from the inner and outer pipe surfaces. The relative alignment of the wedges can be calibrated in terms of both distance and rotation. This enables the calibration tool to deal with roof topping to some extent.

Interpretation software for interpreting IWEX data was improved adding some automation features to the IWEX processor software. Interpretation of current IWEX data can take more time than calibration and data acquisition, especially if the number of indications is large. Improvements in the IWEX processor software used to interpret data has given the interpreter more options for processing the IWEX image data including facilitating detection, identification, and sizing indications with some automation routines and provisions for calculating burst pressure when an anomaly is large enough to warrant it.

Inversion research and development progressed to the point it was tested on real acquired data of a sample with side-drilled holes. Results show full wave field inversion as a potential alternative to IWEX imaging within the framework of a research project. The major problems in setting up an inversion scheme were identified and tackled. The resulting inversion scheme was applied to simulations and real measurements. A simple clearly-defined steel sample was used for experimental tests. Reconstructions, obtained using full wave-field inversion, were compared to an IWEX image based on the same dataset. Results from the test sample showed the resolution obtained using inversion is significantly higher than for simple imaging – at the cost of using an iterative scheme with extensive computational effort. However, although the current developments show the best results in terms of image quality the computation time is much too long and impractical for implementation in the field. Continued development will be needed for practical commercial use.

Immersion IWEX was developed to the point that measurements can be taken on pipe with flexible wedges and processed into an image. Results showed much better alignment and focusing of images on samples with known deviations from perfectly cylindrical pipe. In one

case on a 24-inch pipe with an extra thick seam the images were corrected for the change in ID pipe geometry that led to the miss-interpretation of anomalies during earlier analysis. Earlier data was misaligned because of the extra thick heat-affected-zone near the bond line and led to a misinterpretation of fatigue cracking which was not present upon metallurgical examination. Immersion showed a much clearer image for an anomaly in the same pipe section nearby the original incorrectly identified fatigue crack. In addition, interpretation of a 22-in pipe, with flat zones near the weld and offset plate edges on the ID, was properly imaged clearly showing a side-drilled hole placed in the sample for test purposes. Although the system is mechanically set up and ready for scanning on whole pipe, field work is currently not practical because of the time needed for full matrix capture (FMC) data acquisition (~2 hours) and adaptive IWEX processing of the FMC data (overnight). Improvements in processing speed are possible but further development is needed to implement accelerated processing.

SECTION 3

ENHANCEMENT OF THE CURRENT DATA ACQUISITION IWEX ALGORITHM

This task proposed to improve upon the imaging from the current IWEX processing technique by accommodating for real-time changes in wall thickness, changing inner and outer surface profiles, and accommodating for surface corrosion which may introduce an additional water layer which must be accounted for in the interpretation algorithm. Individual items in this task include the following:

- A parameter study to find which parameters influence the IWEX image the most.
- Develop and test enhanced IWEX data acquisition routines to determine wall thickness variations
- Coordinate In-Kind Field and lab testing with enhanced data acquisition
- Develop Materials test setup for Enhanced IWEX data acquisition
- Develop and test routines to accommodate for the most important parameters
- Implement Updated written IWEX inspection procedure

Parameter study to find which parameters influence the IWEX image the most.

As concluded from an IWEX Interpretation and Training Workshop (Columbus, Ohio, July 16-17, 2015), the quality of the IWEX images needed improvement. Although sizing and positioning of the flaws was possible with imaging quality at that time, interpreting the images was time consuming. Typical images of girth welds (e.g., from the related but separate girth weld project) had higher quality and better alignment between the modes than the seam weld images in this project.

The following factors were found to influence the image quality:

- The calibration of IWEX imaging parameters (wedges, wall-thickness, probe center separation/offset, etc).
- The theoretical pipe model that was used in the IWEX imaging algorithm (a perfectly cylindrical pipe).
- The mechanical alignment of the system.

The sections hereafter describe the effort in analyzing and resolving the first two factors.

Calibration of IWEX imaging parameters

Calibration of the IWEX imaging parameters manually was time consuming and tedious because the optimization of the image quality requires adjusting of all parameters simultaneously. This

was nontrivial, and required experienced operators. Therefore, a calibration tool was developed with the following steps:

- Calibration of wedges.
- Calibration of wall-thickness below the wedge on a single position.
- Calibration of probe center separation/offset.

Calibration of wedges

Calibration of the wedges is based on zero-offset measurements taken with the array probe on the wedge, with the wedge not connected to any surface. Zero-offset measurements are pulse-echo measurements with each of the elements of the transducer array. Based on this dataset, an optimization algorithm searches for the wedge parameters that give best correspondence between the measured pulse-echo travel times to the wedge surface and the pulse-echo travel times that are computed based on a given set of wedge parameters. The remainder of this section describes the details of this algorithm.

The wedges are described by the following set of parameters: vertical index VI, horizontal index HI, and wedge angle α . These parameters may be measured with a caliper. Equivalently, the wedge may be described by the following set of parameters, which is more directly related to the propagation of the ultrasound. The wedge calibration algorithm uses this second set of parameters.

- r-index (the shortest distance between the center of the array transducer and the bottom surface of the wedge),
- array beam angle φ (the angle between the beam direction (normal to the array) and the line corresponding to the shortest distance between the center of the array transducer and the bottom surface of the wedge).

From Figure the following relations may be derived to compute RI (r) and φ from HI (h), VI (v) and wedge angle α :

$$r = \sqrt{h^2 + (R+v)^2} - R$$

$$\varphi = \alpha - \theta; \quad \text{with} \quad \tan(\theta) = h / (R + v)$$

From Figure 3-1 the following relations may be derived to compute HI (h) and VI (v) from RI (r) and φ for a given wedge angle α :

$$h = (R+r) \sin(\alpha - \varphi)$$

$$v = (R+r) \cos(\alpha - \varphi) - R$$

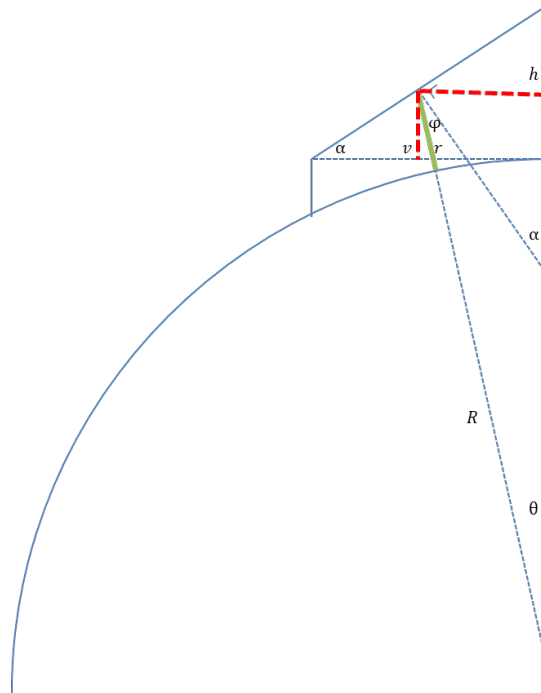


Figure 3-1. Parameters describing a single wedge. This may be the set: horizontal index HI (h), vertical index VI (v), wedge angle (α); or the set: r-index RI (r), array beam angle (ϕ). Pipe radius R .

The calibration of the r-index RI and the beam angle ϕ is based on the travel-time from an array element to the surface of the pipe. A zero-offset measurement is performed and the first arrival in a pulse-echo A-Scan corresponds to the travel-time from the transducer element to the pipe/wedge surface. The shortest distance from a transducer element to the wedge surface is a line that also crosses the middle of the pipe. For a given position of the transducer element, this distance and corresponding travel-time can be computed.

The calibration algorithm is based on an optimization scheme in which the wedge parameters are optimized such that the computed travel-time from each element in the array to the wedge surface matches with the measured travel-times. The r-index RI and the beam angle ϕ are optimized and hereafter converted in the horizontal and vertical indices for given wedge angle α .

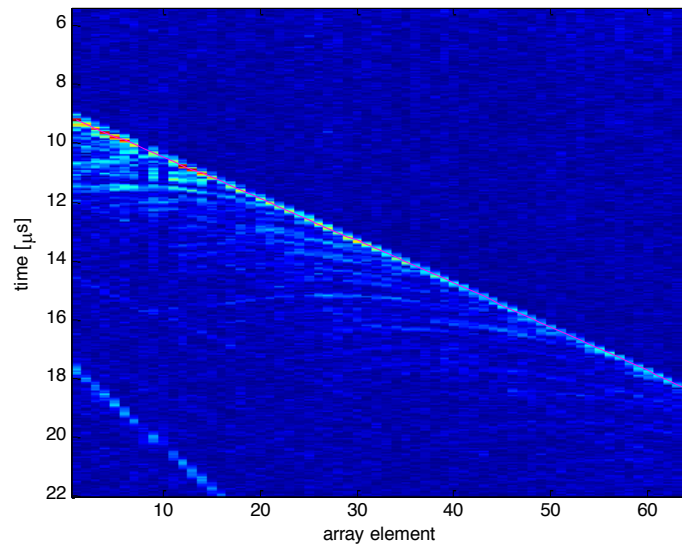


Figure 3-2. Zero-offset measurement with travel-times of the fitted parameters r and ϕ (magenta line) . 24" pipe. It can be seen that the fitted arrival times agree with the measured arrival times.

Calibration of wall-thickness below the wedge on a single position

The wall-thickness may be calibrated using a delay-and-sum approach to form a cylindrical wave. The wave-front is made such that it aligns with the pipe OD surface and thus also with the pipe ID surface. The delay-and-sum delays are both used in sending as well as in transmitting.

The current experiments use all channels of a full-matrix-capture (FMC). This is not fast enough for real-time measurements. Using only a subset of these channels is expected to be sufficient for wall-thickness measurements.

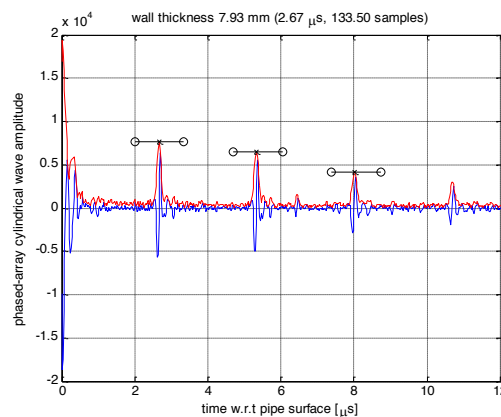


Figure 3-3. Example of wall-thickness measurement, using all channels of the full-matrix-capture (FMC), 24" pipe.

Calibration of probe center separation/offset

The algorithm to calibrate the probe-offset is based on a software delay-and-sum approach to form an ultrasound path that travels horizontally through the pipe. Longitudinal ultrasound-waves are used because this will be the first arrival from the left transducer array to the right transducer array.

The method that finds the probe center separation/offset uses a quarter of the full-matrix-capture (FMC) A-Scans, namely the quarter with source array 1 and receiver array 2.

The travel-times that are used in this method are explained in Figure 3-4. All A-Scans are in the FMC are delayed-and-summed with these travel times. If the offset is correct, then resulting delayed-and-summed A-Scans have an ultrasound peak at zero time ($t=0$).

If an estimated offset is used to compute the travel-times, which differs from the real offset, then the peak in this A-Scan does not show up at $t=0$ but at another time dt . This time difference is related to the error in the estimated offset, approximately via $dx = dt * c_l$ with c_l the longitudinal sound velocity in the pipe. This approximation is valid when dx is not too large, e.g. within approximately 5 mm. The algorithm iteratively updates the estimated offset until the required change in offset is within 3 mm such that the approximation is valid.

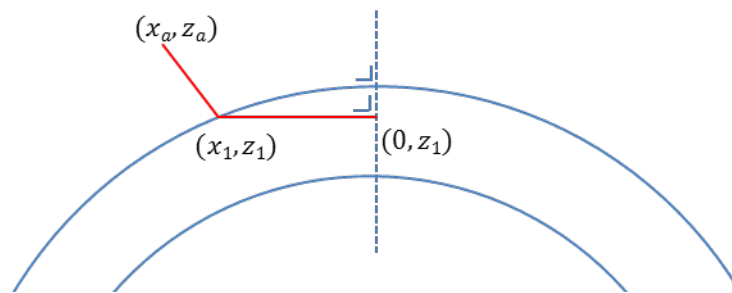


Figure 3-4. Travel-time for offset calibration. Sound path is from transducer element at position (x_a, z_a) , to the pipe surface (x_1, z_1) , and from there horizontally (constant $z=z_1$) through the pipe such that it is tangential to the $x=0$ line.

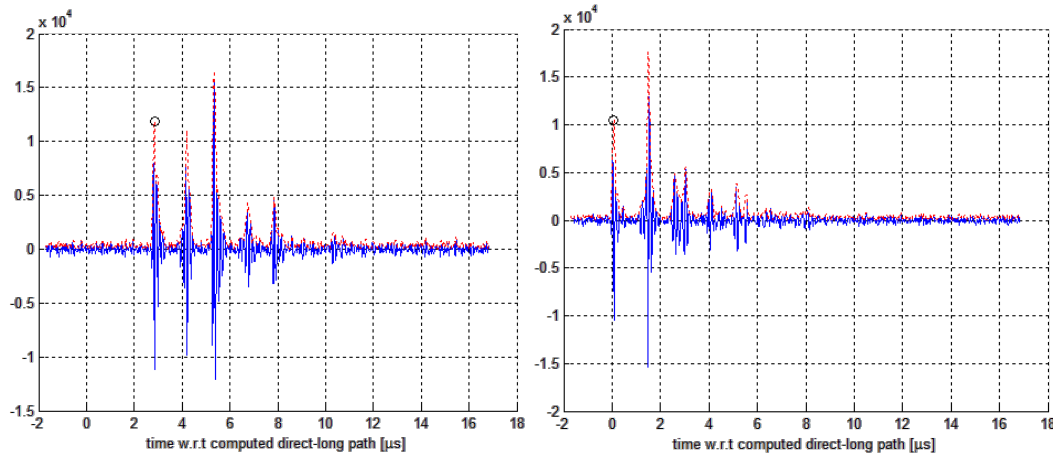


Figure 3-5. Result of the offset calibration method. 8 inch pipe, offset 8.6 mm. Left image: first step. Right image: second step.

Calibration results and tests

The algorithms have been tested in a laboratory environment on pipes with different diameters. However, it has been reported that the stability of the algorithms is not sufficient and that they sometimes fail in field usage. Especially the probe center separation/offset calibration is delicate and may be influenced by poor coupling (e.g., unclean pipe surface) and additionally is influenced by the thickness of the couplant layer.

Deviations from the cylindrical pipe model

In the current seam-weld IWEX imaging algorithm, the pipe wall is assumed cylindrical and with homogeneous wall-thickness. This is not the case in real seams, as the manufacturing process for ERW seam may cause crimping the edges, poor trim, offset plate edges, etc. Deviations from a perfect cylindrical pipe wall result in degradation of the image quality, such as artifacts, lower SNR, lower resolution and misalignment between the IWEX modes. The assumption of a cylindrical pipe wall is not essential to IWEX, any smooth surface is expected to work. However, accurately measuring the ID and OD surfaces is challenging. Therefore, it is recommended to model the surfaces with a minimum number of parameters which still give a sufficient representation of the pipe wall.

Figure 3-6 depicts the problem. From the same full-matrix-capture dataset, IWEX images are generated either with manually calibrated parameters or with automatically calibrated parameters. With manual calibration, the image is in focus but the OD and ID indications are at the wrong position (IWEX-OC at 6.2 mm instead of 7.3 mm). With parameters from the FMC data, the image is blurred but OD and ID indications are at the correct position. No set of parameters was found to generate an image that shows indications both at the correct position

as well as in focus. It is expected that this is due to an incomplete description of the pipe in the IWEX imaging algorithm.

Table 3-1 lists various descriptions of deviations from the theoretical cylindrical pipe and the effect on the IWEX images.

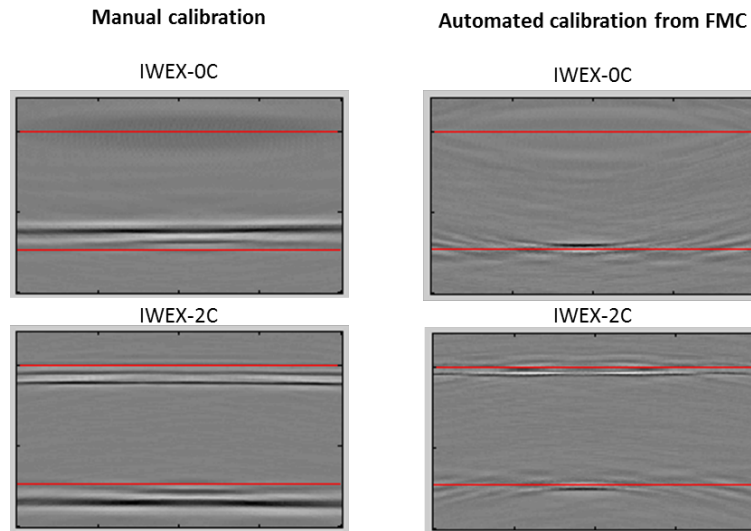


Figure 3-6. IWEX images (cross-modes) of a clean pipe (OD 20 inch, wall-thickness 7.31mm). All four images are computed from the same full-matrix-capture (FMC). Two sets of parameters are used: left column has manually calibrated parameters, right column has automatically calibrated parameters.

Table 3-1: Possible deviations in the pipe from the theoretical cylindrical pipe.

Deviation	ID/OD	Uniform over pipe	Measurement	Compensation	Seen in the field	Effect on image
Pipe wall-thickness left/right, uniform in axial direction	ID	Yes	Easy	Easy	Yes	Focus (mainly modes 1 and 3), mode alignment
Pipe wall-thickness left/right, varying in axial direction	ID	No	Moderate	Moderate	?	Focus (mainly modes 1 and 3), mode alignment
Angle between left and right side of the weld	OD,ID	Yes	(research)	Easy	Yes	Focus (mainly cross modes), mode alignment
Ovality – different curvature but approximately cylindrical in the the probe area close to the weld	OD,ID	Yes	(research)	Image compensation is easy. But requires wedge with curvature of probe area.	Yes	Probe coupling, focus, mode alignment
Ovality – general smooth OD curvature	OD,ID	Yes	(research)	Difficult	Yes	Probe coupling, focus, mode alignment
Arbitrary smooth ID surface, uniform in axial direction	ID	Yes	Difficult	Difficult	Yes	Focus, mode alignment
Arbitrary smooth ID surface, varying in axial direction	ID	No	Difficult	Difficult	Yes/No (Does this vary over pipe or not?)	Focus, mode alignment
ID corrosion	ID	No	Difficult (with OD known)	Difficult	Yes	Focus, mode alignment
OD corrosion	OD	No	Difficult	Difficult	Yes	Probe coupling, focus, mode alignment
OD Reinforcement	OD	Yes ??	Difficult	Difficult	Yes (DSAW)	Artifacts, blind regions
ID Reinforcement	ID	Yes	Difficult	Difficult	Yes (DSAW)	Artifacts, blind regions
Poor ID trim	ID	Yes	Difficult	Difficult	Yes (ERW)	Artifacts
Left/right offset at OD	OD	Yes	(research)	Difficult	No	Focus (mainly cross modes), mode alignment

During the recent field trials, it has become evident that there is still a gap between the image quality that can be obtained in a laboratory setup and the quality of the scans obtained in the field. This impedes interpretation and sizing. Therefore, a study has been set up to determine the parameters that have significant influence on the image. It is assumed that accurate determination of these parameters in the setup phase will lead to an improvement of the image quality.

Currently, a calibration procedure is already in place to determine geometrical parameters of the setup. The parameters are determined by fitting measurements to a model of the wedges and the pipe geometry. This calibration routine assumes a perfect cylindrical pipe model as shown in Figure 3-7(a).

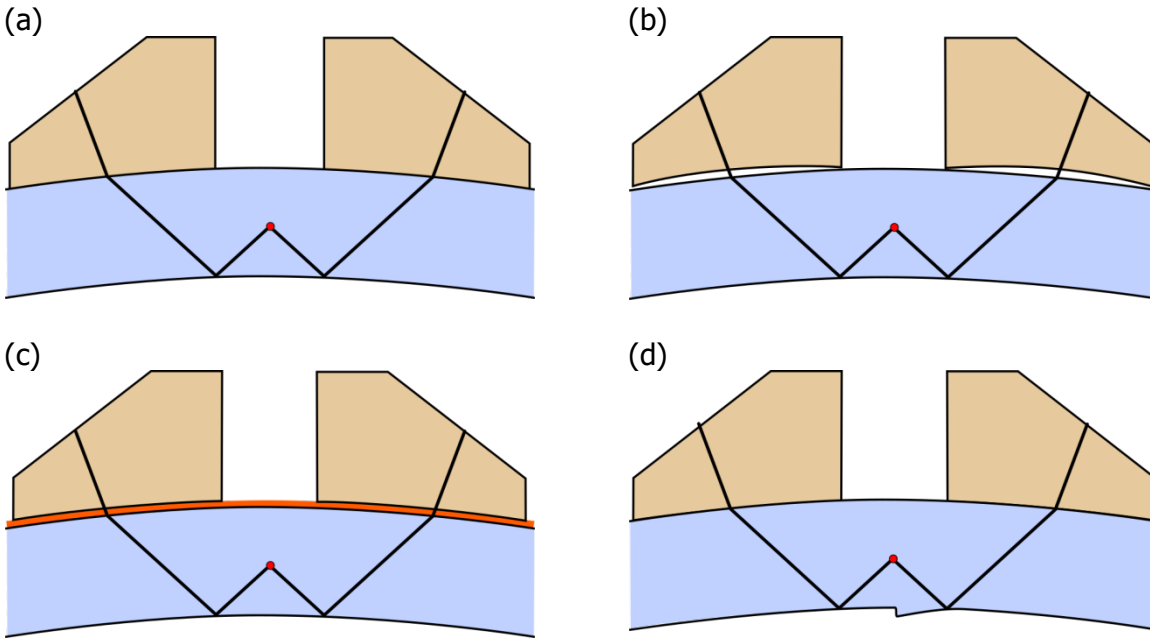


Figure 3-7: Different examples of ideal and non-ideal geometries: (a) cylindrical pipe fitting the wedges perfectly, (b) mismatch in curvature between wedges and pipe, (c) water gap or paint layer between wedges and pipe, (d) wall thickness changes due to trim issues.

The current method used for automatic determination of the setup parameters has been shown to lead to unsatisfactory results when applied in the field. Therefore, users have been forced to tune calibration parameters manually in order to obtain an image of sufficient quality. This process has been cumbersome and not effective in all cases, mainly for two reasons:

- The number of parameters to be changed simultaneously is too high to allow for manual optimization in tolerable time with sufficient accuracy.
- Parameters that are relevant may not be included in the current model and are therefore not accessible for tuning.

During the parameter study, it has been found that the image is mainly sensitive to the following parameters:

- 1) Distance between the two wedges
- 2) Mismatch between the wedges and the pipe surfaces, in particular
 - a) non-matching curvature of the wedges and the pipe surface
 - b) additional material layer between the wedges and the pipe
 - c) tilted wedges due to deformation of the outer pipe surface close to the weld
- 3) Wall thickness of the sample / profile changes near the weld
- 4) Sound velocities in the wedge and pipe material

Based on the relevant parameters found, the method for automatic calibration has been modified:

- The sound velocity of the wedge is calibrated based on measurements instead of using the nominal value. A defined range of velocities is tested, and the value leading to optimal focusing (maximum amplitude) of an image of the bottom surface is chosen.
- The distance between the wedges used to be calibrated based on travel time measurements from one wedge to the other. This approach has been replaced by a method generating several images for different wedge distances and choosing the parameter leading to optimal focusing of the cross mode image.

The modified calibration method was applied to an 8.625" pipe sample with a wall thickness of 4.8 mm. The image shown in Figure 3-8 was obtained. Alignment and focusing were sufficient for interpretation and sizing.

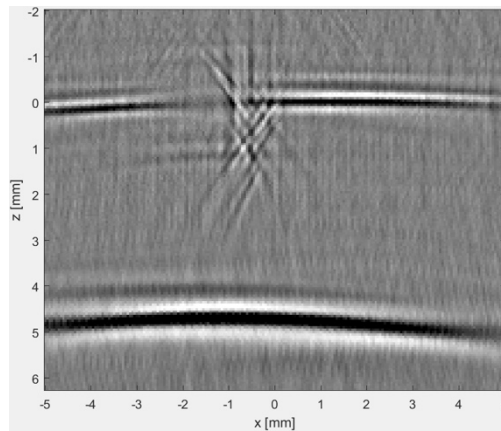


Figure 3-8: Example of an IWEX image of a pipe sample with an artificial surface-breaking defect extending through 20 % of the wall thickness from the outer (top) surface. This result has been obtained in a laboratory environment with the modified calibration routine.

In April 2016, IWEX scans were carried out on a number of samples in the context of the PRCI IM-3 round robin test. Along with the scans, raw datasets (full matrix captures) were recorded at a number of selected positions. These samples were believed to be more representative for field applications.

Full matrix capture datasets allow for calibration of the setup and for the generation of images with different parameters. This enables the determination of relevant parameters and the testing of calibration approaches.

The calibration approach developed in the laboratory environment failed when applied to these datasets. An extra layer between the wedges and the pipe surface turned out to be the main reason. Figure 3-9 presents an example of images calculated below the wedges from which the mismatch between the wedge bottom surface and the outer pipe surface can be seen.

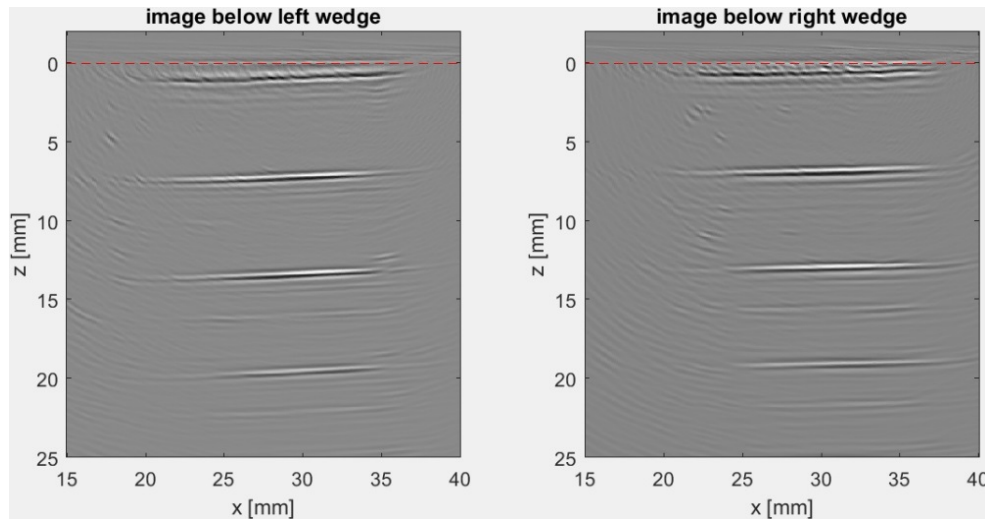


Figure 3-9: Images of the pipe surface below the left and right wedge for a setup showing a mismatch between the wedge bottom and the pipe surface. The dotted lines in the images represent the bottom surfaces of the wedges. The reflection from the outer pipe surface is spatially separated from the wedge bottom reflection. Reflections off the inner pipe surfaces and multiple reflections are shifted accordingly. Note that the curvature of the pipe is removed during imaging such that the interfaces appear flat.

At first, the layer between the wedges and the pipe was assumed to be caused by excessive couplant. However, it turned out that the samples were also painted to facilitate magnetic particle testing and position marking.

Additional steps were included in the calibration routine to determine the thickness of an extra layer between the wedges and the pipe. For the laboratory sample shown in Figure 3-8, the layer turned out to be negligible (less than 0.1 mm), whereas for the round robin samples, the extra layer was found to be a factor 3 to 5 thicker.

Aside from the geometrical shift, the extra layer has also the effect of introducing additional echoes, which can be seen as spurious indications in the IWEX image. It has been tested whether these indications can be removed or at least reduced when the thickness of the layer between wedge and pipe is determined during the calibration step.

The extra layer, depending on the angle at which the material is traversed, affects different sound paths differently. For reasons of simplicity, a compensation assuming a normal path perpendicular to the pipe surface has been applied to assess the effect of a correction step. The approach chosen is based on deconvolution in order to dampen the additional reflections in the ultrasonic signals.

Figure 3-10 shows exemplary images from the scan made with manual setup in rectified (a) and unrectified (b) representation. The image obtained with the modified calibration approach is

shown in Fig. 3-10(c), and the application of deconvolution leads to the result presented in Fig. 3-10(d).

First of all, it can be seen that the flaw at the inner diameter and the lower tip of the flaw at the outer diameter are significantly clearer when using the modified calibration. Furthermore, the deconvolution approach shown in Fig. 4 (d) helps to remove some of the ringing from the image of the pipe surfaces and improves the resolution of the flaws further.

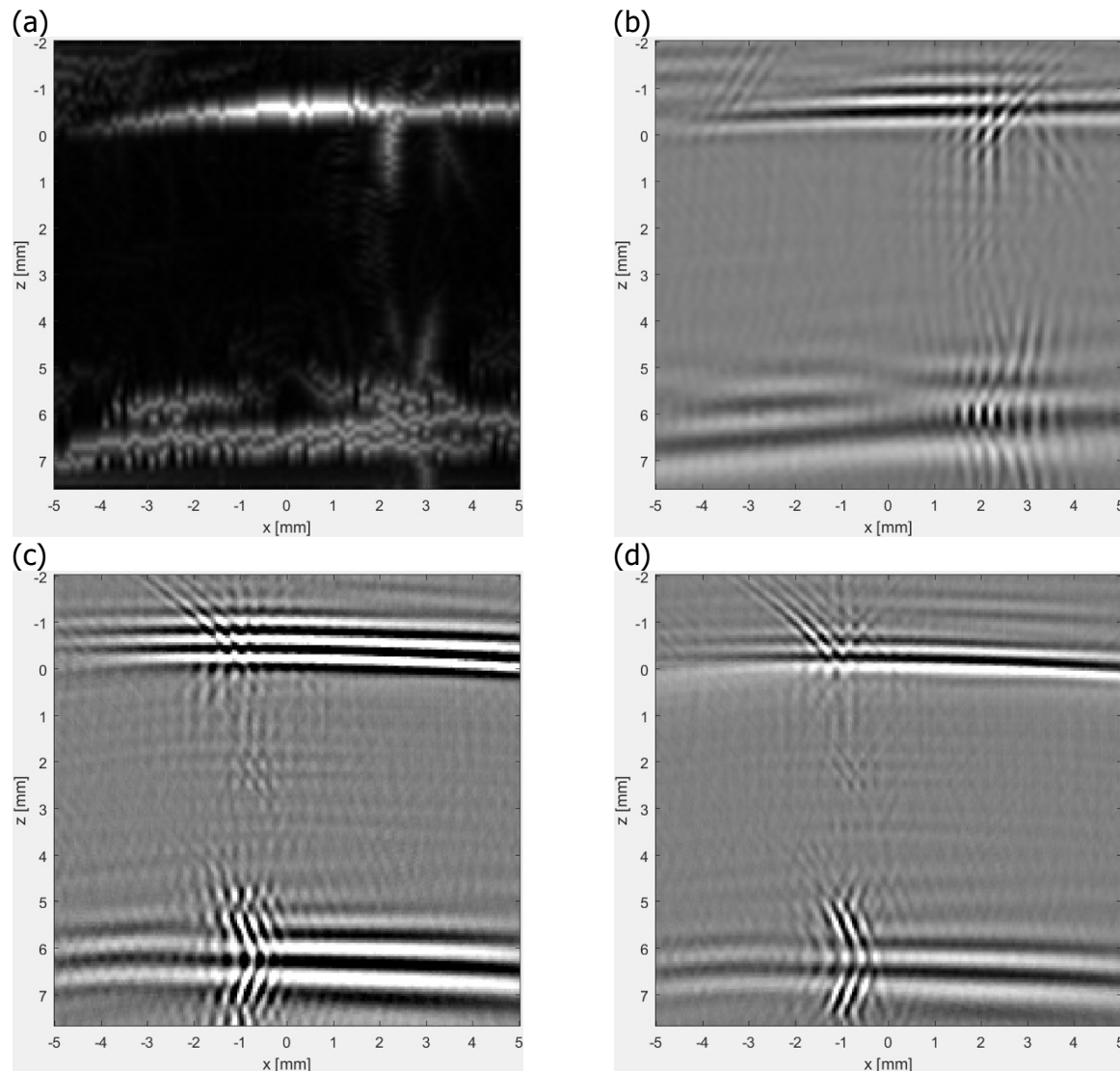


Figure 3-10: Comparison of a scan image and images obtained with the improved calibration routine for pipe UIN 731 from the PRCI trial: (a) rectified image from the scan, (b) unrectified image from the scan, (c) image obtained with the modified calibration routine, (d) image obtained with additional deconvolution to limit the effect of the extra layer between wedge and pipe.

It should be noted that this simplified deconvolution approach does not work under all circumstances. Figure 3-11 presents an example of a different pipe sample. In this case, the modified calibration routine enables improved alignment of the flaw with the material surfaces and improved focusing of the inner diameter surface. The deconvolution approach, however, improves the image of the material surfaces to some extent, but has no significant effect on the resolution of the flaw. Further development is required to take into account different paths traversing the layer between wedge and pipe.

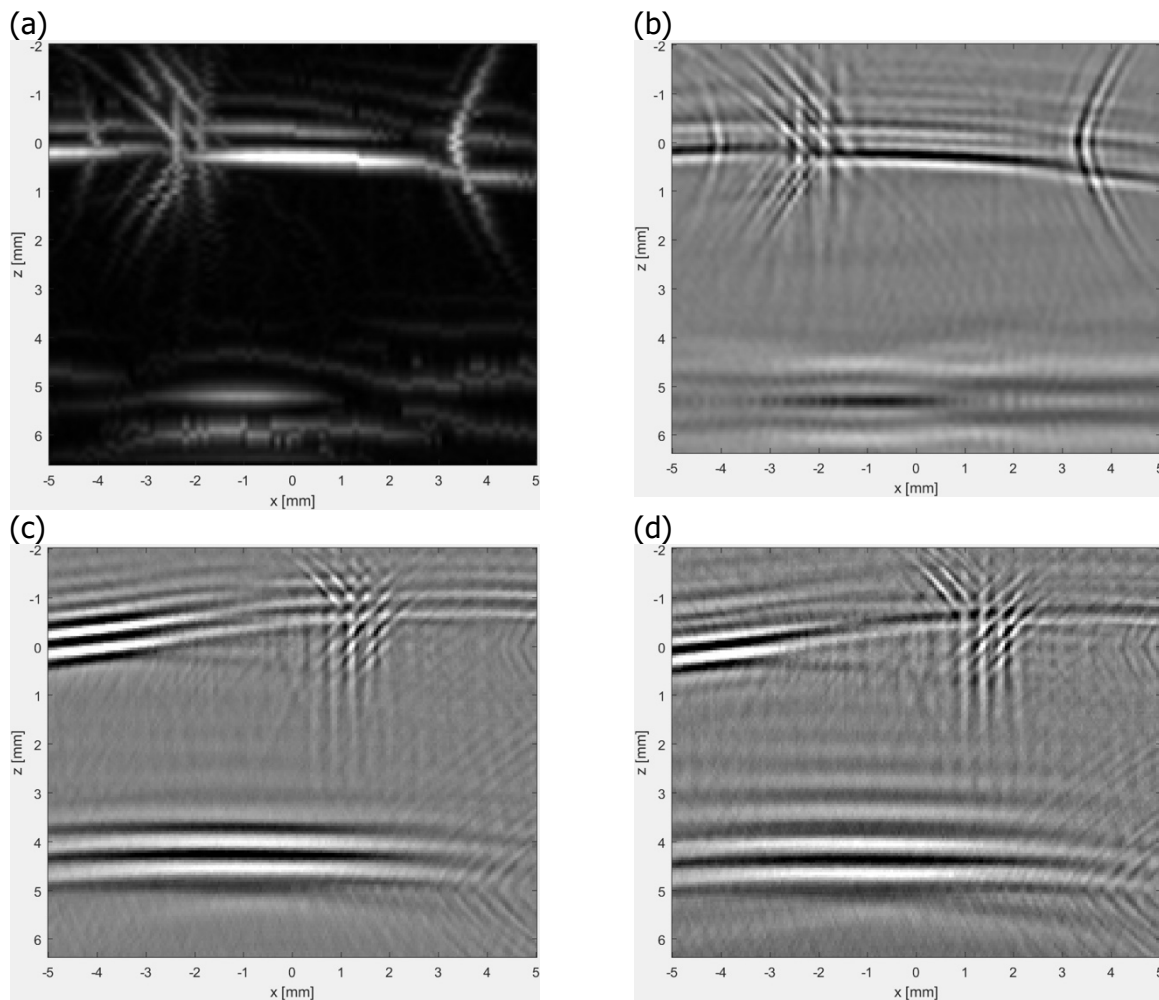


Figure 3-11: Comparison of a scan image and images obtained with the improved calibration routine for pipe UIN 512 from the PRCI trial: (a) rectified image from the scan, (b) unrectified image from the scan, (c) image obtained with the modified calibration routine, (d) image obtained with additional deconvolution to limit the effect of the extra layer between wedge and pipe.

The following conclusions can be drawn:

- For the majority of the samples tested, the modification of the calibration routine constitutes an improvement with respect to image alignment and focusing.
- The calibration remains to be improved to achieve robustness for field application (see items below). It is also required to provide feedback to the user if the calibration fails.
- The effect of an extra layer between the wedges and the pipe has been underestimated in the past. The extra layer turned out to have significant influence on the image alignment and resolution. Some approaches to compensate for these effects have already been tested and resulted in improved images.

The resolution and alignment of IWEX images is influenced by several parameters, which are determined during the setup phase. In order to assess the necessity for calibration and correction for these parameters, their influence on the image is determined.

Two indicators are used to measure the sensitivity of the image to a certain parameter:

- The focus of the image is assumed to be optimal if the image shows maximum amplitude.
- The alignment is determined from the position of indications in the image.

The following parameters are taken into account:

- 1) **System latency**
The system latency specifies the delay in the measurement chain between sending and receiving, without taking travel time in the wedge and pipe material into account.
- 2) **Wedge angle**
The wedge angle specifies the relative angle between the linear array and the pipe surface. It is measured relative to a tangent line touching the pipe at the bond line.
- 3) **Wedge velocity**
The longitudinal sound velocity in the wedge influences the travel time from the array to the outer pipe surface.
- 4) **Wedge index**
The wedge index describes the distance from the array center to the outer pipe surface, measured perpendicular to the pipe surface.
- 5) **Wedge offset**
The offset measures the straight line (secant) between the bond line and the corner of the wedge at the pipe surface towards the bond line.
- 6) **Wall thickness**
The wall thickness specifies the thickness of the pipe material. It influences paths including reflections at the inner diameter.
- 7) **Material velocity**
The shear velocity in the pipe material influences the travel time and the angle of refraction.
- 8) **Water layer**
There may be a layer of couplant between the bottom of the wedge and the outer pipe surface. The sound velocity is supposed to be similar to water.

9) **Curvature / pipe diameter**

The curvature of wedge and pipe may not be exactly as assumed. This is modeled by changing the diameter of the pipe.

10) **Roof topping / weld line peaking**

The pipe may not be perfectly cylindrical due to the way that the sheets are crimped before welding. This effect is described by the angle at which the sheets meet at the bond line. The point of rotation is chosen to be at the outer surface at the bond line. For a perfectly cylindrical pipe, the angle is 0° . A negative angle describes inward peaking; a positive angle describes outward peaking.

The analysis is carried out on a measurement taken with optimal settings in a laboratory environment. The sample consists of a pipe with an outer diameter of 8.625" with an artificial notch at the outer pipe surface. The notch extends about 1 mm into the material; the wall thickness is 4.8 mm. An IWEX image of the setup is shown in Figure 3-12.

The different parameters are then varied to determine their influence on focus and alignment.

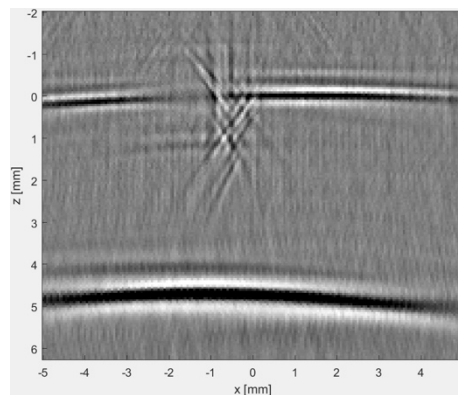


Figure 3-12: Example of an IWEX image of a pipe sample with an artificial surface-breaking defect extending through 20 % of the wall thickness from the outer (top) surface. This result has been obtained in a laboratory environment using automatic calibration of the setup parameters.

Results

In the following tables, the focusing can be assessed using the three columns referring to amplitude. The maximum acceptable variation of the respective parameter is given for an amplitude drop of 1 dB, 3 dB, and 6 dB in the image.

With respect to alignment, the two rightmost columns provide the change of parameter required to obtain a shift of +0.1 mm in the image. For IWEX-0, -1, -2, and -3, the shift refers to the change introduced by changing a model parameter for the left wedge only. Although the

relationship between the parameter and the shift is usually nonlinear, all shifts are provided as linear approximations around the optimum point.

Regarding the system latency, for example, a required change of the system latency parameter by -66 ns for a circumferential shift indicates that a decrease of the system latency by 66 ns in the settings used for imaging leads to the image being shifted by 0.1 mm to the right. The radial shift is positive towards the center of the pipe.

No values are provided for cases in which the influence of the parameter is negligible or could not be determined from measurements.

Table 3-2: Influence of the system latency on the image.

System latency	amplitude			x-position (circumferential) +0.1 mm	z-position (radial) +0.1 mm
	90 % (-1 dB)	70 % (-3 dB)	50 % (-6 dB)		
IWEX-0	-	-	-	-66 ns	-
IWEX-1	-	-	-	-66 ns	-
IWEX-2	-	-	-	-66 ns	+100 ns
IWEX-3	-	-	-	-50 ns	-
IWEX-0 cross	± 60 ns	± 120 ns	-	-	-33 ns
IWEX-2 cross	± 50 ns	-	-	-	+33 ns

Table 3-3: Influence of the wedge angle on the image.

Wedge angle	amplitude			x-position (circumferential) +0.1 mm	z-position (radial) +0.1 mm
	90 % (-1 dB)	70 % (-3 dB)	50 % (-6 dB)		
IWEX-0	-	-	-	+0.2°	-0.1°
IWEX-1	±0.2°	±0.5°	-	+0.2°	-
IWEX-2	-	-	-	+0.2°	+0.1°
IWEX-3	-	-	-	-0.2°	-
IWEX-0 cross	-	-	-	-	-0.2°
IWEX-2 cross	-	-	-	-	+0.2°

Table 3-4: Influence of the wedge velocity on the image.

Wedge velocity	amplitude			x-position (circumferential) +0.1 mm	z-position (radial) +0.1 mm
	90 % (-1 dB)	70 % (-3 dB)	50 % (-6 dB)		
IWEX-0	-	-	-	+20 m/s	+4 m/s
IWEX-1	± 15 m/s	± 30 m/s	-	+10 m/s	-
IWEX-2	-	-	-	+20 m/s	-8 m/s
IWEX-3	± 20 m/s	± 40 m/s	-	+7 m/s	-20 m/s
IWEX-0 cross	± 10 m/s	± 20 m/s	± 25 m/s	-	+7 m/s
IWEX-2 cross	± 10 m/s	± 20 m/s	± 25 m/s	-	-4 m/s

Table 3-5: Influence of the wedge index on the image.

Wedge index	amplitude			x-position (circumferential) +0.1 mm	z-position (radial) +0.1 mm
	90 % (-1 dB)	70 % (-3 dB)	50 % (-6 dB)		
IWEX-0	-	-	-	-0.10 mm	-0.30 mm
IWEX-1	± 0.4 mm	± 1.0 mm	-	-0.10 mm	-
IWEX-2	-	-	-	-0.16 mm	+0.83 mm
IWEX-3	± 0.3 mm	± 0.5 mm	± 0.8 mm	-0.66 mm	-
IWEX-0 cross	± 0.1 mm	± 0.2 mm	± 0.3 mm	-	-0.04 mm
IWEX-2 cross	± 0.1 mm	± 0.2 mm	± 0.3 mm	-	+0.04 mm

Table 3-6: Influence of the wedge offset on the image.

Wedge offset	amplitude			x-position (circumferential) +0.1 mm	z-position (radial) +0.1 mm
	90 % (-1 dB)	70 % (-3 dB)	50 % (-6 dB)		
IWEX-0	-	-	-	-0.10 mm	-
IWEX-1	-	-	-	-0.10 mm	-
IWEX-2	-	-	-	-0.10 mm	-
IWEX-3	-	-	-	-0.10 mm	-
IWEX-0 cross	± 0.1 mm	± 0.2 mm	± 0.3 mm	-	-0.06 mm
IWEX-2 cross	± 0.1 mm	± 0.2 mm	± 0.3 mm	-	+0.05 mm

Table 3-7: Influence of the material thickness on the image.

Material thickness	amplitude			x-position (circumferential) +0.1 mm	z-position (radial) +0.1 mm
	90 % (-1 dB)	70 % (-3 dB)	50 % (-6 dB)		
IWEX-0	-	-	-	-	-
IWEX-1	± 0.5 mm	± 0.8 mm	-	-	+0.20 mm
IWEX-2	-	-	-	+0.30 mm	+0.05 mm
IWEX-3	± 0.1 mm	± 0.2 mm	± 0.3 mm	-0.16 mm	-
IWEX-0 cross	-	-	-	-	-
IWEX-2 cross	-	-	-	-	+0.06 mm

Table 3-8: Influence of the material velocity on the image.

Material velocity	amplitude			x-position (circumferential) +0.1 mm	z-position (radial) +0.1 mm
	90 % (-1 dB)	70 % (-3 dB)	50 % (-6 dB)		
IWEX-0	± 30 m/s	± 60 m/s	-	+10 m/s	-7 m/s
IWEX-1	± 30 m/s	± 70 m/s	-	+10 m/s	-
IWEX-2	± 30 m/s	± 70 m/s	-	+10 m/s	+20 m/s
IWEX-3	± 20 m/s	± 60 m/s	-	+20 m/s	-
IWEX-0 cross	± 10 m/s	± 25 m/s	± 40 m/s	-	+20 m/s
IWEX-2 cross	± 10 m/s	± 25 m/s	± 40 m/s	-	-20 m/s

Table 3-9: Influence of the water layer on the image.

Water layer	amplitude			x-position (circumferential) +0.1 mm	z-position (radial) +0.1 mm
	90 % (-1 dB)	70 % (-3 dB)	50 % (-6 dB)		
IWEX-0	-	-	-	-0.1 mm	-
IWEX-1	-	-	-	-0.1 mm	-
IWEX-2	-	-	-	-0.1 mm	-
IWEX-3	-	-	-	-0.1 mm	-
IWEX-0 cross	± 0.1 mm	± 0.2 mm	± 0.3 mm	-	-0.05 mm
IWEX-2 cross	± 0.2 mm	± 0.4 mm	± 0.7 mm	-	+0.05 mm

Table 3-10: Influence of the curvature / pipe diameter on the image.

Curvature	amplitude			x-position (circumferential) +0.1 mm	z-position (radial) +0.1 mm
	90 % (-1 dB)	70 % (-3 dB)	50 % (-6 dB)		
IWEX-0	± 0.2 inch	± 0.5 inch	± 0.8 inch	+0.50 inch	-0.14 inch
IWEX-1	± 0.1 inch	± 0.3 inch	-	+0.20 inch	+0.10 inch
IWEX-2	± 0.5 inch	± 1.0 inch	-	+0.13 inch	+0.13 inch
IWEX-3	± 0.2 inch	± 0.4 inch	-	+0.33 inch	-
IWEX-0 cross	± 0.4 inch	± 0.8 inch	± 1.1 inch	-	+0.63 inch
IWEX-2 cross	± 0.4 inch	± 0.8 inch	± 1.1 inch	-	-0.63 inch

Table 3-11: Influence of roof topping on the image.

Roof topping	amplitude			x-position (circumferential) +0.1 mm	z-position (radial) +0.1 mm
	90 % (-1 dB)	70 % (-3 dB)	50 % (-6 dB)		
IWEX-0	-	-	-	+4.0°	+3.0°
IWEX-1	-	-	-	-	-
IWEX-2	-	-	-	-	-
IWEX-3	-	-	-	-	-
IWEX-0 cross	± 1.8°	± 4°	-	-	+1.0°
IWEX-2 cross	± 2.0°	-	-	-	-0.8°

In the following, the same results are provided in table sorted by IWEX mode.

Table 3-12: Influence of different parameters on IWEX-0.

IWEX-0	amplitude			x-position (circumferential) +0.1 mm	z-position (radial) +0.1 mm
	90 % (-1 dB)	70 % (-3 dB)	50 % (-6 dB)		
system latency	-	-	-	-66 ns	-
wedge angle	-	-	-	+0.2°	-0.1°
wedge velocity	-	-	-	+20 m/s	+4 m/s
wedge index	-	-	-	-0.1 mm	-0.3 mm
wedge offset	-	-	-	-0.1 mm	-
wall thickness	-	-	-	-	-
material velocity	± 30 m/s	± 60 m/s	-	+10 m/s	-7 m/s
water layer	-	-	-	-0.1 mm	-
curvature	± 0.2 inch	± 0.5 inch	± 0.8 inch	+0.5 inch	-0.14 inch
roof topping	-	-	-	+4.0°	+3.0°

Table 3-13: Influence of different parameters on IWEX-1.

IWEX-1	amplitude			x-position (circumferential) +0.1 mm	z-position (radial) +0.1 mm
	90 % (-1 dB)	70 % (-3 dB)	50 % (-6 dB)		
system latency	-	-	-	-66 ns	-
wedge angle	±0.2°	±0.5°		+0.2°	-
wedge velocity	± 15 m/s	± 30 m/s		+10 m/s	-
wedge index	± 0.4 mm	± 1.0 mm	-	-0.1 mm	-
wedge offset	-	-	-	-0.1 mm	-
wall thickness	± 0.5 mm	± 0.8 mm	-	-	+0.2 mm
material velocity	± 30 m/s	± 70 m/s	-	+10 m/s	-
water layer	-	-	-	-0.1 mm	-
curvature	± 0.1 inch	± 0.3 inch	-	+0.2 inch	+0.1 inch
roof topping	-	-	-	-	-

Table 3-14: Influence of different parameters on IWEX-2.

IWEX-2	amplitude			x-position (circumferential) +0.1 mm	z-position (radial) +0.1 mm
	90 % (-1 dB)	70 % (-3 dB)	50 % (-6 dB)		
system latency	-	-	-	-66 ns	+100 ns
wedge angle	-	-	-	+0.2°	+0.1°
wedge velocity	-	-	-	+20 m/s	-8 m/s
wedge index	-	-	-	-0.16 mm	+0.83 mm
wedge offset	-	-	-	-0.10 mm	-
wall thickness	-	-	-	+0.30 mm	+0.05 mm
material velocity	± 30 m/s	± 70 m/s	-	+10 m/s	+20 m/s
water layer	-	-	-	-0.1 mm	-
curvature	± 0.5 inch	± 1.0 inch	-	+0.13 inch	+0.13 inch
roof topping	-	-	-	-	-

Table 3-15: Influence of different parameters on IWEX-3.

IWEX-3	amplitude			x-position (circumferential) +0.1 mm	z-position (radial) +0.1 mm
	90 % (-1 dB)	70 % (-3 dB)	50 % (-6 dB)		
system latency	-	-	-	-50 ns	-
wedge angle				-0.2°	-
wedge velocity	± 20 m/s	± 40 m/s		+7 m/s	-20 m/s
wedge index	± 0.3 mm	± 0.5 mm	± 0.8 mm	-0.66 mm	-
wedge offset	-	-	-	-0.10 mm	-
wall thickness	± 0.1 mm	± 0.2 mm	± 0.3 mm	-0.16 mm	-
material velocity	± 20 m/s	± 60 m/s	-	+20 m/s	-
water layer	-	-	-	-0.1 mm	-
curvature	± 0.2 inch	± 0.4 inch	-	+0.33 inch	-
roof topping	-	-	-	-	-

Table 3-16: Influence of different parameters on IWEX-0 cross.

IWEX-0 cross	amplitude			x-position (circumferential) +0.1 mm	z-position (radial) +0.1 mm
	90 % (-1 dB)	70 % (-3 dB)	50 % (-6 dB)		
system latency	± 60 ns	± 120 ns	-	-	-33 ns
wedge angle	-	-	-	-	-0.2°
wedge velocity	± 10 m/s	± 20 m/s	± 25 m/s	-	+7 m/s
wedge index	± 0.1 mm	± 0.2 mm	± 0.3 mm	-	-0.04 mm
wedge offset	± 0.1 mm	± 0.2 mm	± 0.3 mm	-	-0.06 mm
wall thickness	-	-	-	-	-
material velocity	± 10 m/s	± 25 m/s	± 40 m/s	-	+20 m/s
water layer	± 0.1 mm	± 0.2 mm	± 0.3 mm	-	-0.05 mm
curvature	± 0.4 inch	± 0.8 inch	± 1.1 inch	-	+0.63 inch
roof topping	± 1.8°	± 4°	-	-	+1.0°

Table 3-17: Influence of different parameters on IWEX-2 cross.

IWEX-2 cross	amplitude			x-position (circumferential) +0.1 mm	z-position (radial) +0.1 mm
	90 % (-1 dB)	70 % (-3 dB)	50 % (-6 dB)		
system latency	± 50 ns	-	-	-	+33 ns
wedge angle	-	-	-	-	+0.2°
wedge velocity	± 10 m/s	± 20 m/s	± 25 m/s	-	-4 m/s
wedge index	± 0.1 mm	± 0.2 mm	± 0.3 mm	-	+0.04 mm
wedge offset	± 0.1 mm	± 0.2 mm	± 0.3 mm	-	+0.05 mm
wall thickness	-	-	-	-	+0.06 mm
material velocity	± 10 m/s	± 25 m/s	± 40 m/s	-	-20 m/s
water layer	± 0.2 mm	± 0.4 mm	± 0.7 mm	-	+0.05 mm
curvature	± 0.4 inch	± 0.8 inch	± 1.1 inch	-	-0.63 inch
roof topping	± 2.0°	-	-	-	-0.8°

Discussion

The following statements can be made with respect to focusing:

- The focusing of the cross modes is significantly affected by the **wedge and material velocities, wedge index and offset**, the thickness of the **water layer**, and **roof topping**.
- The focusing of the tandem modes IWEX-1 and IWEX-3 is strongly affected by the **curvature** of the pipe.
- IWEX-3 is very sensitive to the **wall thickness**.

With respect to alignment of the modes, the following conclusions can be drawn:

- The **wedge angle** and the **wedge and material velocities** as well as the **curvature** have severe influence on the alignment of the images for all modes.
- The **water layer** has the strongest effect on the cross modes in terms of alignment, but affects the other modes as well.
- The cross modes are significantly affected by **wedge index and offset** as well as **roof topping**.
- The **wall thickness** has strong influence on the depth of an indication in the IWEX-2 and IWEX-2 cross modes.

In order to obtain focused images of sufficient quality (amplitude > 70%) and optimal alignment (shift less than 0.2 mm), the following accuracies are required:

Parameter	required accuracy
system latency	± 50 ns
wedge angle	$\pm 0.2^\circ$
wedge velocity	± 10 m/s
wedge index	± 0.1 mm
wedge offset	± 0.1 mm
wall thickness	± 0.1 mm
material velocity	± 20 m/s
water layer	± 0.1 mm
curvature (diameter)	± 0.1 inch
roof topping	$\pm 1.6^\circ$

The current calibration routines do not provide these accuracies. The following parameters use nominal values instead of being calibrated:

- wedge velocity
- material velocity

Furthermore, these parameters are not taken into account in the current calibration approach:

- water layer
- curvature
- roof topping

Therefore, a modification of the calibration approach is required to meet the demands of the application.

For larger pipe diameters, it is assumed that the required accuracy of some of the parameters, such as curvature, may be less strict than in the 8.625-in example considered here. Nevertheless, the calibration routine should aim to achieve the presented accuracies.

The influence of different parameters on the IWEX image was quantified. Furthermore, different ways of inspecting non-cylindrical pipe were tested and compared. A two-pronged approach was proposed:

- Pipe samples that satisfy the constraints of the cylindrical model within reasonable tolerances will continue to be inspected with the current approach using plastic wedges. A typical application belonging to this category is the inspection of stress corrosion cracking in the pipe body. This is the method current in use in the field as of 2017.
- For pipe samples that deviate significantly from the cylindrical model, an immersion type inspection will be developed. First experiments in the previous quarter showed promising results for samples that exhibit significant roof topping (see also drawing below) or changes in wall thickness close to the weld (poor trim). Both geometric anomalies are related to the pipe manufacturing process. This is the process proposed for implementation in late 2018.

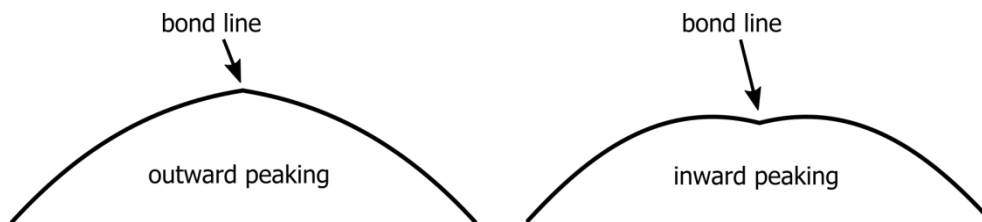


Figure 3-13: Examples of roof topping: outward peaking and inward peaking.

The separation of samples into different classes enables continuation with the current inspection method using scans with plastic wedges, while the proposed extension to immersion is envisioned to provide increased robustness and accuracy in the long term.

To simplify the setup process for the cylindrical pipe, the results obtained from the parameter study were used to develop an updated calibration tool for setting up the inspection.

The calibration consists of two steps:

- 1) The parameters related solely to the measurement system and the plastic wedges are calibrated with the wedges off the pipe sample.
- 2) Once the wedges are calibrated, they need to be put on the pipe sample in the setup used for scanning to calibrate some parameters of the pipe and the relative alignment of the wedges.

Wedge calibration

The calibration of the wedges consists of three different parameters to be determined consecutively: system latency, wedge velocity, and wedge indices.

All parameters are determined from ultrasonic measurements, such that the input of manually determined values, for example using mechanical measurements, is avoided. The information to be entered is limited to parameters of the array (specified by the manufacturer) and the pipe diameter.

In terms of the measurements required and the subsequent processing, several changes were made to the approaches used:

- The system latency can now be calibrated without removing the probes from the wedges.
- The calibration of the wedge velocity and the wedge indices use a higher number of measurements to increase the robustness and accuracy of the calibration.
- All parameters are determined for both wedges independently.

A software tool with a graphical user interface was developed to measure these parameters and provide visual feedback on the outcome of the calibration.

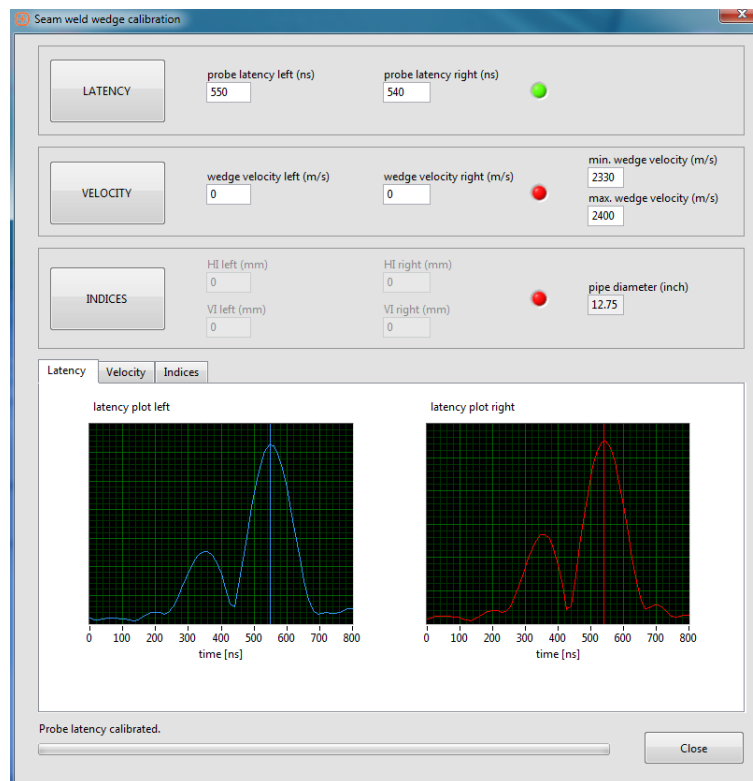


Figure 3-14: Dialog window of the wedge calibration

Scan setup calibration

The calibration of the scan setup provides a measurement tool to determine the thickness of the water layer below the wedges and check the coupling condition. Furthermore, the wall thickness of the pipe sample below the wedges can be measured.

Figure 3-15 provides an example of images made below the wedges. The interface between wedge and pipe is shown, with the dashed lines representing the bottom surface of the wedge, and the horizontal black-and-white indications showing the position of the OD pipe surface. The vertical scale is deliberately exaggerated to simplify the recognition of minor variations.

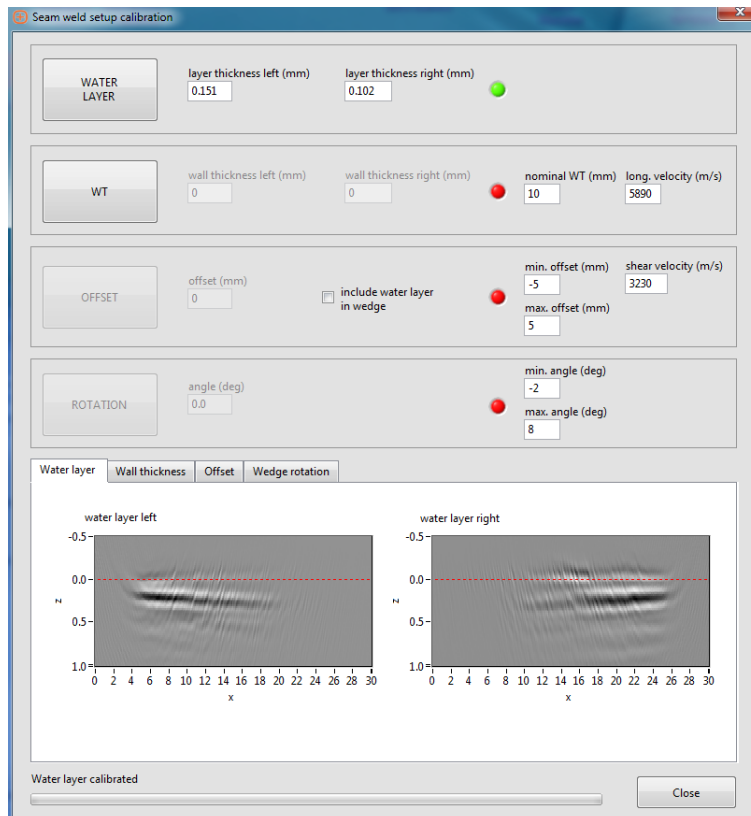


Figure 3-15: Measurement of the water layer; images below the wedge provide visual feedback.

The wall thickness measurement can also be used to analyze the quality of the coupling using the images of the pipe surface made below the wedges. This is illustrated in Fig. 3-16, with the left side showing the better coupling of the two. This kind of feedback can be used to optimize the mechanical setup of the scanner on the pipe before starting the scan.

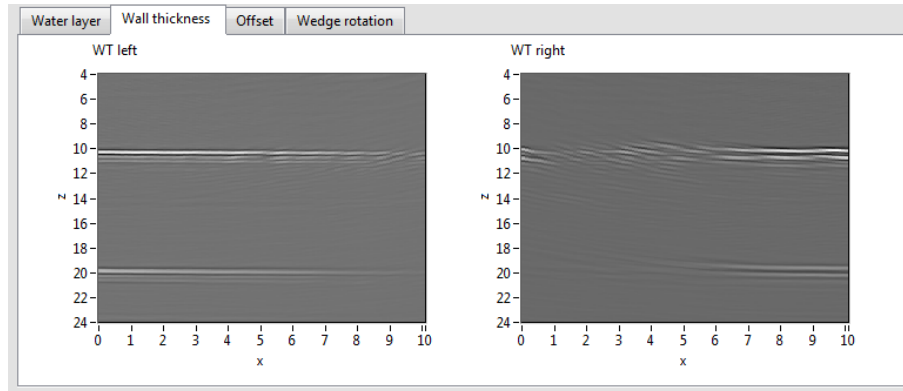


Figure 3-16: Multiple reflections from the inner and outer pipe surfaces provide visual feedback on the coupling condition; in this case, the left side is slightly better coupled.

In a third step, the relative alignment of the wedges is determined. Due to the frequently encountered phenomenon of roof topping, it has been chosen to deviate slightly from the cylindrical model for this final step.

Both the distance between the wedges along the pipe surfaces as well as the relative rotation can be determined in the calibration tool.

First an image made at the outer pipe surface is used to determine the offset between the wedges. Figure 3-17 shows the ultrasonic paths used (blue line) and the region in which the image is made (green rectangle).

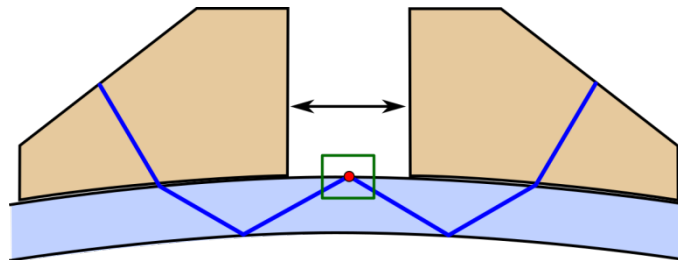


Figure 3-17: Calibration of the distance between the wedges using an image made at the outer pipe surface (green rectangle).

Several values for the offset are tested, and the value leading to an image with maximum amplitude is selected.

If required, the relative rotation between the wedges can be determined using an image made at the inner pipe surface. The rotation is carried out about the origin, shown as the red dot at the outer pipe surface in Figs. 3-17 and 3-18. This way, the offset calibration is not invalidated when determining the relative rotation in a subsequent step.

By providing the option to calibrate the relative rotation of the wedges, the calibration tool can account for roof topping to some extent.

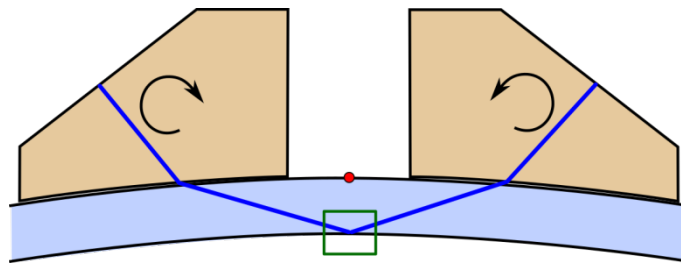


Figure 3-18: Calibration of the relative rotation between the wedges using an image made at the inner pipe surface (green rectangle).

The calibration routine has been tested on samples of 8.625", 16" and 24" diameter in a laboratory environment. Tests under field conditions are pending.

Development of a Written Procedure

During development and trials a written procedure was developed. The procedure has evolved as more experience has been gained with running the IWEX technology. A copy of the RTD IWEX procedure is included as Appendix A. The procedure included in this report should be considered representative and not necessarily the final version that will be used going forward as it is expected to evolve. For instance as of writing of the Phase II report, there is no generally accepted industry practice for producing UT images from FMC data. ASME is developing an industry written practice for FMC data with total focusing method (TFM) processing, but it is yet not finished. (IWEX is a similar processing method to TFM and can be considered a specific flavor of the larger umbrella of TFM types of processing that produces similar results.) As UT imaging becomes more mature and industry practices become established we expect to update our procedure.

Conclusions

A tool for calibrating the wedges and setup on the pipe was developed assuming a cylindrical pipe with some limited variability. The existing calibration routine for the wedges was improved in terms of robustness and simplicity for the user. The calibration tool was extended to provide means for calibrating the seam weld setup on the pipe sample to determine wall thickness and relative alignment of the wedges. The coupling condition can be checked by measuring the thickness of the water layer below the wedges and assessing the strength of the reflections received from the inner and outer pipe surfaces.

The relative alignment of the wedges can be calibrated in terms of both distance and rotation. This enables the calibration tool to deal with roof topping to some extent.

SECTION 4

DEVELOPMENT OF AN AUTOMATED DEFECT DETECTION, IDENTIFICATION, AND SIZING MODULE

The task activity included the following items:

- Develop 3D & 2D GUI to display the IWEX data.
- Project Management program to develop automated defect detection, identification, and sizing module – Kiefner.
- Develop SQL storage of the feature data.
- Develop module to Merge 1-inch wide scans into a continuous data set by calculating the offsets (and overlap) to be able to render it as a continuous image. This will most likely involve some manual correction interface. Unless one of the preview images has already done this operation.
- Develop module for Automatic and Manual Detection of features.
- Develop module for Automatic and Manual Classification of features and calculation of severity using equations from KAPA and possibly API 579 for cracks. Cracks maybe in colonies and require interaction rules.
- Design and develop a module for on-site reporting for Implementation of field application software.
- Develop module for Longitudinally Oriented Crack Assessment.
- Develop module for Reporting of feature data (CSV export for excel & PDF report.
- Develop module for Matching of data to other data sources MT, PA, ToFD, and possibly ILI data. Need to calculate POD, POI, and sizing errors.
- Develop module modifications for Automatic and Manual Detection of features using Immersion Data.
- Testing of Automated Sizing and Report Features.

Develop 3D & 2D GUI to display the IWEX data

The IWEX Processor is a program designed to render and merge multiple IWEX scan data files in an efficient manner, as well as allow detection and analysis of features in the data. It provides pdf reporting and different CSV import/export options.

The program does not require an installation (it is completely self-contained), simply double click on the program and it will run. The program is highly graphics intensive and requires a minimum resolution of 1366x768 pixels to be easy to use.

The GUI development has been through several stages: from viewer for the lab version of the IWEX scan files to analysis software that allows automatic detecting, sizing and characterizing the new field version IWEX scan files. Figure 4-1 shows a sample anomaly as being interpreted by the IWEX processor software. There are 5 strip charts on the bottom half of the screen showing a left and right side-views on the ends and 3 top down C-scan views in the middle for OD, mid-wall, and ID portions of the pipe. The 2 side views and 3 top down views are different perspectives of the same volume of data divided into 2 separate sections for the side views and 3 separate sections for the top down views. Above the strip charts is a cross-sectional view, in this case it represents one slice of the dataset as represented by the yellow line on the strip charts.

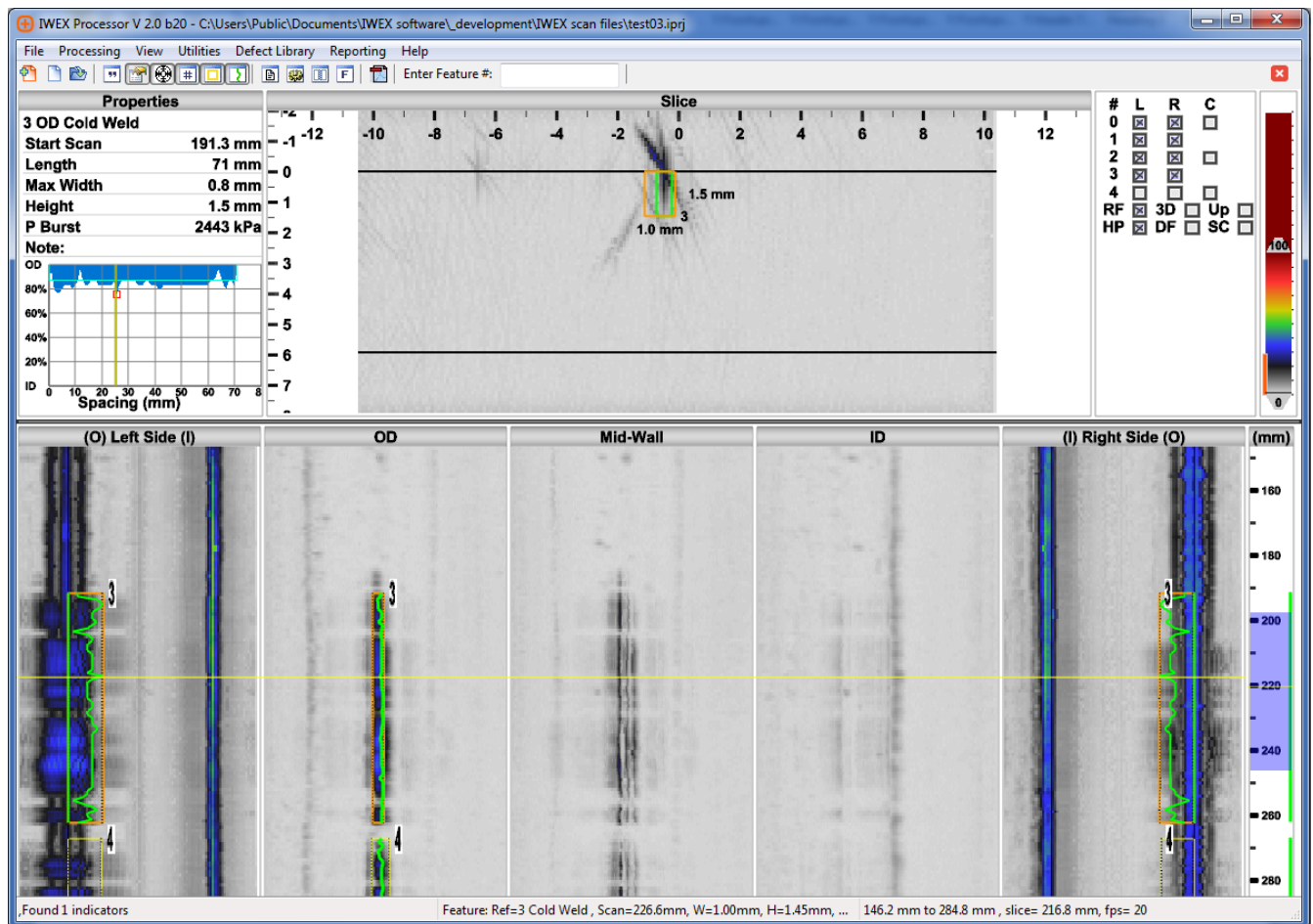



Figure 4-1. IWEX Processor with a project

In addition to the cross-sectional view two white panels flank the cross-sectional view, the properties panel on the left and the mode selection panel on the right.

Properties panel

The Properties panel (Figure 4-2) shows the details and the profile for the selected feature or the one nearest the mouse. The profile shows blue for each profile box, green is used to indicate the distance to the surface if the defined profile box does not quite reach the surface.

Currently Burst Pressure can be calculated only for surface breaking features using the Ln-Sec Method (from KAPA). When it is calculated a horizontal line shows the Effective depth.

When editing a feature, it is possible to change the feature type and add a note clicking on  and then **Save**.

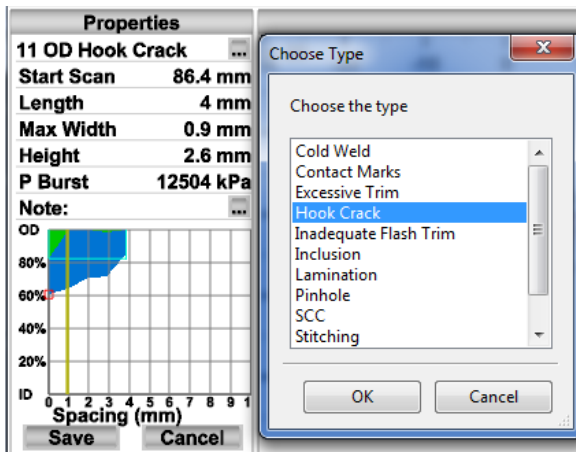


Figure 4-2. Properties panel

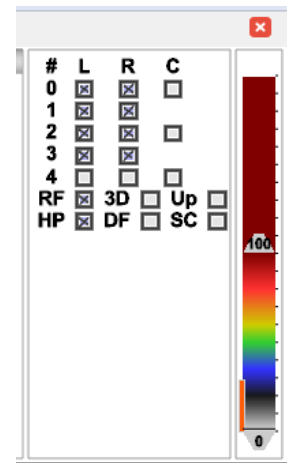


Figure 4-3. Mode control panel

Mode selection panel

In the Mode Selection panel (Figure 4-3) it is possible to turn on and off the various modes (see Section 1 Figure 1-4), in addition to selecting different filters. A description of the filters is as follows:

- **RF** is for rectification and thinning, Figure and 4-6.
- **HP** applies the High-Pass filter to filter out the low frequencies, Figure4-5 and 4-6.
- **DF** is a Differential Filter is used by the Feature Detection Routine to quickly find areas of interest, Figure4-7. It shows you exactly what the algorithm 'sees' when it is trying to determine the Indicators for the current slice.
- **UP** applies the up-sampling filter, Figure 4-4-8.
- **3D** opens the three-dimensional view of part of the scan file, Figure 4-9.
- **SC** rebuilds the strip charts using the visible views.

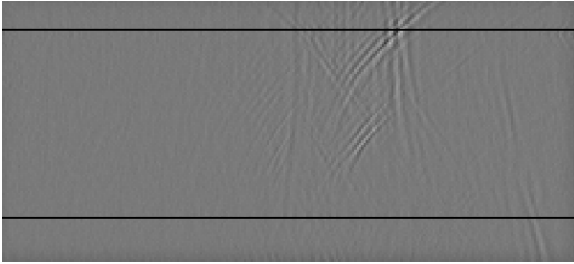


Figure 4-4. RF off

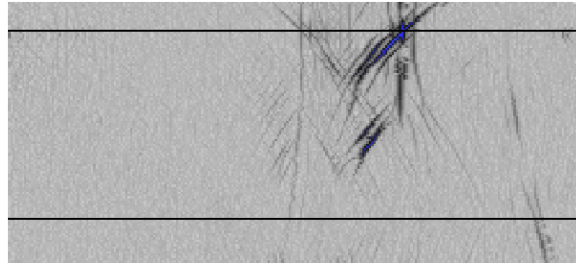


Figure 4-5. RF on, HP off

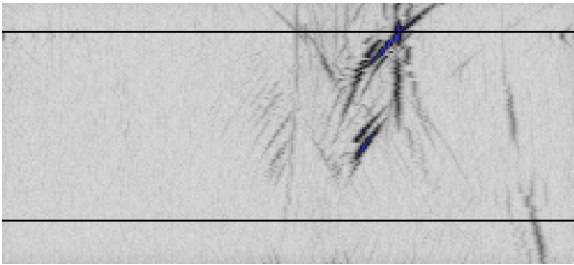


Figure 4-6. RF on HP on

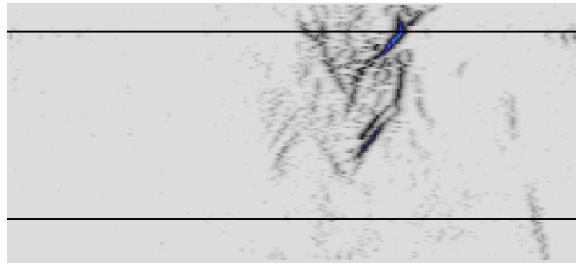
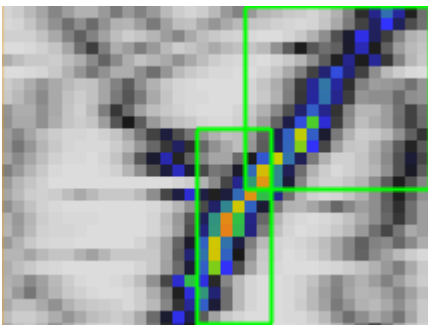
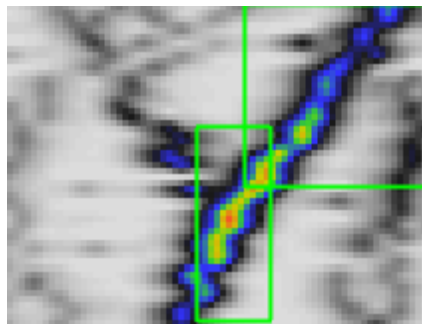


Figure 4-7. DF on



a)



b)

Figure 4-8. a) UP filter off, b) UP filter on

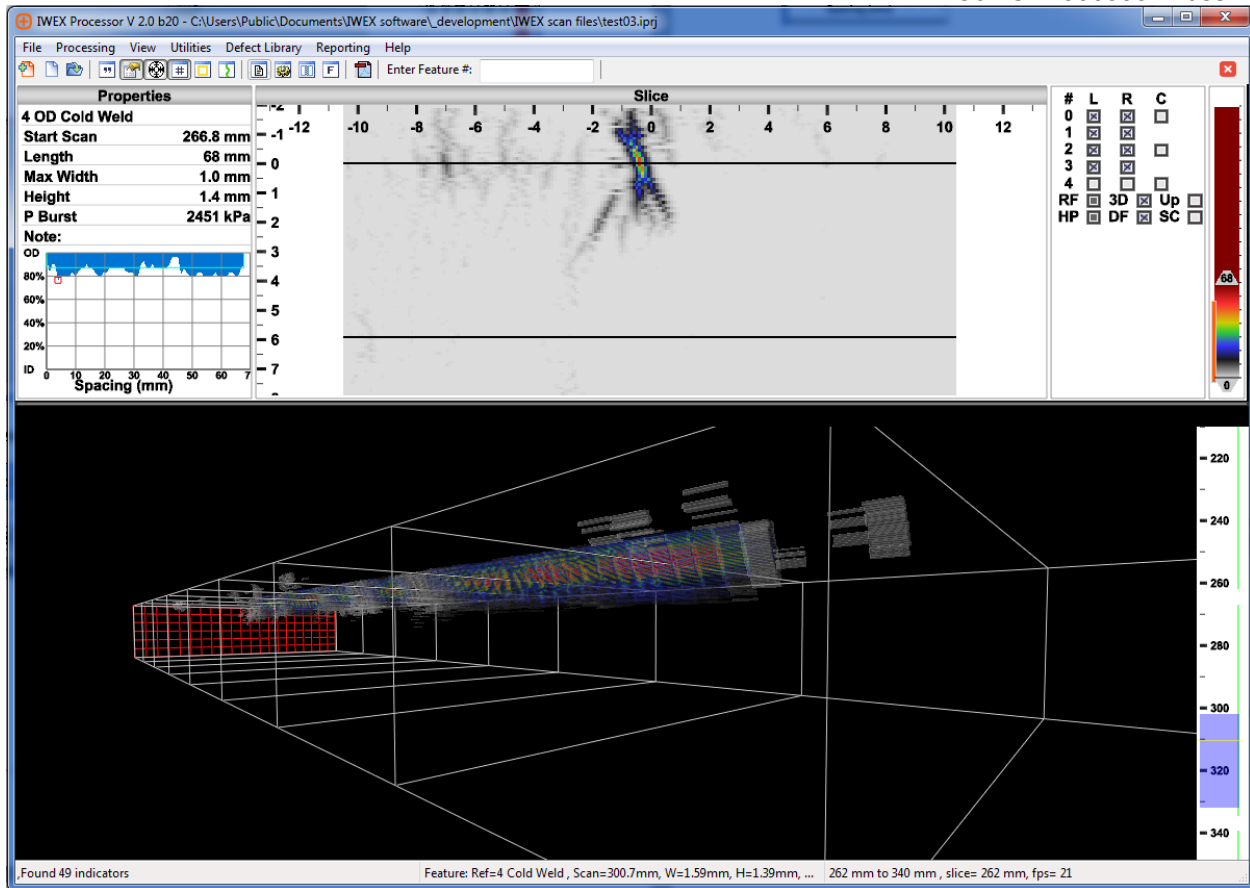


Figure 4-9. 3D view

The GUI can also display data in text form but is not shown here for brevity. The data are contained in tables from the SQL database, which are described below.

Develop SQL storage of the feature data

The features data, together with other information necessary for other functions, are stored in a SQLite database which is also the format of the IWEX project file with extension **(.iprj)**. The features data is stored in tables within the database. Examples of the tables are as follows and shown in Figures 4-10 through 4-17:

- **ILI_DATA:** ILI data basic information according the Pipeline Open Data Standard, Figure 4-10
- **autodetect:** interaction rules, detection threshold and statistics for every run of the Auto detection algorithm, Figure 4-11
- **data_file:** file names: used when merging more files together, Figure 4-12
- **feature:** information about the features (type, position, profile, KAPA, analyst, etc.), Figure 4-13

- **information:** the information from the IWEX data file header Figure 4-14
- **offset:** axial, circumferential and depth offset is saved for each file. The offsets are added to each feature according the data file on which is created, Figure 4-15
- **pipe:** contains name, diameter, wt, smys, cvn, safety factor, Figure 4-16
- **prefs:** information about the last active view options, Figure 4-17

The tables show the data can be exported so others can use the data for comparison purposes. This will be important for future studies where accuracy of ILI data needs to be studied or improved and integrity studies where the shape and type of flaws will be studied.































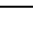
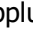
	ILI_Data_ID	integer	'ILI_Data_ID' integer
	Dig_Number	integer	'Dig_Number' integer
	Item	integer	'Item' integer
	Anomaly_Type_CL	text	'Anomaly_Type_CL' text
	Internal_External_CL	text	'Internal_External_CL' text
	Feature_Description	text	'Feature_Description' text
	Ovality	double	'Ovality' double
	Axial_Ovality	double	'Axial_Ovality' double
	Absolute_Odometer	double	'Absolute_Odometer' double
	Milepost	double	'Milepost' double
	Max_Depth_Pct	double	'Max_Depth_Pct' double
	Max_Depth_Measured	double	'Max_Depth_Measured' double
	Average_Depth	double	'Average_Depth' double
	Length	double	'Length' double
	Width	double	'Width' double
	Orientation	integer	'Orientation' integer
	US_Weld_Distance	double	'US_Weld_Distance' double
	DS_Weld_Distance	double	'DS_Weld_Distance' double
	US_Weld_Number	double	'US_Weld_Number' double
	DS_Weld_Number	double	'DS_Weld_Number' double
	US_Weld_Odometer	double	'US_Weld_Odometer' double
	DS_Weld_Odometer	double	'DS_Weld_Odometer' double
	Seam_Orientation	integer	'Seam_Orientation' integer
	MAPL_ID	double	'MAPL_ID' double
	Joint_Length	double	'Joint_Length' double
	Outside_Diameter	double	'Outside_Diameter' double
	Measured_Wall_Thickness	double	'Measured_Wall_Thickness' double
	Nominal_Wall_Thickness	double	'Nominal_Wall_Thickness' double
	Latitude	double	'Latitude' double
	Longitude	double	'Longitude' double
	Pipe_Depth	double	'Pipe_Depth' double
	Comments	text	'Comments' text

Figure 4-10. ILI_DATA table, according PODS

















 id	integer	`id` integer
 m_nAutoDetectVersion	integer	`m_nAutoDetectVersion` integer
 m_dMinDistCirc	double	`m_dMinDistCirc` double
 m_dMinDistDepth	double	`m_dMinDistDepth` double
 m_dMinDistScan	double	`m_dMinDistScan` double
 m_dMinLength	double	`m_dMinLength` double
 m_dMaxLength	double	`m_dMaxLength` double
 m_dMinHeight	double	`m_dMinHeight` double
 m_dMaxTrigger	double	`m_dMaxTrigger` double
 m_dTriggerFactor	double	`m_dTriggerFactor` double
 m_dStdDevFactor	double	`m_dStdDevFactor` double
 m_dAvgFactor	double	`m_dAvgFactor` double
 m_nIndicators	integer	`m_nIndicators` integer
 m_nProfileBoxes	integer	`m_nProfileBoxes` integer
 m_nFeatures	integer	`m_nFeatures` integer
 m_sAnalyst	text	`m_sAnalyst` text

Figure 4-11. autodetect table



 id	integer	`id` integer
 file_name	varchar (255)	`file_name` varchar (255)

Figure 4-12. data_file table





















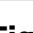
 id	integer	`id` integer
 ref	varchar (20)	`ref` varchar (20)
 category	varchar (20)	`category` varchar (20)
 depth_cat	varchar (2)	`depth_cat` varchar (2)
 scan_start_mm	double	`scan_start_mm` double NOT NULL
 scan_end_mm	double	`scan_end_mm` double NOT NULL
 circ_start_mm	double	`circ_start_mm` double NOT NULL
 circ_end_mm	double	`circ_end_mm` double NOT NULL
 depth_start_mm	double	`depth_start_mm` double NOT NULL
 depth_end_mm	double	`depth_end_mm` double NOT NULL
 profile_mm	text	`profile_mm` text
 burst_kpa	double	`burst_kpa` double NOT NULL DEFAULT 0.0
 eff_startdist_mm	double	`eff_startdist_mm` double DEFAULT 0.0
 eff_enddist_mm	double	`eff_enddist_mm` double DEFAULT 0.0
 eff_len_mm	double	`eff_len_mm` double DEFAULT 0.0
 eff_area_sqmm	double	`eff_area_sqmm` double DEFAULT 0.0
 analyst	text	`analyst` text
 comment	text	`comment` text
 display_settings	text	`display_settings` text
 weld_zone	text	`weld_zone` text
 data_file_id	int	`data_file_id` int DEFAULT 0

Figure 4-13. feature table



 field_name	varchar (255)	`field_name` varchar (255)
 value	varchar (255)	`value` varchar (255)

Figure 4-14. information table







 id	integer	`id` integer
 data_file_id	integer	`data_file_id` integer NOT NULL
 scan_mm	double	`scan_mm` double NOT NULL DEFAULT -9e9
 dist_mm	double	`dist_mm` double NOT NULL DEFAULT 0.0
 circ_mm	double	`circ_mm` double NOT NULL DEFAULT 0.0
 depth_mm	double	`depth_mm` double NOT NULL DEFAULT 0.0

Figure 4-15. offset table










 id	integer	`id` integer
 line_name	text	`line_name` text
 diameter_mm	double	`diameter_mm` double NOT NULL DEFAULT 1.0
 wt_mm	double	`wt_mm` double NOT NULL DEFAULT 1.0
 smys_kpa	double	`smys_kpa` double NOT NULL DEFAULT 1.0
 safety_factor	double	`safety_factor` double NOT NULL DEFAULT 1.0
 cvn_joules	double	`cvn_joules` double NOT NULL DEFAULT 0.0
 comment	text	`comment` text
 depth_start_mm	double	`depth_start_mm` double DEFAULT 0.0

Figure 4-16. pipe table

 id	integer	`id` integer
 key	text	`key` text
 val	text	`val` text

Figure 4-17. prefs table

Develop module to Merge 1-inch wide scans into a continuous data set by calculating the offsets (and overlap) to be able to render it as a continuous image.

The merging of data was recognized as a need because the inspection width for IWEX inspections is about 1-inch, but the width of an integrity anomaly may be wider. This is especially important for SCC colonies where the circumferential extent of a colony is more often wider than this. For flexibility the Data File Offset Editor window allows editing the offsets for all the three directions: circular, longitudinal and radial (depth). This will allow data to be merged regardless of the application.

The software allows adding multiple files to a project. For every new file, the software asks if the file is going to be merged axially or circumferentially. For axial merging the scan start value of the added file is used. For circular merging the width of the scan area is used.

Using the dialog in Figure 4-18 (Processing->Edit Project and Offsets) it is possible to define the offsets between the scans along any of the three axes. Values can be adjusted to take any overlap between the scans in account.

Figures 4-18 and 4-19 show an example with 5 files merged in circular direction. The width of each scan file was 20mm (0.8in) and each scan overlaps the other of 10mm (0.4in) hence the position of each added file was previous **Circ Offset + Scan Width – Overlap**.

Data File	Scan Start (mm)	Scan End (mm)	Scan Direction	For Scans GT (mm)	Scan Offset (mm)	Circ Offset (mm)	Depth Offset (mm)
20in.-6.5,CGO-TS-2017-001_0000_Grid-1-00-rev	-1 (-1)(-0.0ft)	201 (201)(0.7ft)	Backward	0	0	0	0
20in.-6.5,CGO-TS-2017-001_0001_Grid-1-01-rev	-1 (-1)(-0.0ft)	201 (201)(0.7ft)	Backward	0	0	10	0
20in.-6.5,CGO-TS-2017-001_0002_Grid-1-02-rev	-1 (-1)(-0.0ft)	201 (201)(0.7ft)	Backward	0	0	20	0
20in.-6.5,CGO-TS-2017-001_0003_Grid-1-03-rev	-1 (-1)(-0.0ft)	201 (201)(0.7ft)	Backward	0	0	30	0
20in.-6.5,CGO-TS-2017-001_0004_Grid-1-04-rev	-1 (-1)(-0.0ft)	201 (201)(0.7ft)	Backward	0	0	40	0

Figure 4-18, Table of merged scan strips

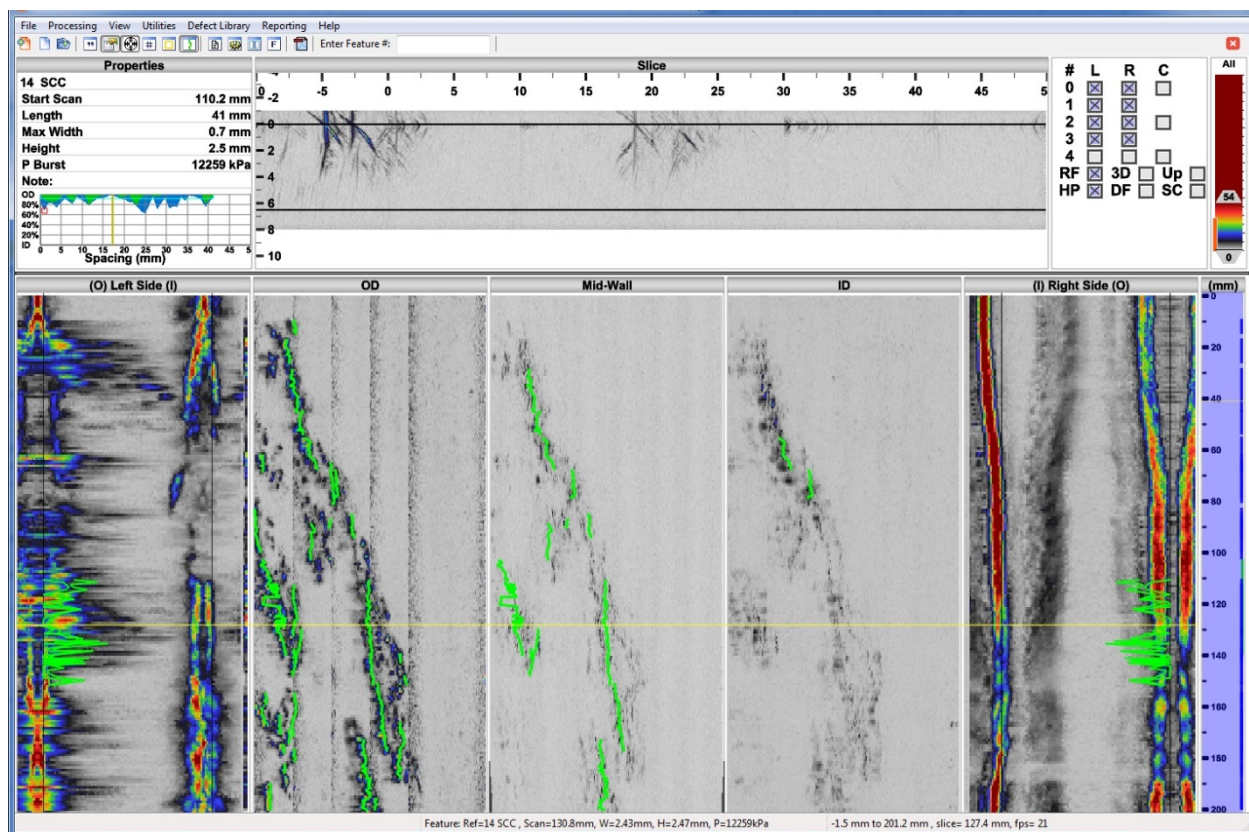


Figure 4-19, Display of merged scan strips

Develop module for Automatic and Manual Detection of features

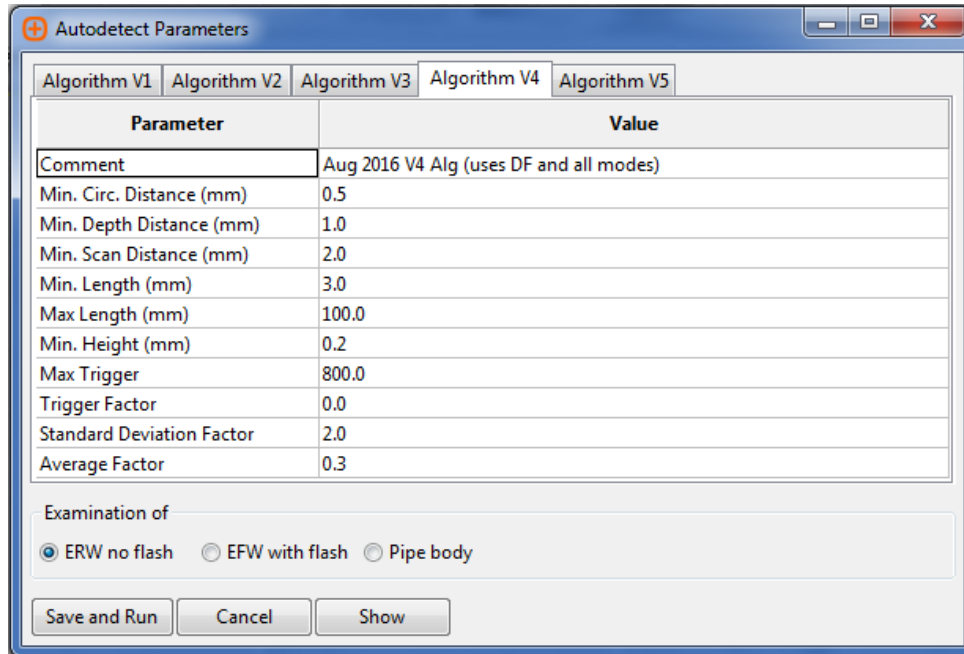
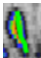


Figure 4-20. Autodetect Parameters dialog opened by *Processing->Auto Detect features*

The automatic detection feature can be used to build a profile when editing a single feature or for all the scan files of the project. It consists of 5 different algorithms that can be tuned adjusting the interaction distances and the trigger value (Figure 4-20). This last one is used to change the threshold level above which a signal is detected or not. The algorithms differ on whether or not the differential filter is used, whether or not it is possible to use fewer modes for the evaluation, whether or not they are applied for external or internal SCC.

A "feature line" system  has been implemented to let the analyst check the quality of the automatic detection: in Figure 4-21 it is possible to see how the profile boxes follow the depth of the profile on the side view and the path of the feature on the OD view.

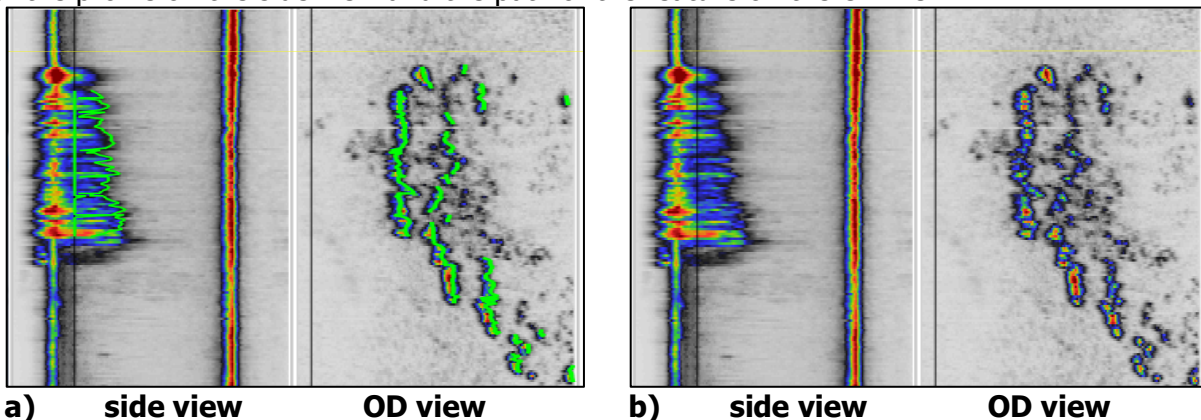


Figure 4-21. a) scan with profile/feature line, b) scan without profile/feature line

Develop module for Automatic and Manual Classification of features and calculation of severity using equations from KAPA. Cracks maybe in colonies and require interaction rules.

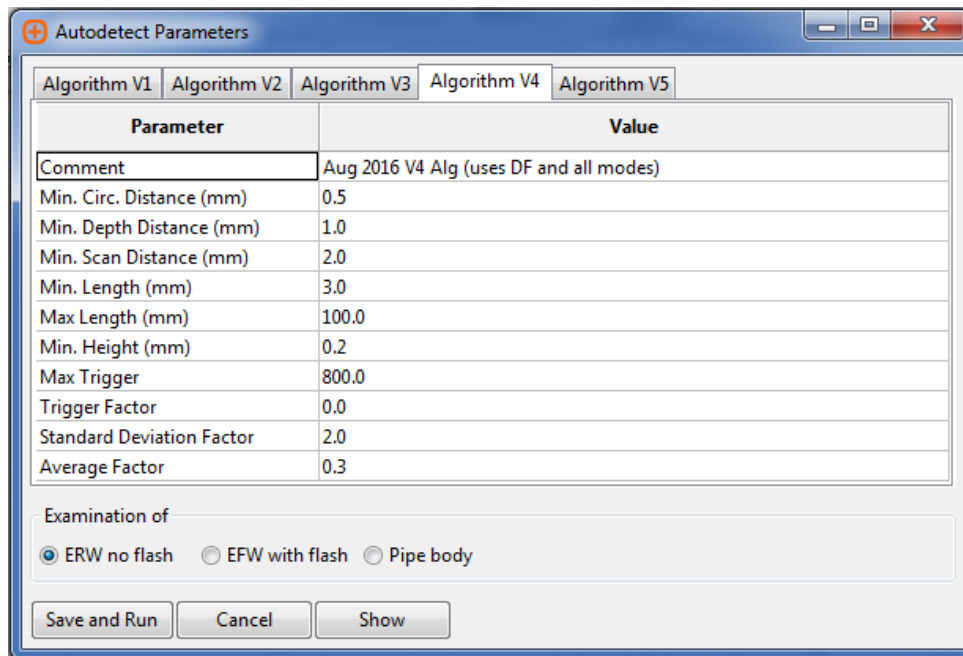


Figure 4-22

In the Autodetect Parameters dialog, Figure 4-22, it is possible to change the interaction distances to have the software grouping small features in to bigger features. A module has been implemented to classify automatically the features once the "Examination of" value has been set. Automatic classification is made according the distance from the surfaces and from the centerline.

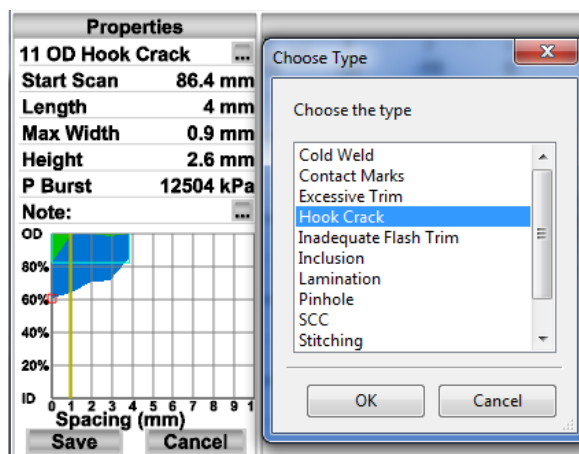


Figure 4-23

Manual classification can be done by using the "Choose type" list box from the Properties panel when editing the feature, Figure 4-23.

A module for calculation of severity using the Ln-Sec Method equation from KAPA was implemented. The burst pressure "P Burst" is calculated using the SMYS, CVN and safety factor values from the "Pipe Parameters Editor" dialog, Figure 4-24. Every time any of the values in this dialog is modified, the software re-calculates the burst pressure for all the features.

Property	Value	Metric Units	Value	Imperial Units
Line Name				
Diameter	114.3	mm	4.5	inches
Depth Start	-2	mm	-0.079	inches
Wall Thickness	5.588	mm	0.22	inches
SMYS	414375	kPa	60100	psi
CVN	33.9	J	25.003	ft*lb
Safety Factor	0.72			
Comments				

Set Diameter from NPS Save

Figure 4-24

Design and develop a module for on-site reporting for Implementation of field application software.

The reporting process starts with choosing the sections to include in the report, Figure 4-25. The module allows the generation of the report in different formats: from a simple field report with a table with the screenshots of the features, to a final report with all the information about the project, the settings, etc.

Choose which sections you want to include...

- ☒ Front Page
- ☒ Job Page
- ☒ IWEX Setting Pages
- ☒ Project and Line Information Page
- ☒ Auto Detect Parameters
- ☒ ILI Data Information
- ☒ Profile Box List
- ☒ Properties
- ☐ Horizontal Slice View
- ☒ Vertical Slice View

< Back Finish Cancel

Figure 4-25

ILI_Data_ID	Dig_Number	Item #	Anomaly Type	US Weld #	Max Depth (%)	Max Depth (mm)	Length (mm)	Width (mm)	Orientation (HH:MM)	Dist US Weld (mm)	Internal/ External	Comments
<div> <input type="button" value="Add"/> <input type="button" value="Edit"/> <input type="button" value="Delete"/> </div>												

ILI_Data_ID New

Parameter	Value
Dig_Number	
Item	
Anomaly_Type_CL	
Internal_External_CL	
Feature_Description	
Ovality	
Axial_Ovality	
Absolute_Odometer(m)	0.00
Milepost	
Max_Depth_Pct	
Max_Depth_Measured(mm)	0.000
Average_Depth(mm)	0.000
Length(mm)	0.00
Width(mm)	0.00
Orientation(hh:mm)	0000
US_Weld_Distance(m)	0.00
DS_Weld_Distance(m)	0.00
US_Weld_Number	
DS_Weld_Number	
US_Weld_Odometer(m)	0.00
DS_Weld_Odometer(m)	0.00
Seam_Orientation(hh:mm)	0000
MAPL_ID	
Joint_Length(m)	0.00
Outside_Diameter(in)	
Measured_Wall_Thickness(mm)	0.000
Nominal_Wall_Thickness(mm)	0.000
Latitude	
Longitude	
Pipe_Depth(m)	0.00
Comments	

ILI_Data_ID New

Parameter	Value
Dig_Number	
Item	
Anomaly_Type_CL	
Internal_External_CL	
Feature_Description	
Ovality	
Axial_Ovality	
Absolute_Odometer(ft)	0.00
Milepost	
Max_Depth_Pct	
Max_Depth_Measured(in)	0.000
Average_Depth(in)	0.000
Length(in)	0.00
Width(in)	0.00
Orientation(hh:mm)	0000
US_Weld_Distance(ft)	0.00
DS_Weld_Distance(ft)	0.00
US_Weld_Number	
DS_Weld_Number	
US_Weld_Odometer(ft)	0.00
DS_Weld_Odometer(ft)	0.00
Seam_Orientation(hh:mm)	0000
MAPL_ID	
Joint_Length(ft)	0.00
Outside_Diameter(in)	
Measured_Wall_Thickness(in)	0.000
Nominal_Wall_Thickness(in)	0.000
Latitude	
Longitude	
Pipe_Depth(ft)	0.00
Comments	

April 2018

Develop module modifications for Automatic and Manual Detection of features using Immersion Data

Due to the position of the OD IWEX signal above the OD line and the possible variation in thickness, adjustments were made to the algorithms to re-position correctly the features on the cross-section view. The features are now linked to the data file and they take in account the offsets variations.

Testing of Automated Sizing and Report Features

Testing of the Automated sizing showed consistency in finding features. It is possible to tune the threshold level of the algorithms to catch low image amplitude signals, and the interaction rules such as axial distance, circular distance and depth distance between indications to combine small indications in one feature.

Axial or longitudinal length sizing is very accurate and it depends upon the above tuning parameters.

Errors in height sizing still depend strongly on the quality of the scan: image amplitude, signal to noise ratio, focusing and alignment of the modes are factors that influence the analysis of the data.

Automated sizing, especially for crack profile sizing, can reduce the sizing time up to 80%.

Conclusions

UT images are generated as IWEX data files in binary format by means of the "*IWEX for Seamweld Inspections*" software. When the UT image contains only a few indications the "Seamweld Inspection" software can be used by the inspecting technician to evaluate the data and produce a report with an acceptable evaluation and in reasonable time. When sizing a single indication frame by frame or when the number of indications is not a just few but tens or even hundreds of indications, analyzing the data can become overwhelming producing interpretation errors, in addition the time spent on producing a report can increase proportionally.

The IWEX Processor is a tool to evaluate the IWEX data files and was developed to improve the performance and reduce errors during analysis and reporting. Detection, sizing, and characterization (including burst pressure calculation when pertinent) of the indications can be done with the assistance of automatic detection algorithms that can improve the accuracy of evaluation and reduce the reporting time by up to 80% (i.e. days rather than weeks for large numbers of features and/or hours rather than days for normal smaller datasets).

SECTION 5

DEVELOPMENT OF AN INVERSION ALGORITHM

Develop Inversion scheme

An iterative full-wavefield inversion scheme was developed. This scheme is based on approaches used in the fields of seismic imaging and medical imaging. Those media are often described by acoustical wave propagation, while an elastic model is more appropriate for NDT to naturally include longitudinal waves, shear waves, and their conversion at interfaces. Also, medical and seismic media have relatively small differences in material properties compared to NDT. The approaches typically used for inversion are robust in the presence of these small variations.

An inversion algorithm comprises a forward model that describes the propagation of sound and predicts the measurement for a given medium, as well as an update algorithm that adjusts the medium parameters such that the computed transducer recordings agree with the measured transducer recordings. In the iterative scheme that is currently under study, the forward model is necessarily based on an integral equation approach (rather than on a finite difference or finite element approach).

The following steps have been taken in the development of the algorithm:

- Derivation of the modeling functions for the two-dimensional elastic wave equation.
- Implementation of the two-dimensional elastic wave equation for forward modeling in Matlab.
- A preliminary study of a numerical method to include an ID reflection that mimics a steel-air interface. Whereas such a transition is standard for NDT, it is difficult to include in the modeling method due to the significant differences between the two media.

Figure 5-1 below presents preliminary results of the forward simulation algorithm. The sample under study is a metal plate. The reflection at the back-wall of this plate is simulated. Although this seems a trivial example, the integral equation in the inversion approach is prone to have difficulties with strong reflections. A numerical method was introduced to simulate this strong reflection. It can be seen that this method works well up-to angles of 30 degrees from the normal. This is sufficient for relevant pipe samples that will be studied.

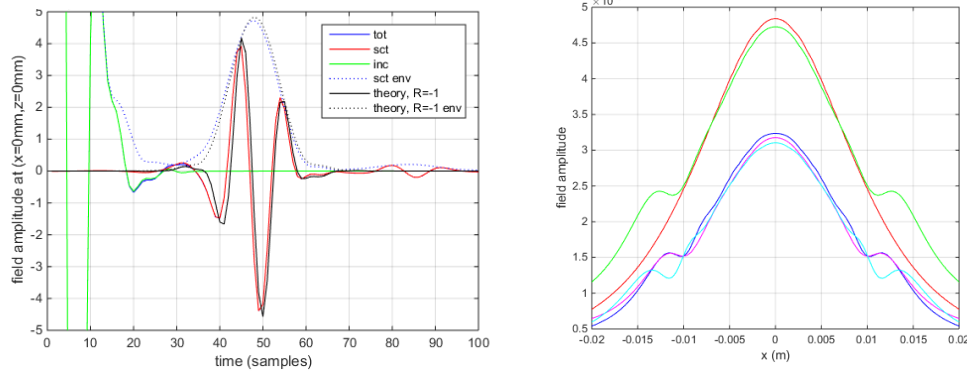


Figure 5-1, Preliminary results of the forward modeling algorithm based on an integral equation approach. The studied medium is a uniform metal plate. An ultrasound source is placed on the middle of the top of the plate. (Left) Modeled ultrasonic response of the plate at the same position as the source. Red curve is the simulation result. Black curve is the theoretical response. (Right) Modeled ultrasonic response at various positions at the top of the plate. Green curve is obtained with the proposed approach with the numerical method to mimic a back-wall included. Red curve is an analytical approximation of the back-wall reflection. Other curves are various tests of the method.

Depth sizing of stress corrosion cracks and crack families is difficult with current ultrasonic inspection techniques because cracks may obscure each other even when using reflections off the ID pipe surface. Based on a full-matrix-capture (FMC) recording of an ultrasound array transducer, the crack families may be reconstructed using a full wave-field inversion scheme that includes multiple scattering (multiple reflections off cracks in addition to the ID and OD pipe surfaces). For seismic and medical imaging applications, inversion can use the simplified model of acoustic media (longitudinal sound waves only). Also, these media have a low contrast, i.e., relatively small differences between the acoustic properties of the different materials. For non-destructive testing, it is necessary to model wave propagation in elastic media, thereby including longitudinal waves, shear waves, and their conversion at interfaces.

We have developed and programmed an iterative full wave-field inversion scheme for two-dimensional elastic media. Although inversion is a technique used in Geophysics and has been used on Seismic (or subsonic) data, to the best of our knowledge, this is the first inversion scheme of this kind for use in NDE to produce ultrasonic images using full waveform elastic data.

The scheme was tested on a numerical example that comprises a slit with a height of 4 mm and a width of 0.4 mm and with acoustic properties that are quite similar to that of steel, such that the acoustic contrast remains relatively small. The virtual transducers have been positioned above the slit and use longitudinal waves with a center frequency of 2.5 MHz. Because a full inversion scheme is applied, the resolution of the resulting image is not limited by the

wavelength in the medium. A reflecting surface representing the inner pipe wall has been added. Results showed a good reconstruction of the slit and the reflecting surface (see Figure 5-2), although there are some artefacts visible at the reflecting surface below the slit.

It remains to be tested how the inversion scheme will respond to ultrasonically open cracks that are filled with air (i.e., high contrast). Furthermore, the current scheme does not include transmission through the OD nor reflections at the OD surface. The modeling of the transducers needs to be adapted to take directivity into account. The cause of the artifacts which are visible in Fig. 1 needs to be investigated. These issues need to be addressed with numerical modeling studies before the scheme can be tested with measurements.

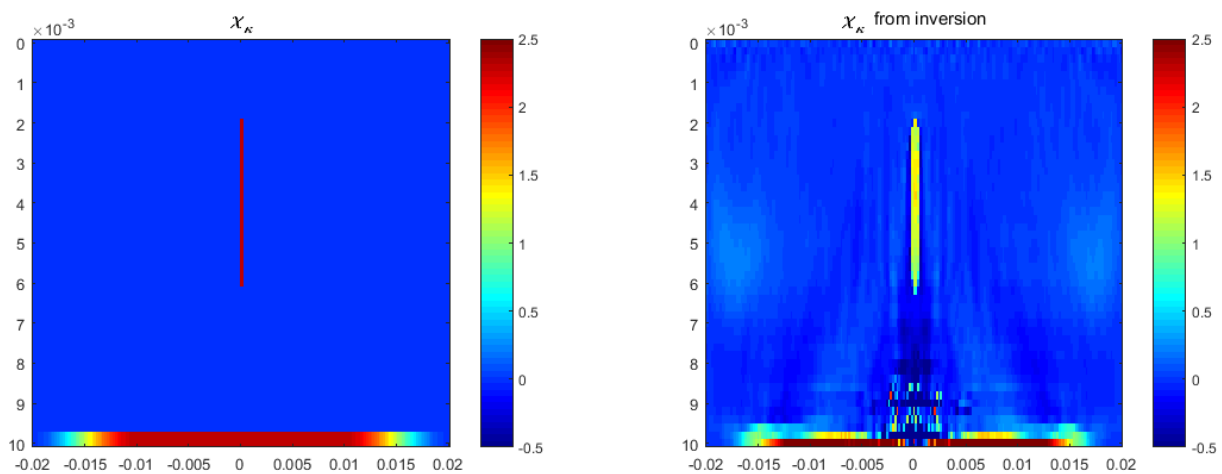


Figure 5-2. (Color figure) Example of a numerical result of the inversion algorithm. The input is the medium depicted on the left image. The modelled window is 40 x 10 mm with a 4 mm high and 0.4 mm wide and slit. The slit and back-wall are of a material with longitudinal-wave sound velocity of 4000 m/s, shear-wave sound velocity of 2185 m/s, and density of 5277 kg/m³, which is different from an actual crack.

For this second test, the following improvements have been made to the inversion scheme:

- The linear array ultrasound probe consists of small transducer elements, which each have a very large beam spread. In the previous implementation, the width of the elements was neglected resulting in a perfectly omnidirectional beam. We have implemented the actual beam spread of the transducer elements, by including the width of the elements in the algorithm. We found that directivity is not a very strong effect in our case. This can be understood from the fact that the width of the transducer elements is smaller than the wavelengths of the data.
- Regularization of the inversion has been extended, solving the problem of noisy images in poorly illuminated regions. This new regularization has significantly improved the algorithm over the first test. First, because the new regularization has removed the

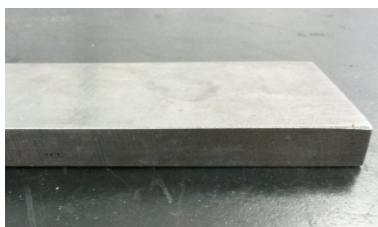
artifacts that were visible on the synthetic inversion results reported previously. Second, because the new regularization has enabled us to reduce the number of sources and frequencies. With this regularization, the algorithm may use fewer computations to achieve the same image quality. The possibility to reduce computation time and memory has been studied, as is described hereafter.

- The computation time and the memory usage of the algorithm scale with the size of the region to be reconstructed, with the amount of sources that is used in the algorithm, and with the amount of frequencies that is used in the algorithm. It has been studied if the number of sources and frequencies could be reduced without affecting the quality of the image. It was found that the number of sources and frequencies could be halved. This yields a significant speed-up in run-time and a factor four reduction of the required computer memory. Memory is a bottleneck for the size of the region to be reconstructed, so this result allows the method to be used for pipes with a larger wall-thickness. Or alternatively, it allows inspecting the same pipe with a higher ultrasound frequency.

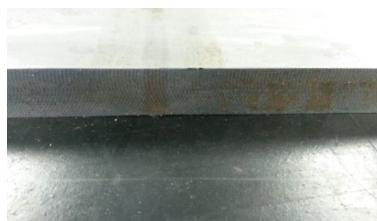
Validation of the inversion method

There are two paths that are followed to validate the inversion algorithm. First is to validate the inversion algorithm with the finite element method (FEM) which is known to simulate open cracks well. This provides a well-defined numerical experiment to assess how the inversion algorithm responds to the strong reflections of open cracks. Second is to validate the inversion with measurements of well-defined samples that have fabricated cracks.

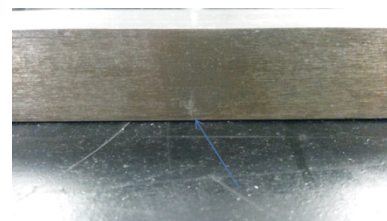
Three samples with well-defined structures have been selected and full-matrix-captures (FMC) have been recorded (Figure 5-3). FMCs have been recorded with probe frequencies of 2 MHz, 4 MHz, and 10 MHz. Additionally, IWEX images have been made using this FMC datasets.



Thickness 10.1 mm, three boreholes with 0.5 mm diameter, separated 1 and 1.5 mm.



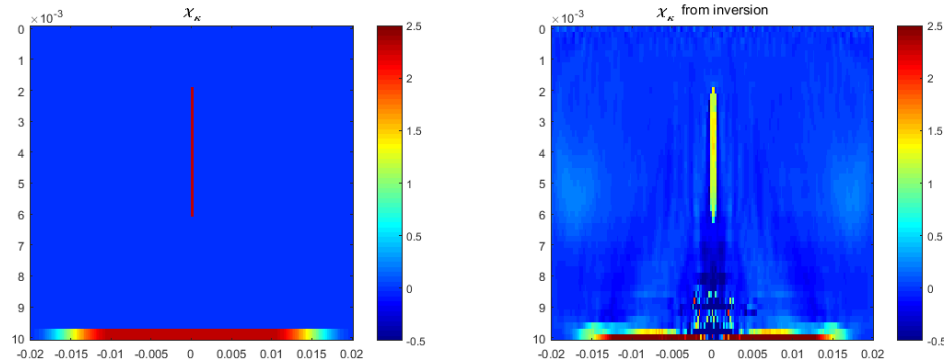
Thickness 19.0 mm, crack at top surface and also a welding defect.



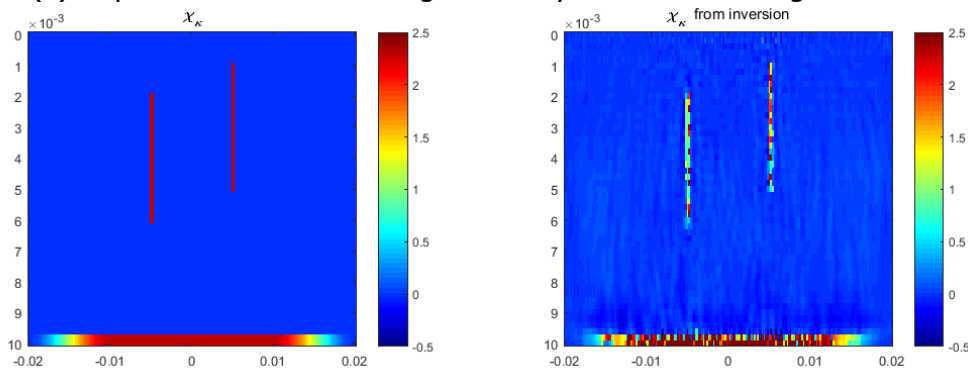
Thickness 25.4 mm, fatigue crack at bottom surface.

Figure 5-3. (Color figure) Samples to test the inversion algorithm.

(a) Previous results, (figure 5-2)



(b) Improved method including directivity and extended regularization



(c) Improved method and reduced number of sources and frequencies

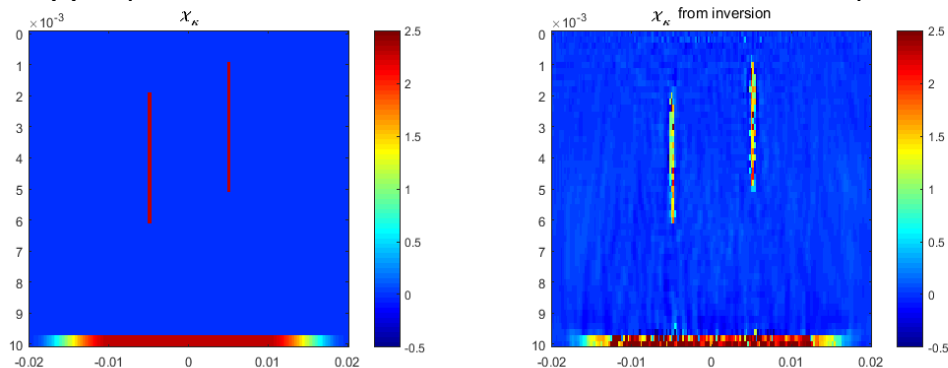


Figure 5-4. (Color figure) Example of a numerical result of the inversion algorithm. The input is the medium depicted on the left images. The modeled window is 40 x 10 mm with a 4 mm high and 0.4 mm wide slits. The slit and back-wall are of a material with longitudinal-wave sound velocity of 4000 m/s, shear-wave sound velocity of 2185 m/s, and density of 5277 kg/m³. The transducer has a center frequency of 2.5 MHz. (a) Results of earlier modeling (Figure 5-2). (b) Improved inversion method including transducer directivity and extended regularization. Data modelled with 19 sources and 41 receivers along the top of the model, using 14 frequencies. (c) Improved method, modelled with only 10 sources, 41 receivers, and 7 frequencies.

Development of a finite-element method to model free-surfaces and cracks

So far, we successfully tested the current inversion scheme with synthetically generated data. The examples considered, however, do not replicate realistic scenarios in that:

- material crack defects are transparent to wave propagation, and
- reflections at the pipe surfaces were not included in the model.

In order to further validate the inversion scheme, we developed a modeling tool based on the standard finite-element method (FEM). The advantage of FEM over other popular methods, such as finite-differences, is in the treatment of the boundary conditions necessary to model void regions. Indeed, FEM is able to account for void-filled cracks and free-surfaces very handily.

Validation of the inversion scheme with FEM-generated data

A first synthetic example scheme with crack defects (Figure 5-5) is considered, to validate the inversion. Here, the front-wall (outer pipe surface) is not present and the back-wall (inner pipe surface) is simulated with a thin layer of hard material (hence, it does not correspond to a free-surface). We are assuming the knowledge of position and contrast size of the back-wall. The synthetic data has been generated using the FEM code. The result depicted in Figure 5 shows that the inversion scheme is rather successful, even in this difficult scenario.

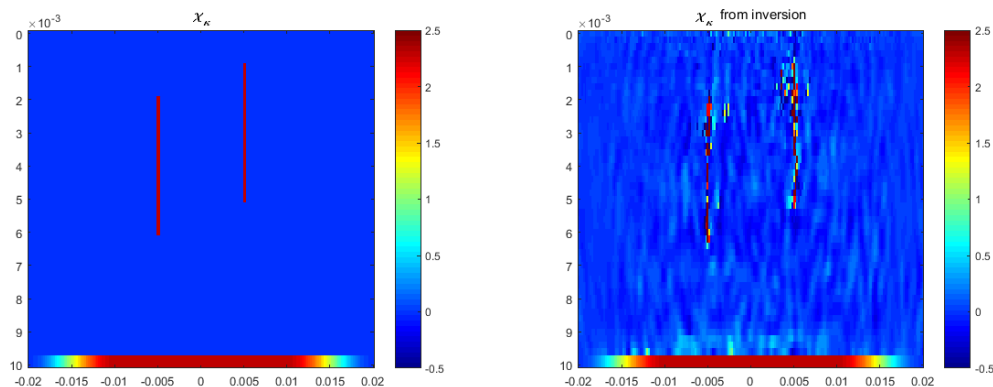


Figure 5-5: Inversion result with a model with void-filled cracks and known back-wall (note that, in the previous results, the cracks were transparent to wave propagation). The contrast values are cropped, for ease of display, and they correspond to infinity inside the crack.

With the example in Figure 5 and many other experiments, we experienced that the prior knowledge of the front-wall and the back-wall is important for a successful inversion.

Implementation of front-wall and back-wall in the inversion scheme

The current inversion code is not able to benefit from the prior knowledge of front-wall and back-wall, meaning that, for field data, it will be forced to invert for material heterogeneities and boundary shapes all at once. As the experience matured so far suggests, this can be detrimental for the convergence of the scheme. Therefore, we have developed an analogous inversion algorithm that can handle arbitrary boundary shapes. Clearly, these shapes must be determined prior to the inversion, using alternative methods.

To demonstrate the effectiveness of the modified scheme, we propose the synthetic example in Figure 5-6. The settings for this experiment are nearly identical to those of Figure 5-5, except for the presence of a (known) free back-wall. As in the previous example, the cracks are filled with void. The result in Figure 5-6 validates the new inversion scheme. The much superior result in Figure 5-6 with respect to Figure 5-5 might be partially due to inverse crime, which consists in inverting data generated by the same FEM modeling subroutine used within the inversion algorithm.

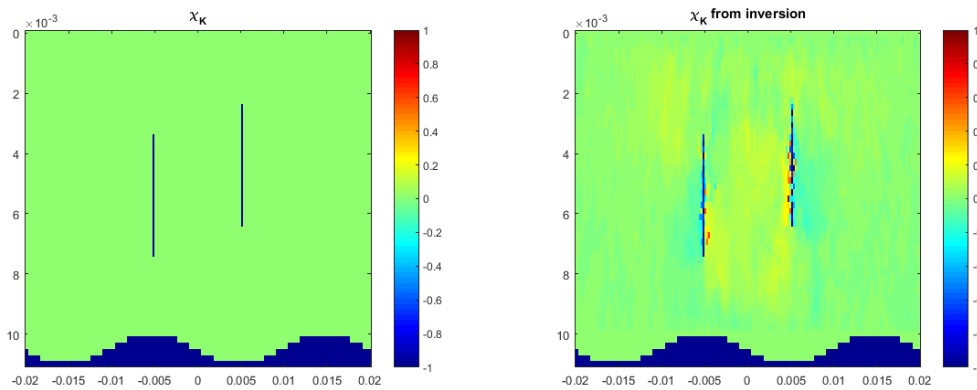


Figure 5-6: Inversion result for a crack model with known free back-wall. The contrasts shown here are relative to the bulk modulus K , rather than compressibility κ (as in Figure 5-5).

The next logical step is the study of the effect of the front-wall on the inversion result. The results for a model comprising front- and back-wall are depicted in Figure 5-7.

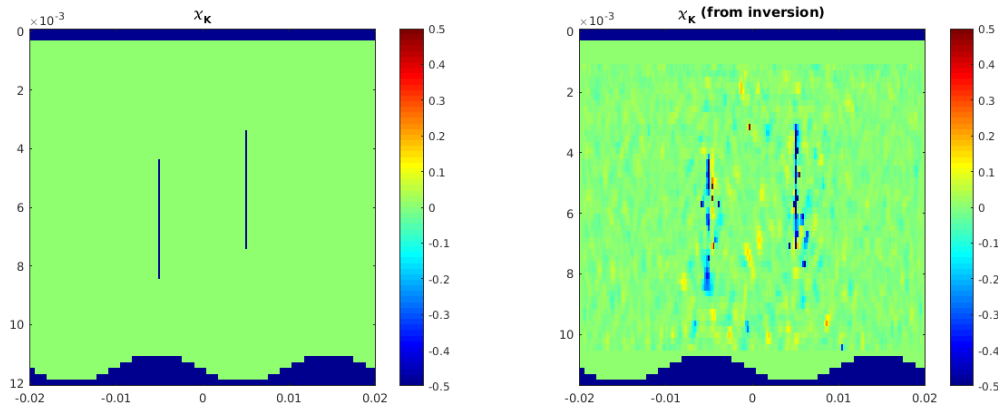


Figure 5-7: Inversion result for a crack model with known free front-wall and back-wall.

Other details of the original inversion scheme, such as sparse regularization, handling of the source mechanism and type of recorded data, need also to be adapted to the new scheme.

Progress in Ultrasonic Full Wave-field Inversion for UT inspection

Depth sizing of stress corrosion cracks and crack families is difficult with current ultrasonic inspection techniques because cracks may obscure each other even when using reflections off the ID pipe surface. Previously we developed an elastic two-dimensional full wave-field inversion scheme. To the best of our knowledge, this is the first inversion scheme of this kind. The scheme was significantly improved with a new mathematical formulation that made it robust to strong reflections (air-filled flaws as are common in NDT but absent in medical imaging or seismology). Reflections at OD and ID surfaces were explicitly included in the model. The scheme is detailed in Figure 5-8. This full wave-field inversion scheme was tested using a numerical simulation of the experiments and showed good agreement.

With this testing the focus has been on measured data. As a first step, the modelling of ultrasonic response of the OD and ID profiles was studied in detail (the box "Modelled ID and OD response" in Figure 5-8). However, significant disagreement was found which precludes correct convergence of the inversion algorithm. The observed differences between the simulated response and the measured response are now understood.

The ultrasonic response of a flat plate is measured with a 2 MHz transducer with 64 elements, a pitch of 0.85 mm, and an element width of 15 mm (in the scanning direction, perpendicular to the cross-sectional image). The test sample is depicted in Figure 5-9.

With these transducer elements (0.7 mm x 15 mm), it turns out that for shorter travel distances the measured data behaves similar to wavefields generated by infinitely long line-sources, whereas for longer travel distances the data behaves similar to wavefields generated by point-sources (see Figure 5-10). Line-sources (with infinite width) have an amplitude decay that scales as one over the square-root of the distance. In contrast, point sources have an amplitude decay that scales with one over the distance. Moreover, the phase of the ultrasonic signal is different for the two regimes. The inversion model assumes infinitely long line-sources which is only valid in the regime close to the transducer elements. The options to address this issue are: (1) adapt the forward modeling code to reflect this behavior or (2) correct the measured data to perfect line-source behavior. Both options are currently being investigated.

In addition, the measured data contains additional arrivals caused by internal reflections in the probe (see Figure 5-10). For inversion, this behavior of the probe will have to be mimicked.

After addressing the two issues listed above, we are ready to validate the full wave-field inversion scheme on measured data to show its capabilities. Results will be compared to IWEX imaging. Future improvements are necessary to accommodate for a real measurement setup and natural flaws, either with wedges or using an immersion technique. This would include OD and ID profiling, including the wedge or immersion response in the model, and studying regularization conditions for natural flaws.

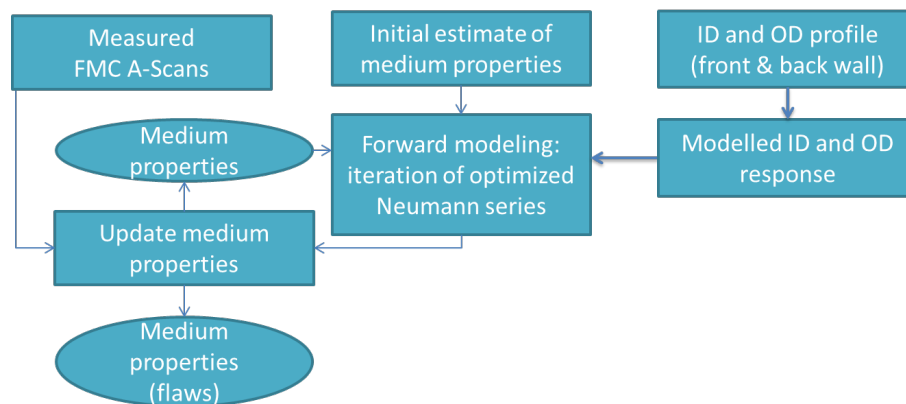


Figure 5-8. Full-Wavefield Inversion scheme. Upper three boxes are the inputs of the scheme: measured FMC A-Scans, an initial estimate of the medium (clean weld), and the profile of the ID and OD interfaces. The inversion scheme adjusts the estimate of the medium, i.e., by including flaws, until that the simulated ultrasonic response of this medium estimate agrees with the measured ultrasonic response. After convergence, this algorithm has found all details of the medium (i.e., an image depicting one or more flaws and the surfaces of the sample).

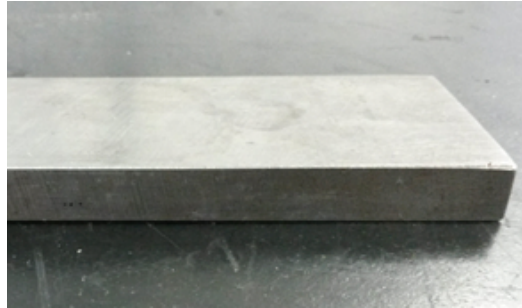


Figure 5-9. Test sample. Thickness 10.1 mm, three boreholes with 0.5 mm diameter, separated 1 and 1.5 mm.

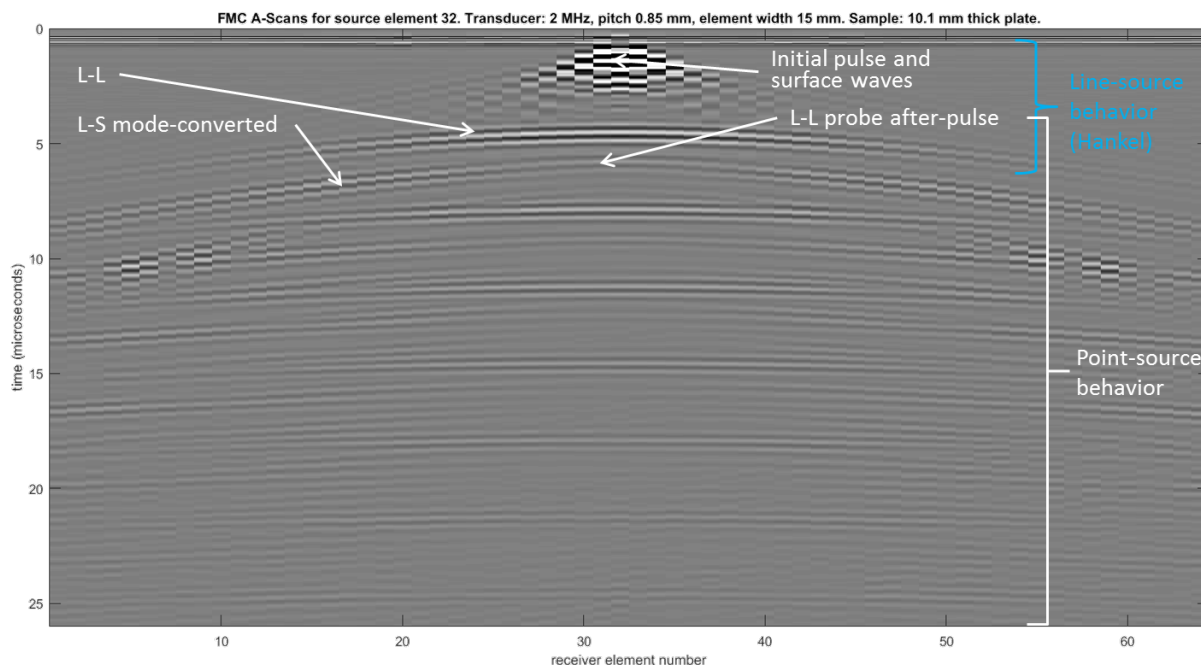


Figure 5-10. Test sample. Thickness 10.1 mm, three boreholes with 0.5 mm diameter, separated 1 and 1.5 mm.

Disagreement was found which precludes correct convergence of the inversion algorithm. The observed differences between the simulated response and the measured response are now solved or incorporated in the model.

Modelling of the source type

This first issue is the modelling of the source type. The modelling applied in the inversion process is truly 2D, assuming an infinitely long line-source. True 3D modelling of a finite length line-source is not practical in view of the computational effort. The measured data shows an amplitude decay that changes from a true line-source decay in the near-field, to point-source decay behavior in the far-field. A complicating factor is the fact that on theoretical grounds it can be stated that this decay behavior is different for compression (P) waves and shear (S)

waves. Although theoretically not entirely correct it was decided to design an approximate, time-domain scaling function, to turn the mixed decay measured data into true line-source data. The real data inversion carried out below is based on this approximation.

Ghost events in measured data

The second issue is the presence of spurious events in the measured data, which has been identified as a ghost echo response from the 2 MHz probe used for collecting the measurement data. This effect gave some delay in the inversion of the real data, because it was first believed that the modelling failed to produce an event that should be there. In addition, it looked like there was going to be compression (P) to shear (S) wave type conversion at normal incidence. It was decided to try to capture the ghost in the wavelet extraction and that way bring it into the modelling. It is to be expected that this kind of event can be avoided in the design of dedicated probes for use of Inversion algorithms in the field in the future.

Wavelet extraction and calibration of frequency components

The third issue is the source pulse. For inversion of measured data it is essential to know the strength and spectral shape of the outgoing pulse, for every source. Because the forward modelling is only carried out for a limited set of frequencies, extracting the wavelet from a match between measured and modelled data is an underdetermined problem. This can be solved by imposing a compactness criterion in the time domain. On this basis a time-domain wavelet can be extracted from a frequency domain match with relatively few (30) frequencies. Also causality can be imposed, if applicable. From the time-domain wavelet, sparse frequency domain calibration factors can be obtained. See Figure 5-11 for an example of wavelet extraction for the source pulse.

With the wavelet extraction process and the modelling of the source-type in place, the modelled data can be matched to the measured data. See Figure 5-12 for a single source record of the modelled data reflecting the measured data from the same source. The next step is the actual inversion of the measured data. This will be performed shortly.

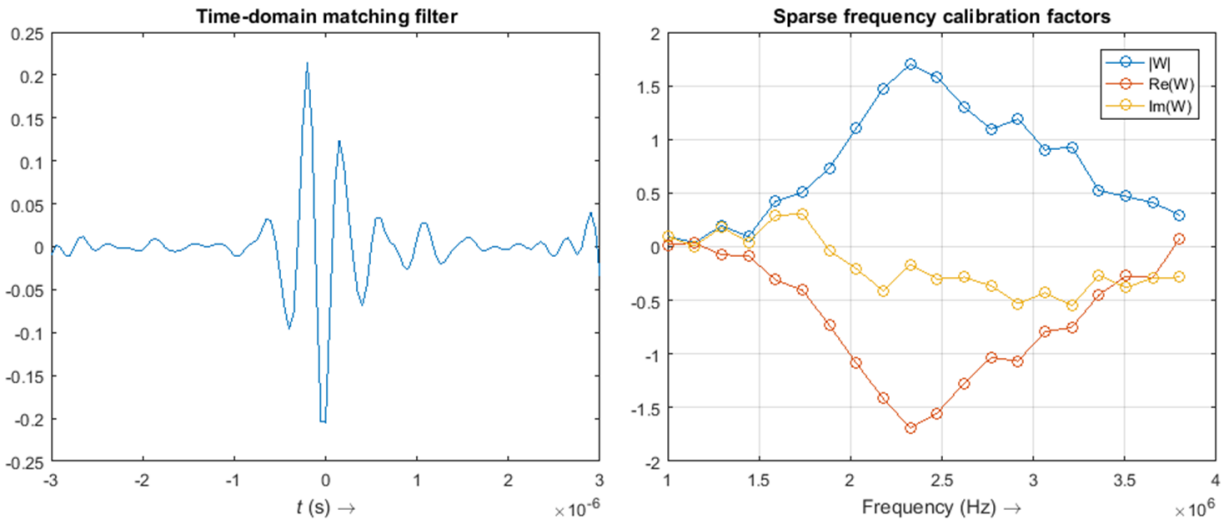


Figure 5-11: Source pulse extraction process. Compact, time-domain pulse, extracted from matching measured and modelled data (left), complex calibration factors for sparse frequencies (right)

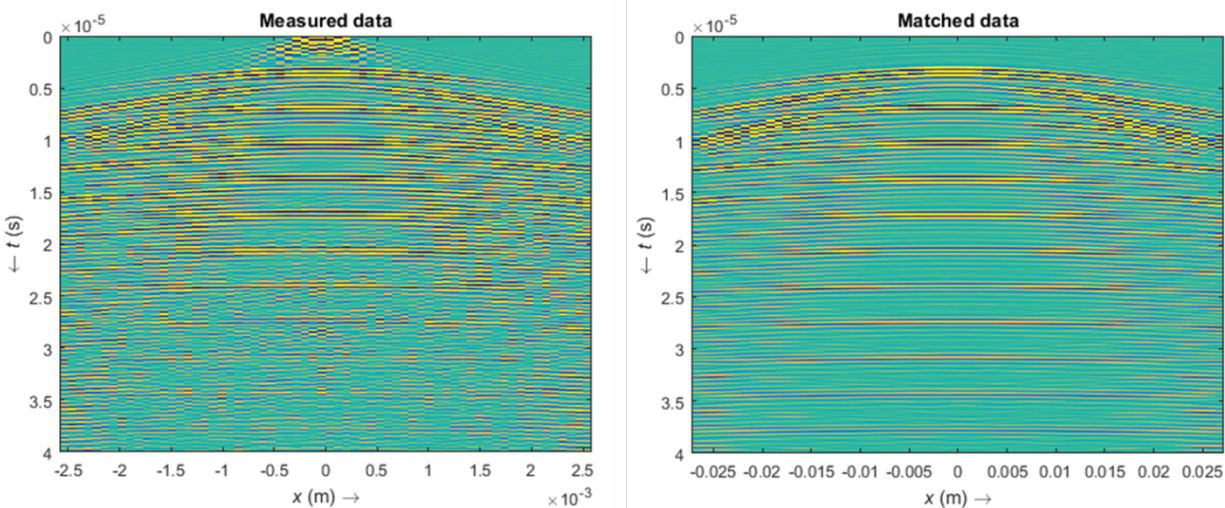


Figure 5-12: Single source record after time-variant scaling of measured data (left) and application of extracted wavelet to matching data (right).

Evaluate the performance of the inversion method and compare to IWEX images

Finalization of the inversion scheme

With the inversion scheme completed, there were three main obstacles to be overcome to finalize the inversion scheme:

- The source model has to be adapted to match the behavior of the linear array elements with finite extent in the passive direction, i.e., the scanning direction.

- Additional acoustical echoes caused by the array probe used for the experiments has to be taken into account in the data modeling;
- The source wavelet has to be extracted from the measured data to estimate the frequency content accurately.

After tackling these issues, the inversion was applied to measurements. The center frequency of the array probe was chosen to be 2 MHz. This frequency is relatively low for IWEX imaging, but sufficient for reconstruction using full wave field inversion. The application of the inversion scheme was successful.

Analysis of the inversion result and comparison of the inversion result to an IWEX image

Figure 5-13 present the images obtained from the experiment with a 2 MHz array probe placed on a flat steel block. In Fig. 5-13(a), a photograph of the side face of this block is shown. The array with an element spacing of 0.85 mm was positioned on top at the vertical position $z=0$ mm. The side-drilled holes in this block have a distance of 1.0 and 1.5 mm, respectively.

A typical IWEX image of this setup is shown in Fig. 5-13(b). A rectified representation of the image is chosen to simplify comparison to the inversion results. In the IWEX image, both the indications of the holes and the position of the lower surface of the steel block can be seen. The resolution is low due to the fact that longitudinal waves at a relatively low frequency are used for generating the IWEX image. The dominant wavelength is approximately 3 mm. Typically details with a size in the order of half the wavelength are resolved by imaging methods like IWEX.

Figure 5-13(e) shows a horizontal profile through the IWEX image at the depth of the holes, approximately at $z=7$ mm. It can be seen that the holes with 1.0 mm distance cannot be resolved, but the holes with a distance of 1.5 mm (half the wavelength) can be identified as separate indications.

The results of the inversion are based on the same measured dataset and reconstructed for exactly the same region of interest to enable a fair comparison. Fig. 5-13(c) presents the outcome after the first iteration of the inversion, while Fig. 5-13(d) presents the final result after five iterations. The horizontal profiles through the reconstructions are shown in Figs. 5-13(f) and (g), respectively. It can be seen that the inversion is able to resolve significantly more detail, such that all three holes can be identified.

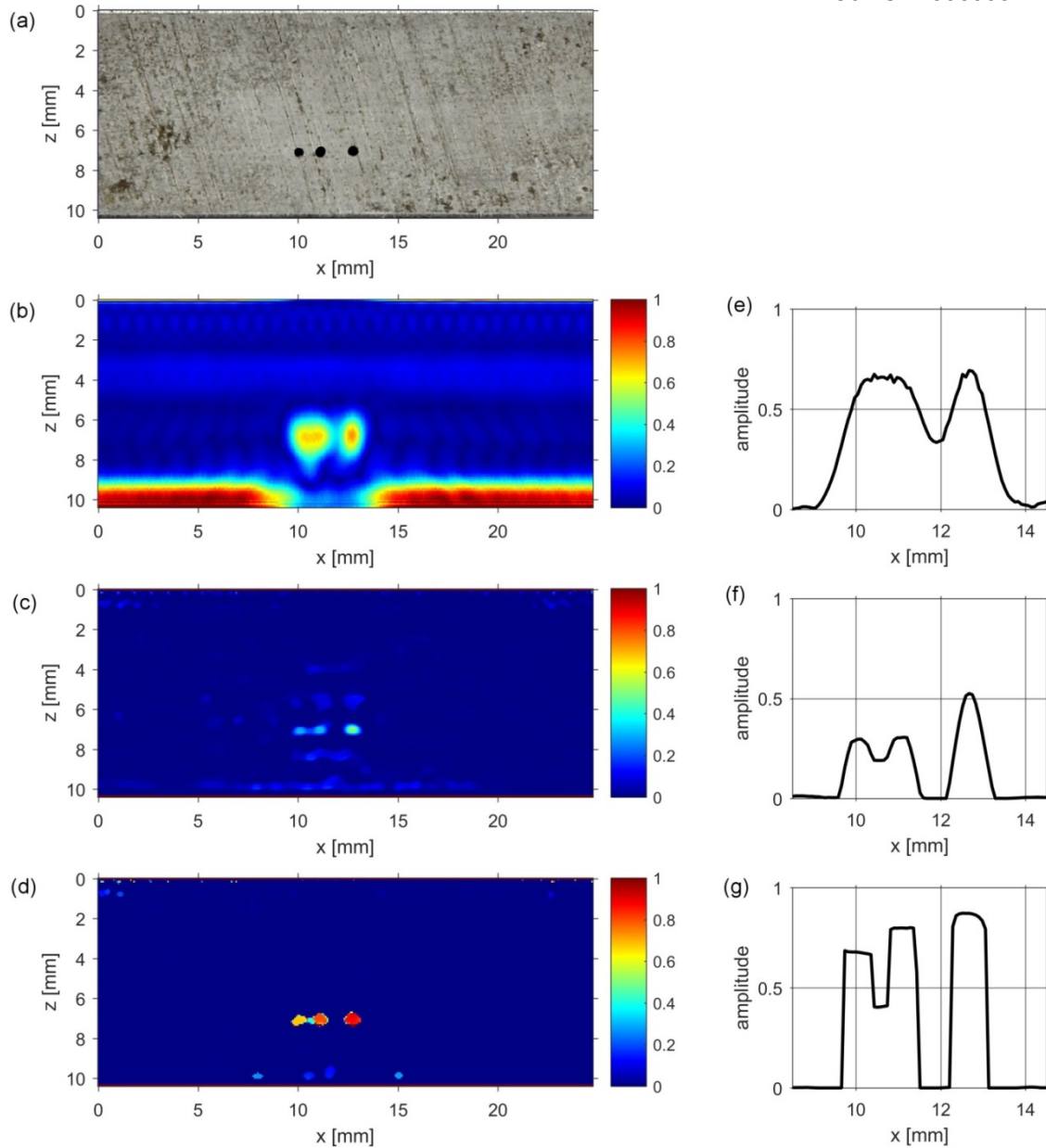


Figure 5-13: Comparison of inversion results to an IWEX image based on the same measurement.

(a) Photograph of the flat test block of 10 mm thickness showing three side-drilled holes with diameter 0.5mm, spacing 1.0 mm and 1.5 mm apart;

(b) IWEX image of the same region obtained from a measurement with an array probe with a nominal center frequency of 2 MHz.

(c) Reconstruction result after the first iteration of the inversion scheme.

(d) Reconstruction result after the fifth iteration of the inversion scheme.

(e), (f), (g) horizontal profiles through the reconstructions (b), (c), and (d) of the three holes at a depth of 7 mm.

The higher level of detail in the inversion result is because the inversion uses information from both longitudinal and shear arrivals contained in the data as well as their reflections from the upper and lower surface of the sample.

The difference between the first and fifth iteration of the inversion is characterized mainly by the contrast and clearness of the result. It should also be noted that the inversion produces indications of flaws with clearly defined boundaries. This trend is also because of the regularization used to stabilize the inversion. This regularization has a tendency to promote 'blocky' results with contiguous regions. This trend is observed in later iterations of the inversion, as can be seen by comparing the profiles in Figs. 13(f) and (g). In the final result shown in Fig. 13g), the highest amplitudes corresponding to the defect locations exhibit a nearly flat profile.

In contrast to this, the extent of the flaw in an IWEX image is usually estimated from a smooth transition between low and high amplitudes, or from smaller indications like tip diffractions related to the outer boundaries of the flaw. In general, this leaves more room for interpretation by the observer about the actual shape and extent of the flaw.

Conclusion from inversion development

This comparison concludes the research on full wave field inversion as a potential alternative to IWEX imaging in the framework of this project. The major problems in setting up an inversion scheme were identified and tackled. The resulting inversion scheme was applied to simulations and real measurements. A simple clearly-defined steel sample was used for experimental tests. Reconstructions, obtained using full wave-field inversion, were compared to an IWEX image based on the same dataset. It could be shown that the resolution obtained using inversion is significantly higher than for simple imaging – at the cost of using an iterative scheme with extensive computational effort.

However, although the current developments show the best results in terms of image quality the computation time is much too long and impractical for implementation in the field. Continued development will be needed for practical commercial use.

SECTION 6

DEVELOP IMMERSION PROBE ALGORITHMS FOR IMPROVED ALIGNMENT AND SIZING

Work on immersion probe algorithms started after it was realized that compensation for the poor fit of hard plastic wedges was not always possible for some pipe joints with out-of-roundness, where the out-of-roundness could either be on the outside (OD) or inside (ID) surfaces or both. The term immersion comes from immersing a sample in water tank to provide a path for the ultrasonic wave from the ultrasonic transducer array to the pipe to be inspected. The water in the immersion tank allows for the pipe to deviate from a perfect cylindrical shape. In the field immersion in a water tank is impractical, so water filled flexible wedges are used to conform to the pipe surface. In addition to the flexible wedge adaptive IWEX processing was needed to map the exact shape of the OD and ID surfaces. Thus the development of immersion probe algorithms is described by three different terms immersion, water wedge, and adaptive IWEX; although the three terms have specific meanings they are often used interchangeably. Tasks for development of immersion probe algorithms, currently called Adaptive IWEX, included the following:

- Immersion probe design
- Algorithm development
- Automated calibration and pipe surface detection
- Testing of automated calibration and pipe surface detection
- Full Matrix Capture (FMC) scanning of lab samples
- Development of software for viewing and interpreting immersion IWEX scan files
- Modification of the probe holder for water wedge measurement of seam welds
- Scanning of lab samples
- Improvements of adaptive IWEX algorithms based on the lab testing

Introduction

IWEX ultrasonic inspection of seam welds is usually done with two linear array transducers, with each mounted on a wedge that fits the pipe surface. However, with experience from this DOT project we have found that pipes are not always sufficiently cylindrical to assume a circular cross-section for IWEX imaging, in some cases the local pipe surface below the wedge does not match the wedge curvature. To overcome this issue, we investigated an immersion measurement setup and immersion imaging algorithm. The volume between the array transducers and the pipe surface is filled with water, e.g., by placing pipe coupon in a water tank. This may be thought of as an adjustable wedge which is made from water that perfectly fits any pipe surface. For usage in the field, solutions exist with a wedge-like water cushion

between the probe and the pipe. In an immersion measurement, it is necessary to extract the surface profiles of the outer diameter (OD) and inner diameter (ID) from the data before the IWEX imaging can be performed. Extracting the ID profile has the added benefit that geometry such as root reinforcement, misalignment, or poor trim, is taken into account and does not distort the IWEX images.

In the previous quarter of this project (Q12), we demonstrated that Immersion IWEX is a feasible method to inspect pipes with non-cylindrical surfaces. First versions of algorithms have been developed for the configuration calibration, extraction of the OD surface, extraction of the ID surface, and Immersion IWEX imaging based on the measured OD and ID profiles. The resulting Immersion IWEX images are better aligned than images obtained with wedge, which is extremely relevant to flaw characterization and sizing. We pioneered a configuration with two transducer arrays tilted with an angle of 20 degrees which predominantly generates shear-waves in the steel pipe, similar to conventional inspection with plastic wedges. This configuration shows much clearer indications than a configuration with a transducer array parallel to the pipe surface that is based on longitudinal waves.

Transducer design (1): frequency, pitch, inter-element spacing

Transducer arrays for immersion measurements have different requirements than transducers for measurements with plastic wedges. It is not only necessary to image the weld area but also to profile the OD. Moreover, the sound velocity of water is nearly two times slower compared to plastic hence the wavelength in water is also shorter.

Theory

The following parameters are considered: the center frequency f of the transducer elements, the pitch p of the transducer array and the inter-element spacing i between the transducer elements. The size of the elements $a = p - i$. The aperture of a 64-element transducer array $A \approx 64 \cdot p$.

Frequency	The center frequency determines the wavelength of the ultrasound in the steel and in the water. A high frequency provides a high resolution in the direction of the beam. However, for similar performance a high frequency requires a smaller pitch hence a smaller array aperture which causes a lower resolution in the direction normal to the beam path.
Pitch	The pitch should be sufficiently small to avoid significant aliasing. However, the aperture of the array also scales with the pitch hence a too small pitch causes a lower image resolution in the direction normal to the beam path.
Inter-element spacing	The inter-element spacing determines the size of the transducer elements. Small elements have large beam spread while larger elements have a narrower beam spread.

Directivity of transducer elements

For ultrasonic imaging, it is necessary that the beam width of the individual elements of the transducer array is sufficiently large to cover the weld area. The radiation pattern of the elements is given by

$$P(\theta) = \text{sinc}[a/\lambda \sin(\theta)],$$

with radiation direction θ , element size a , and $\text{sinc}(t) = \sin(\pi t)/\pi t$ for $t \neq 0$. The radiation patterns of several transducers and the corresponding -6 dB beam widths are plotted in Figure 6-1 (top-right).

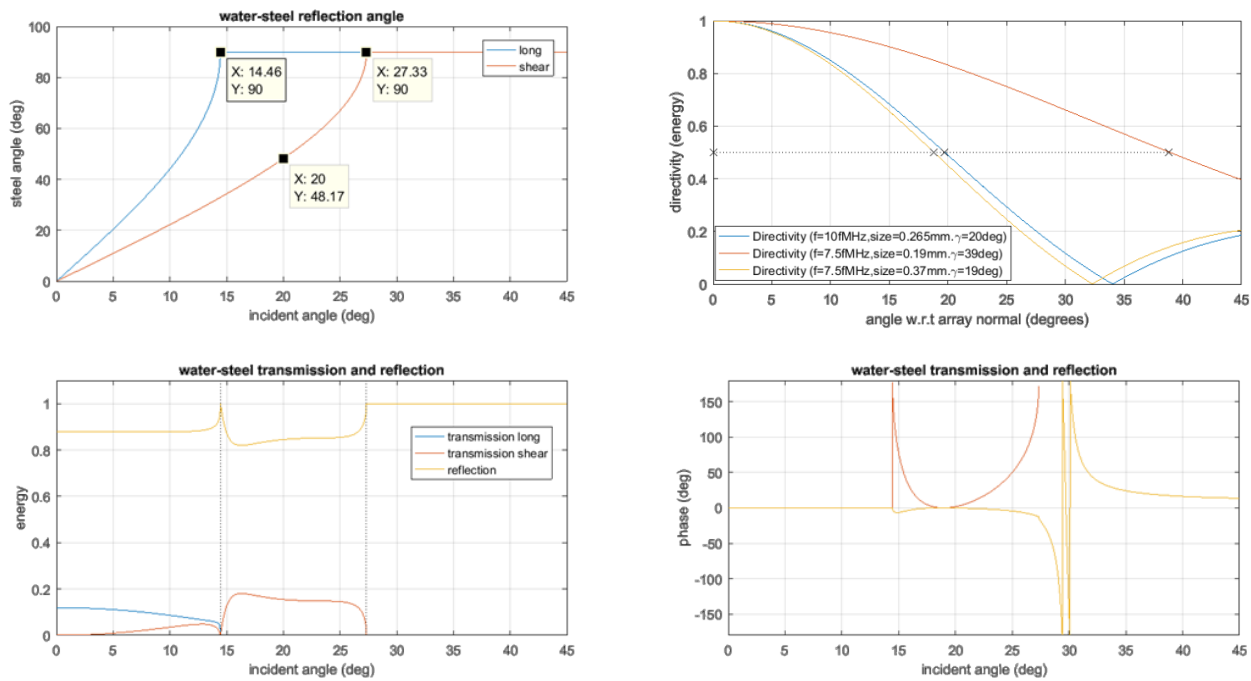


Figure 6-1 Physics plots for the design of the array transducer.

Aliasing

Aliasing is an effect that occurs due to the spatial undersampling of the ultrasonic wavefield with the discrete number of transducer elements. To avoid aliasing, it is necessary to choose the pitch p of the array no larger than the Nyquist pitch

$$p_{\text{Nyquist}} = c_{\text{water}} / (2 \sin(\theta_{\text{max}}) f_{\text{max}}) = \lambda_{\text{min}} / (2 \sin(\theta_{\text{max}})),$$

with water sound velocity c_{water} , maximum incident angle θ_{max} , maximum frequency f_{max} , and minimal wavelength $\lambda_{\text{min}} = c_{\text{water}}/f_{\text{max}}$. The maximum incident angle is the maximum angle under which plane waves arrive at the transducer array or are emitted from the transducer array. For

phased arrays, this is typically the steering angle. For IWEX, θ_{max} includes all angles that are used to generate the digital focus in the weld.

Aliasing may be avoided by either

- 1) choosing the pitch p sufficiently small,
- 2) ensuring that no ultrasound waves arrive under an angle larger than θ_{max} ,
- 3) ensuring that ultrasound waves that arrive under an angle larger than θ_{max} have different arrival times than the arrival times that correspond to the weld image, or
- 4) choosing large array elements such that beam angles above θ_{max} are not measured by the elements.

In conventional phased array applications with a plastic wedge and 30 – 70 degrees shear-wave angles in steel with a wedge of 37 degrees, a pitch of 1.0λ gives typically good results.

Filtering of aliasing using the transducer element directivity

The maximum allowed angle to avoid aliasing, θ_{max} , for a given pitch p and wavelength λ , is given by

$$\sin(\theta_{max}) = \lambda / 2p.$$

Reducing aliasing by choosing large array elements that have the -6 dB point of the radiation pattern at this angle, i.e., $P(\theta) = 0.5$, gives $\sin(\theta) = 0.6 \cdot \lambda/a$. Combining this with the equation above gives $a > 1.2 p$ which is not possible as the element size cannot exceed the pitch.

Simulations to assess the cause of the aliasing

Ray-trace simulations were used to study the cause of the aliasing. The test case that was studied was a 7.5 MHz transducer, 128 elements, pitch 0.5 mm, element size 0.19 mm. The radiation pattern of the transducer elements was computed at the center frequency. The test sample was a 10.1 mm thick plate and transducers are placed under an angle of 20 degrees.

The following reflections contributing to the aliasing were studied:

- OD reflection (longitudinal waves).
- ID reflection (longitudinal- and shear-waves).
- Reflection of a flat reflector at twice the wall-thickness (2*WT). This simulates the OD reflection over skip, i.e., transducer → transmission through OD → skip at ID → reflection at OD (longitudinal- and shear-waves).
- Reflection of a flat reflector at three times the wall thickness (3*WT, longitudinal- and shear-waves)
- Reflection of a flat reflector at four times the wall thickness (4*WT, longitudinal- and shear-waves)

In Figure 6-2, the influence of the various reflections on the aliasing is shown. The Nyquist pitch for this setup is 0.1 mm while the pitch of the simulated transducer array is 0.5 mm. It may be seen that aliasing is non-trivial and that different reflections contribute to different areas in the weld IWEX image.

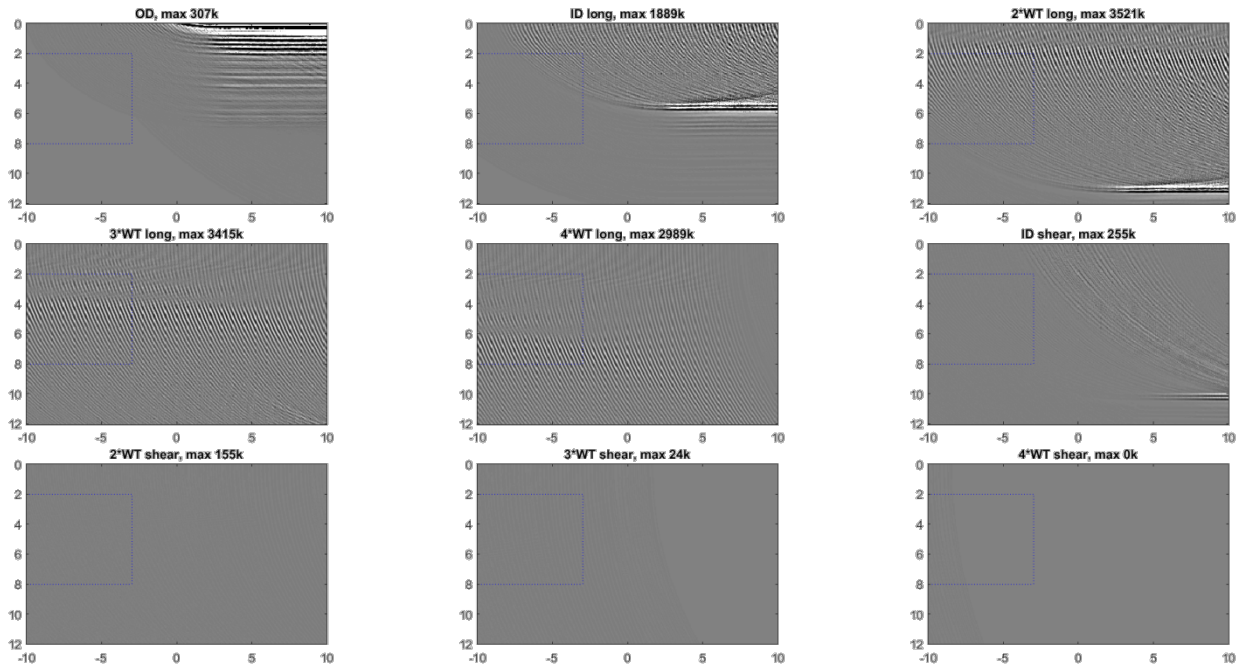


Figure 6-2, Numerical simulations of IWEX images of a clean plate, wall-thickness 10.1 mm. IWEX-OR mode. OD and ID reflections are taken into account. These reflections result in aliasing as the simulated pitch is larger than the Nyquist pitch. Note that the color-axis of the images is chosen very narrow such that the adverse aliasing effect is well visible.

Experiments: frequency, pitch

As the theoretical predication of the effect of aliasing and defect resolution in the image is difficult, the probes have mainly been designed based on experiments. IWEX immersion experiments have been performed with two probes that are placed under an angle of ~ 20 degrees with a flat surface and with a vertical index of ~ 15 mm.

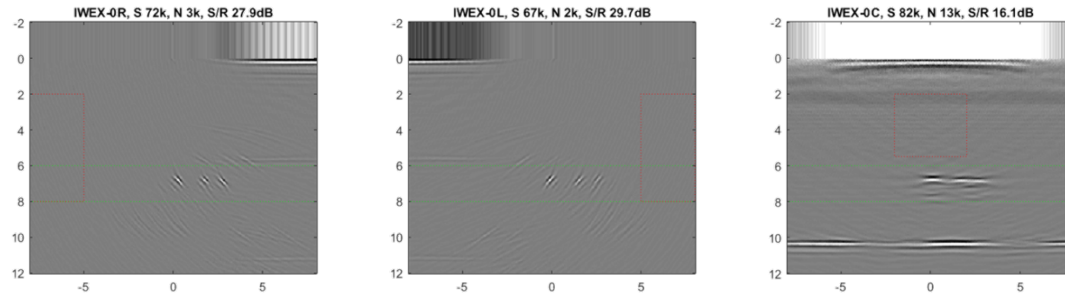
Figure 6-3 compares the results of 7.5 MHz transducers with 10 MHz transducers. The array aperture, beam directivity (scale with a/λ) and relative pitch (p/λ) are equal for both configurations. It may be seen that although the resolution in the direction of the beam is slightly higher, the detectability of these 0.5 mm boreholes is not significantly influenced when

using a lower frequency. Therefore, it was chosen to use a frequency of 7.5 MHz as that allows for a larger pitch and hence a larger aperture when 64 elements are used.

Figure 6-4 compares two 7.5 MHz transducers, one with a pitch of 0.25 mm and one with a pitch of 0.43 mm. The transducers also have different element sizes hence different beam-widths. The number of active elements is chosen such that the probes have similar aperture. The transducers with a pitch of 0.43 mm caused aliasing that is more pronounced visible than the transducers with a pitch of 0.25 mm. However, the amplitude of the aliasing noise was not always significantly weaker for the arrays with a pitch of 0.25 mm (see the IWEX-0L image). As will be shown hereafter, a pitch of 0.25 mm with 64 elements would cause the aperture to be too small.

Figure 6-5 compares IWEX images made with 7.5 MHz probes with pitch 0.43 mm where different apertures (number of elements) have been used. The following cases are depicted apertures 27.5 mm, 25.6 mm, and 22.4 mm, which correspond to transducers with 64 elements with pitches of 0.43, 0.4, and 0.35 mm, respectively. It may be seen that the indications in the IWEX-2L mode get a very poor resolution when 52 elements were used (52 elements have an aperture of 22.4 mm which is the same aperture as 64 elements with pitch 0.35 mm). The IWEX images generated with an aperture of 25.6 mm, corresponding to 64 elements with a pitch of 0.4 mm, showed a good resolution in the direction normal to the beam. The same results were seen for IWEX images of a 22-inch pipe with 8 mm wall-thickness, an ERW weld, significantly poor trim, and an OD notch (Figure 6-6). Therefore, it was chosen to use transducers with 64 elements and a pitch of 0.43 mm.

7.5 MHz, 0.43 mm pitch, 49 elts



10 MHz, 0.325 mm pitch, 64 elts

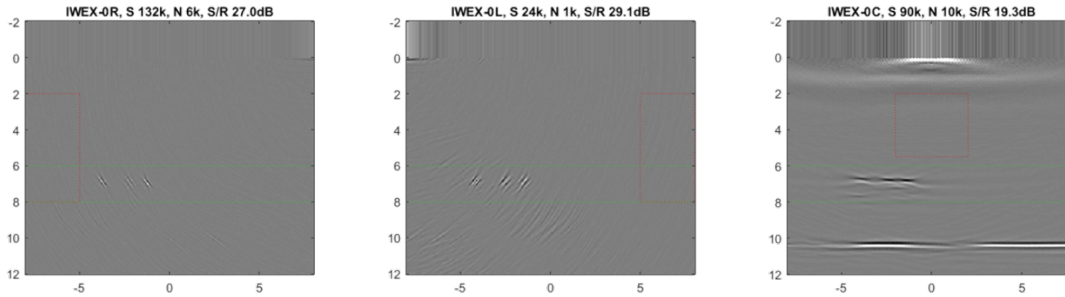
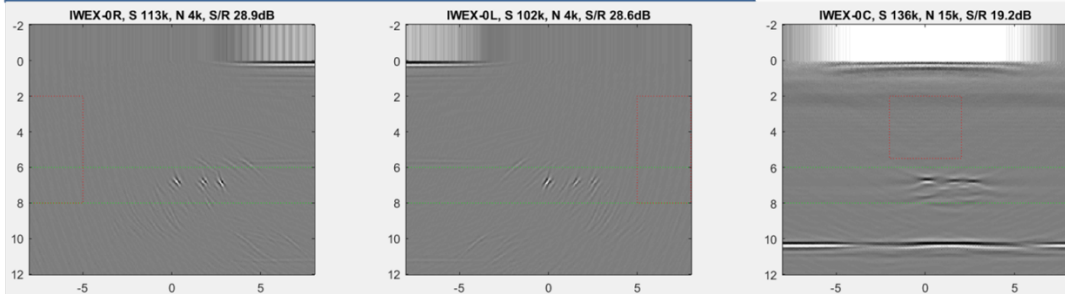


Figure 6-3, IWEX measurements of a 10.1 mm flat plate with three 0.5 mm boreholes. Upper and lower plots have a different frequency, the same p/λ ratio, the same element beam-width, and the same array aperture.

7.5 MHz, 0.43 mm pitch, 74 elts



7.5 MHz, 0.25 mm pitch, 128 elts

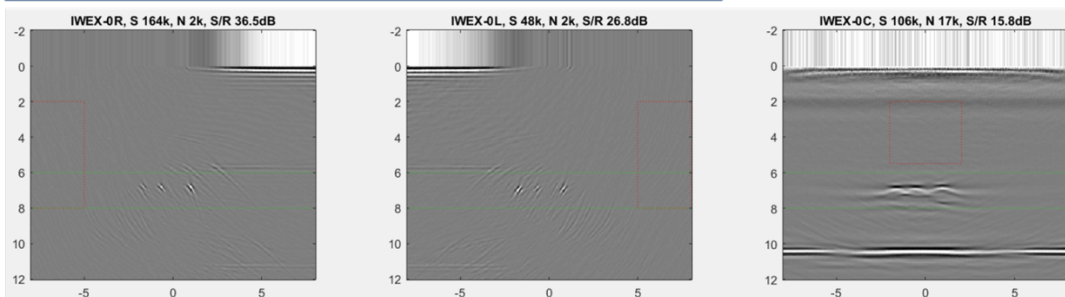


Figure 6-4, IWEX measurements of a 10.1 mm flat plate with three 0.5 mm boreholes. Upper and lower plots have a different pitch, different element sizes (hence different element beam-widths), the same frequency and the same aperture.

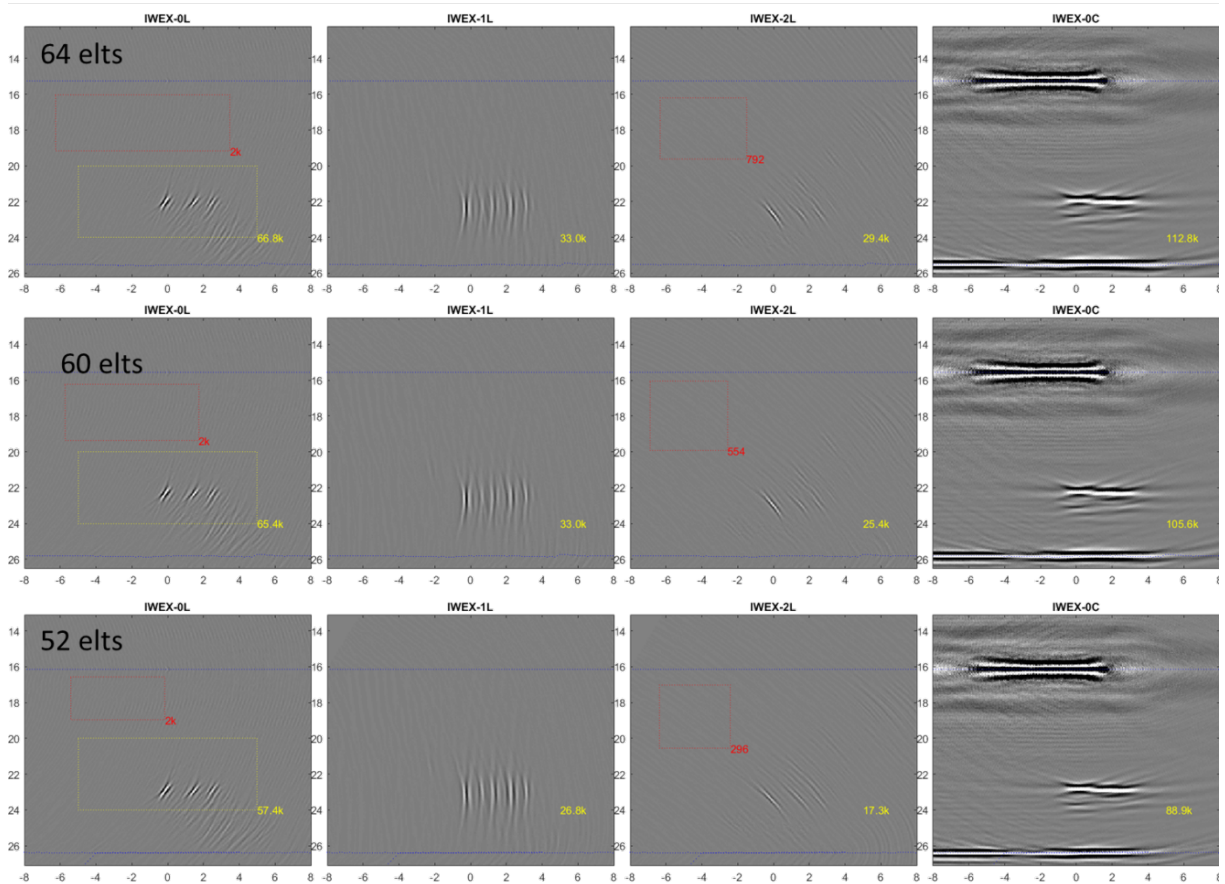


Figure 6-5, IWEX measurements of a 10.1 mm flat plate with three 0.5 mm boreholes. 7.5 MHz, pitch 0.43 mm. Each row has a different number of elements that is used in the IWEX image.

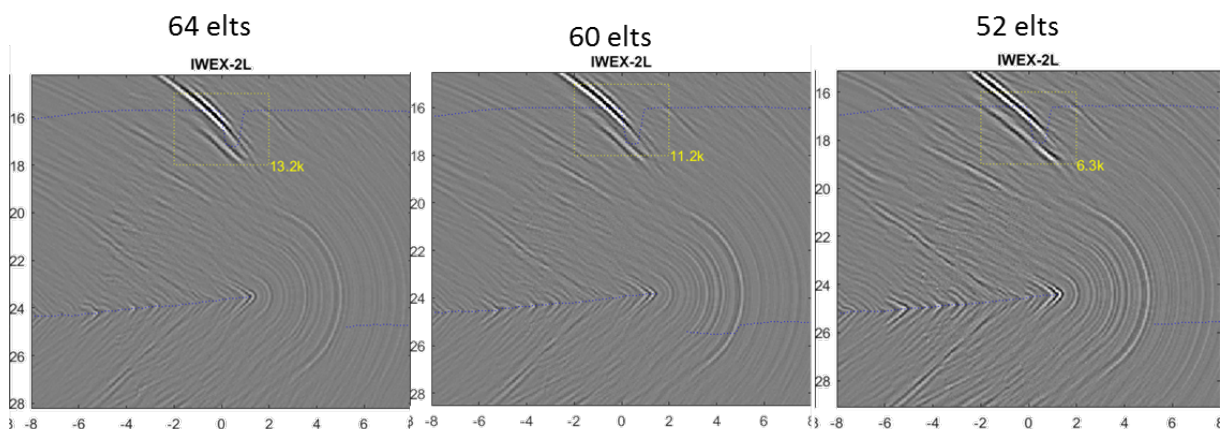


Figure 6-6, IWEX measurements of a 22 pipe, ERW weld, 8 mm wall-thickness, with an OD notch. 7.5 MHz, pitch 0.43 mm. Each IWEX image is generated using a different number of elements.

Design of inter-element spacing (element size)

The element size was designed using Figure 6-16-1. Shear-waves are predominantly generated between the first and the second critical angles of the water-steel interface, 14 – 27 degrees. With the transducer placed under an angle of 20 degrees, the required beam directivity is thus limited to 6 degrees. Therefore, the inter-element spacing was chosen as small as possible for a transducer with acceptable cross-talk. Larger elements have the benefit of suppressing aliasing and a better transducer element signal-to-electronic-noise ratio.

Transducer design (2): element width, curvature (lateral focus)

For accurate ultrasonic imaging it is not only necessary that the image in the imaging plane is in focus but the ultrasound also needs to be focused in the direction out of the image plane, i.e., the scan-direction. This is normally achieved by using an acoustical lens in the wedges. For immersion measurements, this focus may be achieved using focused linear array transducers which have elements that are curved.

The width and the curvature of the transducer elements are optimized for inspection of pipe with wall-thickness up to 10 mm, including the IWEX-1 (tandem) and IWEX-2 (skip) modes. Also, the detection of the OD profile is taken into account in the design.

It was shown that the same transducers may be used for inspection of flat plate as for the inspection of pipe with 16-inch diameter.

Algorithm improvements

The Immersion IWEX algorithms consist of the following steps: calibration of transducer position with respect to each other, imaging and extraction of OD profile, imaging and extraction of ID profile, IWEX immersion imaging. Various improvements have been made on these algorithms, as listed in Table 6-1.

Table 6-1: Q13 Improvements of the various Immersion IWEX algorithms.

Probe position calibration

- Removed need to specify IWEX window. Approximate position of probes with respect to the surface is now estimated using a new algorithm based on zero-offset A-Scans.
- Removed need for accurate estimate of center-to-center offset between the two transducer arrays. A new algorithm uses the FMC to estimate this offset from the direct through-water arrivals from the left to the right transducer array.
- Removed the need to specify the IWEX windows for the center-to-center offset calibration. These are now computed from the left and right transducer positions.
- Better graphical output of the algorithms, which is necessary for manual verification of the calibration.

OD IWEX imaging and detection

- New algorithm that first estimates the OD profile from zero-offset A-Scans.

- OD detection with IWEX images that follow the estimated OD profile. This is faster and also is a step towards processing of FMC scans where the OD profile of the previous scan position is a good estimate of the OD profile.
- Improved algorithm for OD detection based on a single IWEX image (IWEX-OL + IWEX-OR + IWEX-OC) instead of three separate images with user-specified boundaries.

ID IWEX imaging and detection

- ID detection with IWEX images that follow the estimated OD profile plus the specified wall-thickness. This is faster and also is a step towards processing of FMC scans where the ID profile of the previous scan position is a good estimate of the ID profile.
- Algorithm to automatically detect which points of the ID are valid. This algorithm is based on a simple relative amplitude threshold. In the first version of the algorithm, the user has to specify manually which parts of the ID were well detected, which is not feasible for the processing of entire FMC scans. Interpolation of the validity of the ID to the resolution of the IWEX travel-time and scale-matrix computations is done in such a way that end-points, which give non-physical travel-times resulting in artefacts, are removed.

Immersion IWEX algorithm

- Added a filter that reduces the longitudinal-wave artefacts in the IWEX images. The beam-paths found using travel-time minimization that have angles (in water) below the first critical angle are excluded from the IWEX imaging.
- Added additional requirements on the ultrasound beam-paths. Skip paths should travel upwards after skip. Transmission at OD or reflection at ID should cause sound-paths that travel in the same x-direction. The beam-paths that were found in the travel-time minimization but do not obey these requirements are excluded from the IWEX imaging.
- Added the possibility to exclude beam-paths that skipped at a region of the ID that was marked as invalid.

Immersion IWEX travel-time computation

In the IWEX imaging algorithms, the ultrasonic beam paths from each transducer element to image each pixel are found using travel-time minimization of the travel-times between the two points (see Figure6-7). For the direct path (IWEX-0 modes) it is unknown through which point at the OD surface the beam-path travels and this point is found by computing the travel times for all grid-points at the OD surface and then using the point that resulted in the minimal travel-time. A similar algorithm is used to compute the skip paths, but in that case both the OD and ID surfaces are considered. However, there are some issues that are not taken into account in this algorithm.

The transmission coefficient at the OD or reflection coefficient at the ID surface may be very low for the particular beam-path. Similar to conventional ultrasonic inspection, certain beam angles will result in mode-conversion to longitudinal waves. Compared to conventional ultrasonic inspection, the focus that is used in the IWEX imaging algorithm comprises many different beam angles thereby reducing this problem. In fact, individual beam-paths may be

excluded in the IWEX imaging algorithm, which is used in the filter to remove longitudinal wave artefacts that is describe in the next section.

For smooth surfaces such as flat or cylindrical surfaces this travel-time minimization algorithm always finds the physically correct paths. For the fitted OD and ID surfaces, the travel-time minimization might also find paths that are physically incorrect despite the minimal travel-time. For example, if the ID profile is not measured wide enough (in the x-direction) then the algorithm will report that elements that are far away from the weld all contain reflection points at the end-points of the measured ID profile, whereas the reflection would actually take place at a part of the ID surface that is not measured and hence not included in the IWEX travel-time computation.

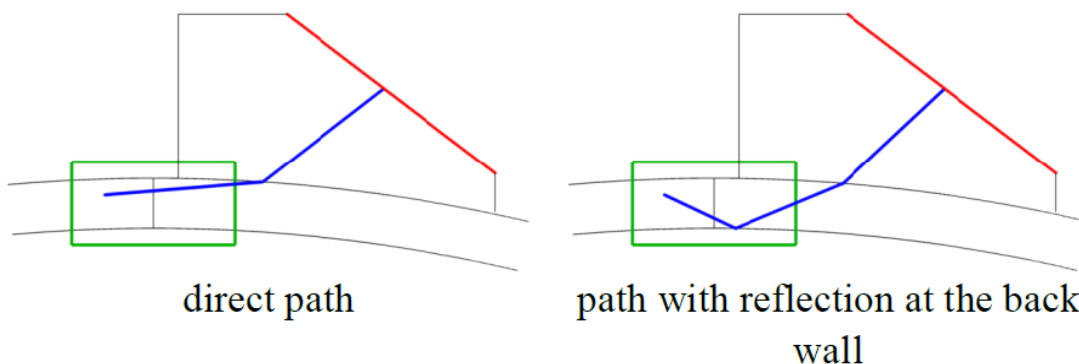


Figure 6-7. IWEX imaging paths (here depicted for normal seam weld imaging with a wedge).

Filter to reduce long-wave artefacts

The shear-wave IWEX images contain artefacts that originate from longitudinal-wave energy that is thus imaged at the wrong position of the weld (see left images of Figure 6-8, Figure 6-9, and Figure 6-10).

In Figure 6-16-1 (left-bottom plot), it may be seen that shear waves in steel are predominantly generated for incident angles between the first and second critical angles of the water-steel interface. Incident ultrasound waves that arrive with an inclination that is less than the first critical angle do result in some shear-wave energy but most energy is converted to longitudinal waves.

Therefore, a longitudinal-wave artefact filter was designed. The beam-paths in the IWEX algorithm that have an incident angle below the first critical angle of the steel are excluded

from the image computation. In the algorithm, the incident angle is estimated and the surface is approximated horizontally in the computation of this angle.

The results of this filter are shown in Figure 6-8, Figure 6-9, and Figure 6-10. It may be seen that the longitudinal wave artefacts are strongly reduced using this filter. The shear-wave indications in these shear-wave IWEX images are nearly unaffected, as is expected from the fact that only little shear-wave energy is generated with the removed beam-paths. However, in Figure 6-8 it may be seen that the resolution of the IWEX-1L mode is slightly reduced when the filter is applied.

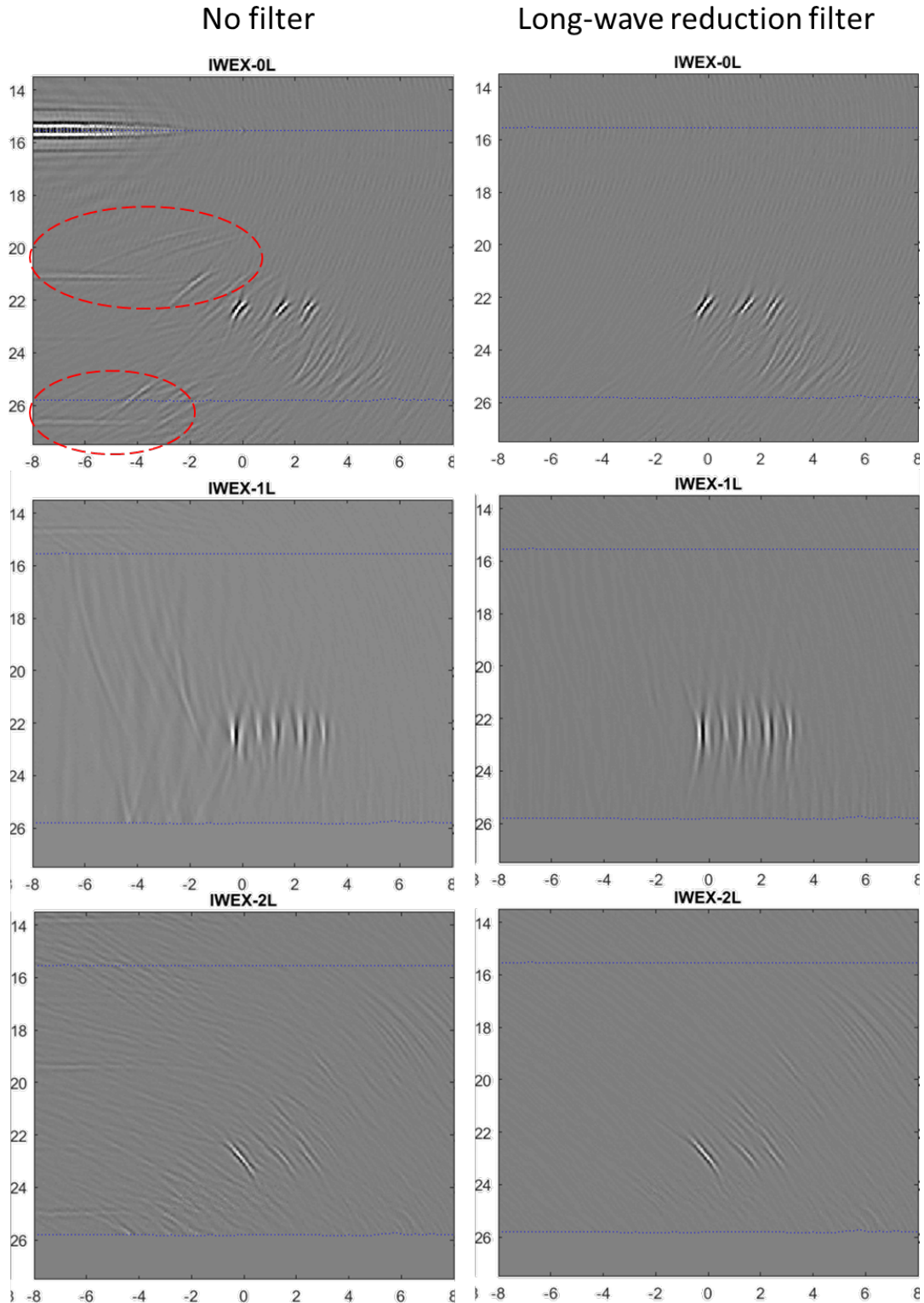


Figure 6-8, Immersion IWEX measurements of a flat plate, 10.1 mm wall-thickness, with three 0.5 mm boreholes. (left) IWEX images without filter. (right) IWEX images with filter to reduce longitudinal wave artefacts. Red markings in the left IWEX-0L image indicate some examples of longitudinal-wave artefacts.

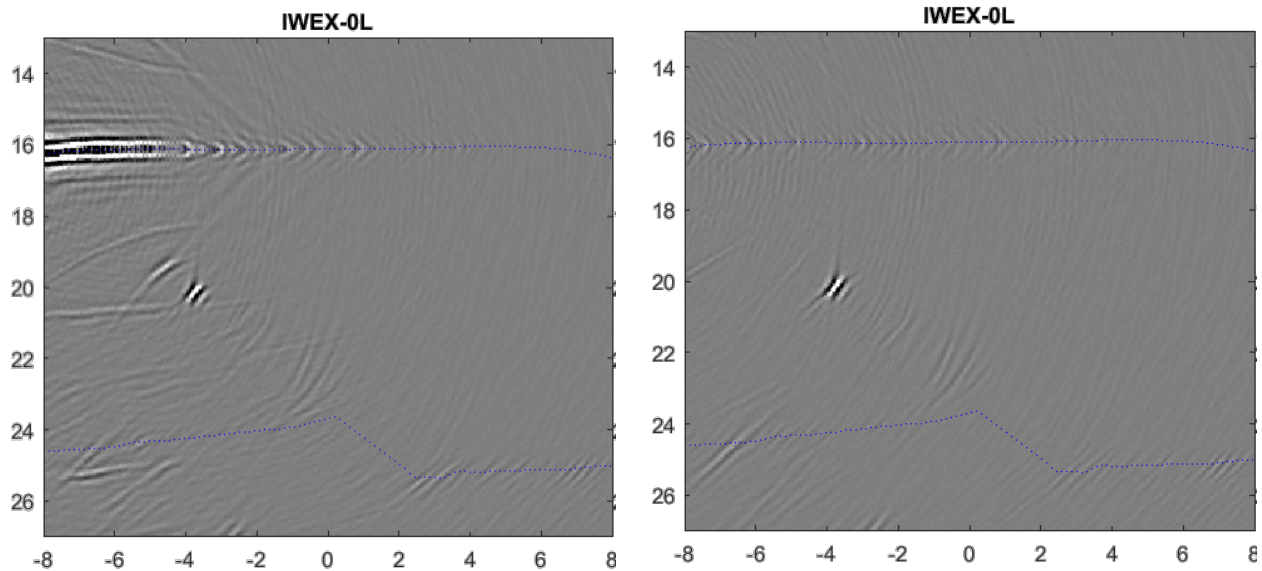


Figure 6-9, Immersion IWEX measurements of a 22" pipe, ERW weld, 8 mm wall-thickness, with a side-drilled-hole. IWEX-0L mode. (left) IWEX image without filter. (right) IWEX image with filter to reduce longitudinal wave artefacts.

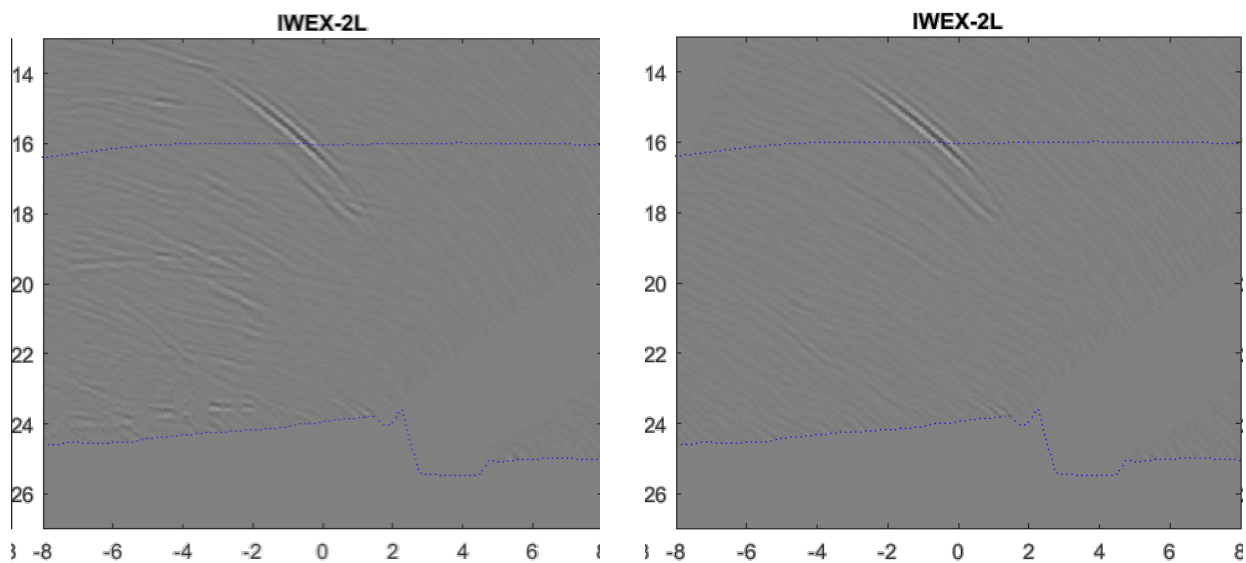


Figure 6-10, Immersion IWEX measurements of a 22" pipe, ERW weld, 8 mm wall-thickness, with an OD notch. IWEX-2L mode. (left) IWEX image without filter. (right) IWEX image with filter to reduce longitudinal wave artefacts.

Exclude beam-paths with transmission or reflection in wrong direction

As explained above, the travel-time minimization that is used in the IWEX imaging algorithm may result in non-physical beam paths. For relatively smooth surfaces, it is expected that all segments of the beam-path (in the water, in the steel, and after skip) all travel in the same x-direction, i.e., they are expected to travel either to the left or to the right. For skip beam-paths

with a reflection at the ID, it is expected that the wave travels upwards after the skip. Beam paths that do not obey these expectations are excluded from the IWEX imaging.

For the flat plate and for the 8-in pipe with a reasonably flat surface, the resulting IWEX images are nearly identical apart from the region below the ID where the IWEX-1 and IWEX-2 modes are zero per definition.

For the 22-in pipe with significant poor trim, Figure 6-11, the results of excluding the invalid beam-paths are depicted. It may be seen that some of the clutter is removed from the IWEX images but not all of it.

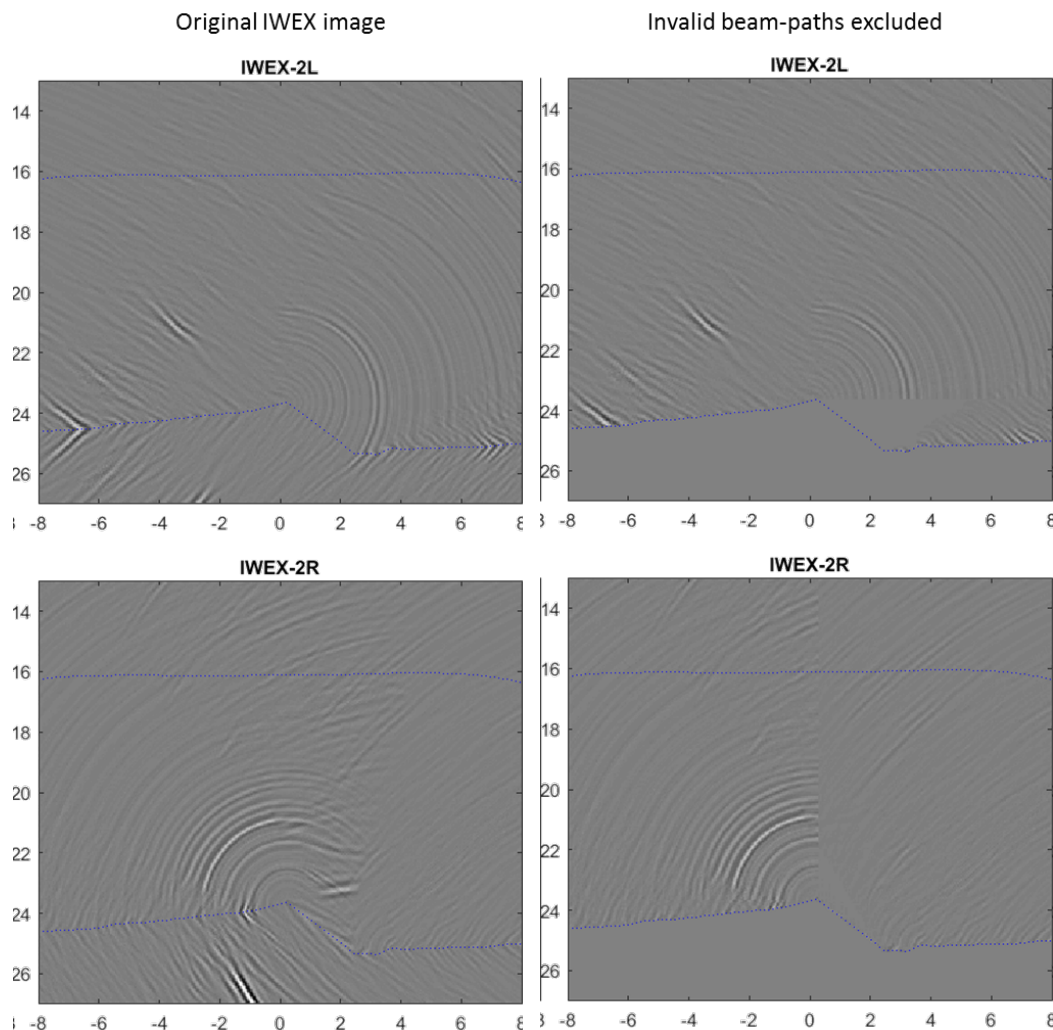


Figure 6-11, Immersion IWEX measurements of a 22" pipe, ERW weld, 8 mm wall-thickness, significantly poor trim, and a side-drilled-hole. Selection of IWEX modes (IWEX-2L and IWEX-2R) that suffered most from invalid beam-paths. Longitudinal-wave reduction filter enabled for all images. (left) original IWEX image including most beam-paths. High contrast to show artefacts more clearly. (right) IWEX image with beam-paths that are most likely un-physical excluded.

Exclude beam-paths that skipped at invalid points of the extracted ID interface

The ID profile is extracted from the FMC data using an IWEX image of the ID. However, this image does not always show the entire ID interface clearly and positions below a certain amplitude threshold are interpolated in the ID extraction algorithm.

With this option enabled, beam-paths that reflect at interpolated points of the ID surface are excluded from the IWEX image computation. In addition, beam-paths that reflect at the end-points of the measured ID interface are excluded.

Figure 6-12 to 6-16 show the results of excluding the beam-paths that reflect at interpolated points of the ID interface. The advantage of excluding these points is best visible for the 22-inch pipe with poor trim at the ID of the ERW weld (see Figure 6-14 and Figure 6-15). The artefacts caused by these wrong beam-paths are removed while the indications remain similar. However, for the flat plate points of the ID interfaces that are actually well extracted are marked as invalid by the algorithm. The result of the ID extraction may be seen in Figure 6-12. The resulting IWEX images are shown in Figure 6-13 where it may be seen that the boreholes are less visible. Note that the IWEX images that are not depicted (e.g., from the right-hand-side) are very similar for both cases. It is desired to have a better ID extraction algorithm that is capable of extracting the profile at positions where the ID interface is less visible in the IWEX-0C image. The width of the extracted ID profile is just too small to image the complete OD in the IWEX-2C mode; this may be seen in Figure 6-13 (flat plate) and Figure 6-16 (8-inch pipe with ERW weld).

As the algorithm significantly improved the ERW with poor trim, but resulted in degradation of the image quality for the cases with a smooth ID profile, this algorithm is now included as an option such that it may be enabled or disabled depending on the weld geometry.

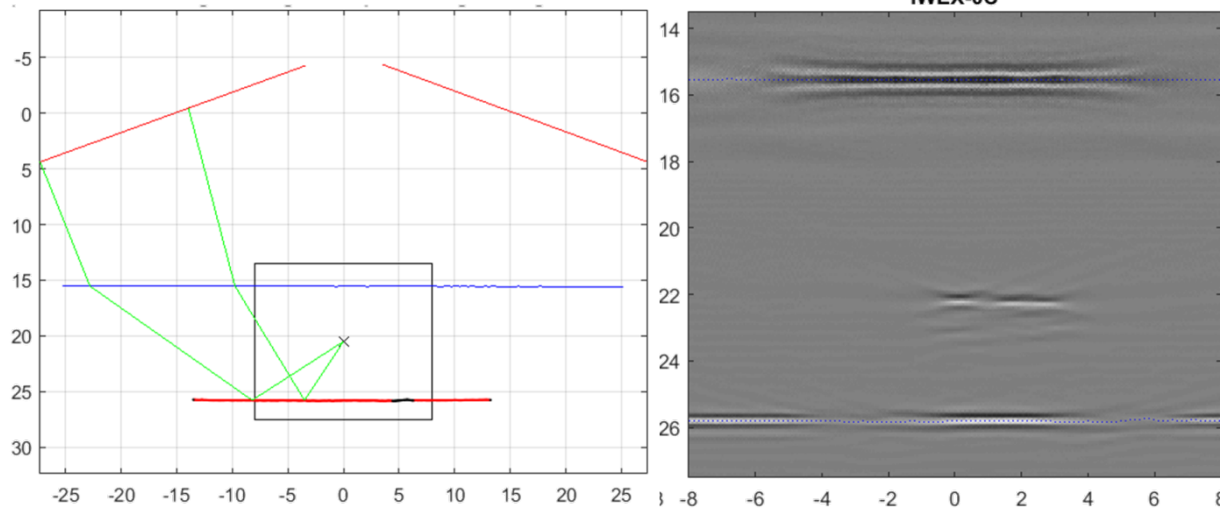


Figure 6-12. Flat 10.1 mm thick plate with three 0.5 mm boreholes. (Left) result of profile extraction showing valid regions of the ID (red) and invalid regions of the ID (black). (Right) IWEX-0C image showing the ID profile. The part where the ID profile has a weak amplitude and is only vague visible is marked as invalid by the algorithm.

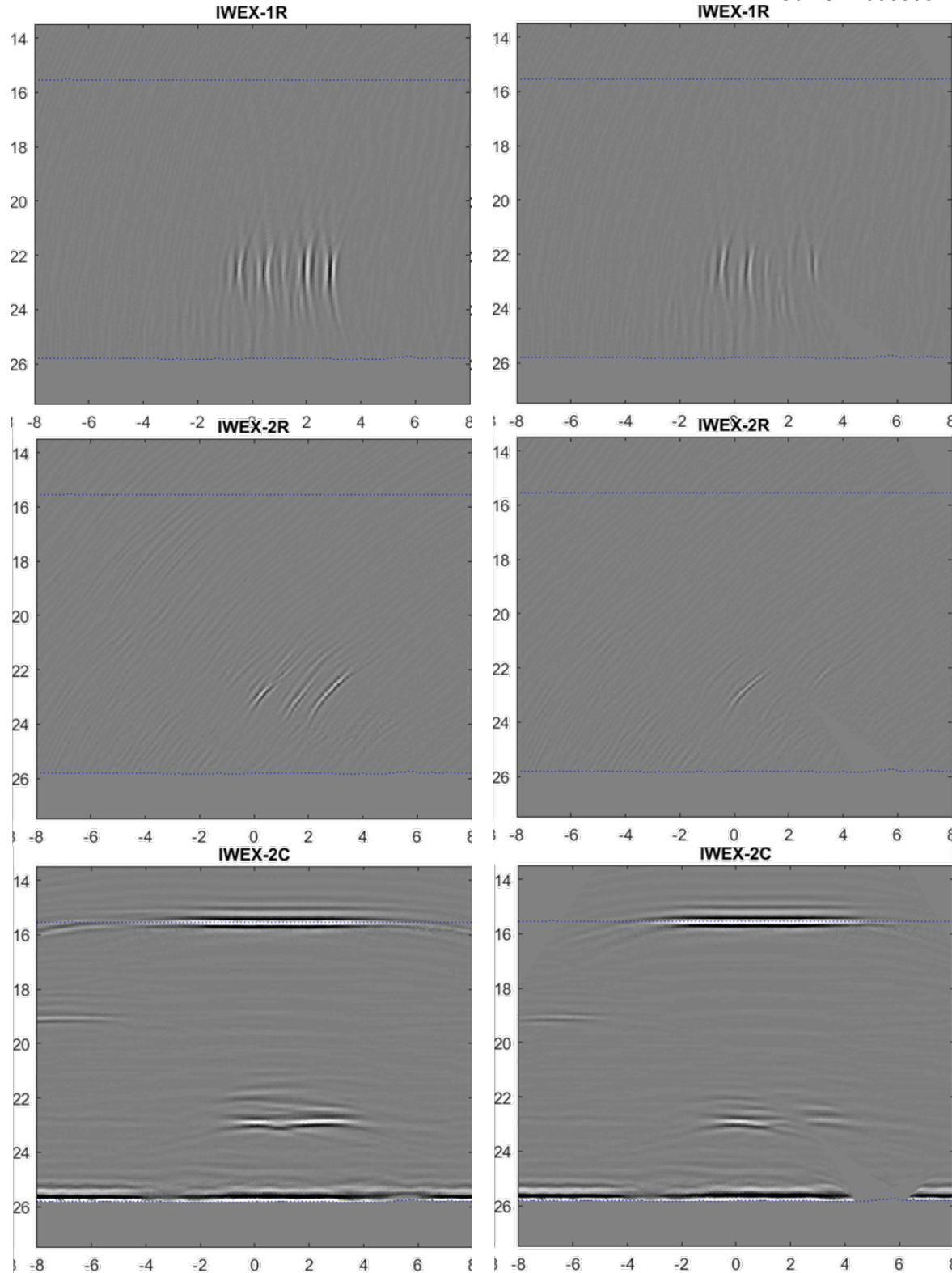


Figure 6-13. Flat 10.1 mm thick plate with three 0.5 mm boreholes. (left) skipping on all ID points including interpolated points. (right) excluded beam-paths that skip at invalid ID points. (both images) long-wave filter enabled, only valid beam-path directions. IWEX modes not depicted are similar for both cases.

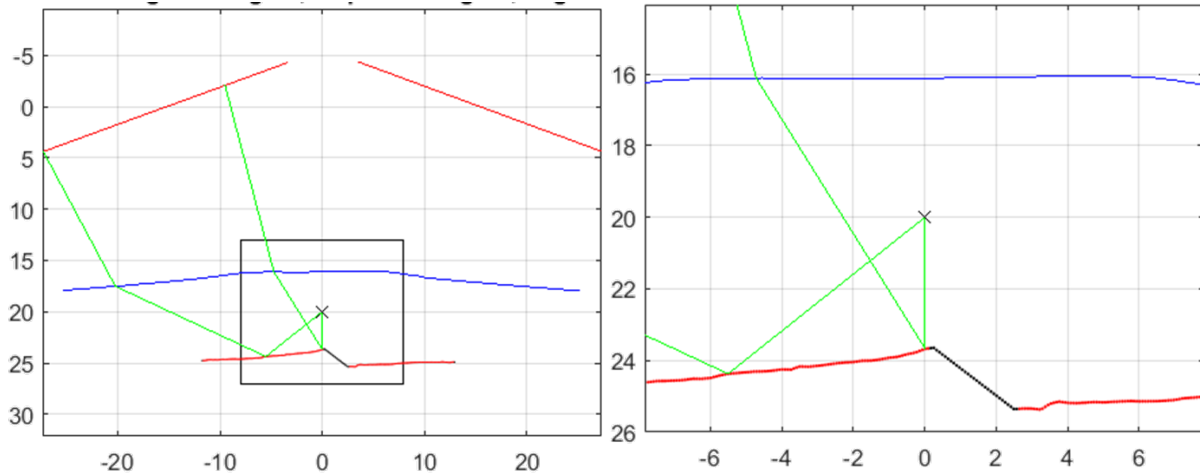


Figure 6-14, Result of ID extraction showing valid regions of the ID (red) and invalid regions of the ID (black).Results of the 22" pipe, ERW weld, 8 mm wall-thickness, significantly poor trim.

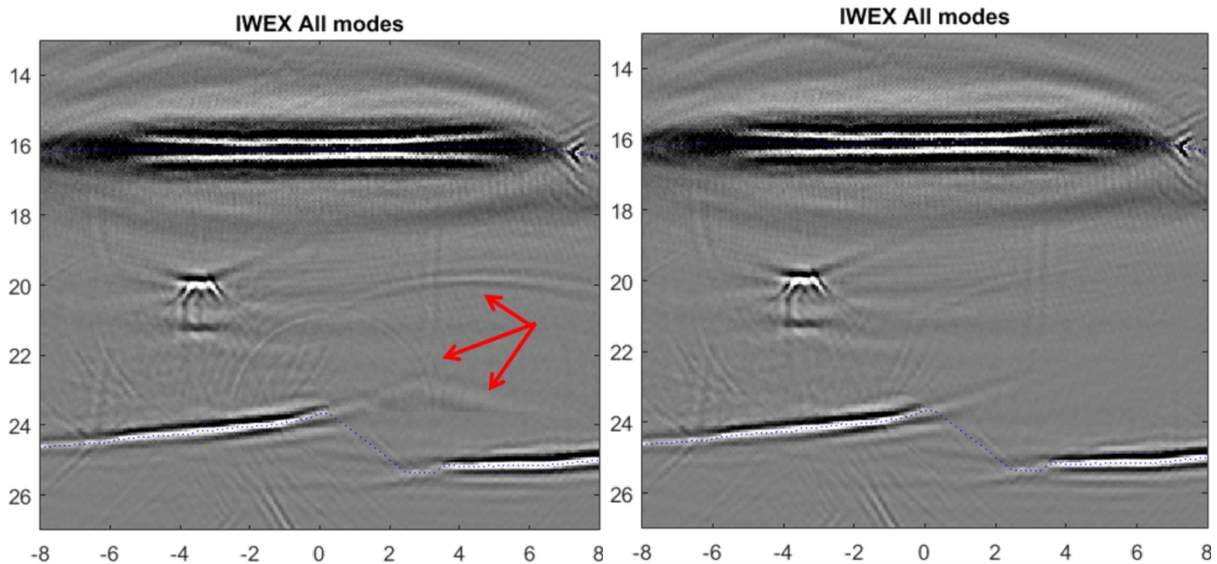


Figure 6-15, Results of the exclusion of skip-paths on invalid ID points. Immersion IWEX measurements of a 22" pipe, ERW weld, 8 mm wall-thickness, significantly poor trim, and a side-drilled-hole. All IWEX modes shown in a single image. Longitudinal-wave reduction filter enabled for both images. (left) original IWEX image excluding only invalid beam-paths based on direction. (right) excluding beam-paths based on skip on invalid ID points.

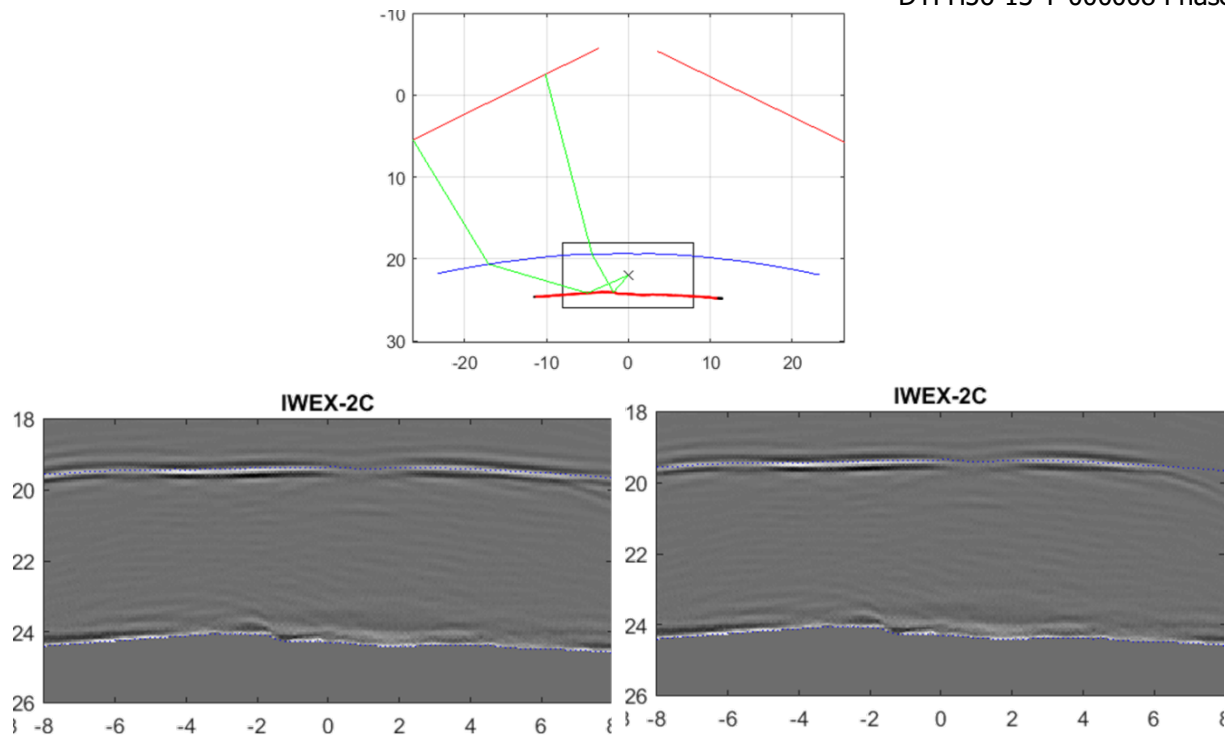


Figure 6-16, Results of the exclusion of skip-paths on invalid ID points. Immersion IWEX measurements of a 8" pipe, ERW weld, 5 mm wall-thickness, with an OD notch. (top) Nearly the entire ID is valid except from the left and right ends. IWEX-2C images are depicted; the other IWEX images were similar for both cases. Longitudinal-wave reduction filter and invalid beam-direction filter enabled for both images. (left) IWEX image with skips at all possible ID points. (right) Beam-paths with skips at invalid ID points not in the IWEX image.

Results

The results presented in this section are both a validation for the new probe design as well as for the improved and more automated algorithms.

Test cases

The following test cases are considered:

- Flat plate, 10.1 mm thick, with three 0.5 mm boreholes
- 22 inch pipe, 8 mm wall-thickness, ERW seam, poor trim, with a 1.1 mm side-drilled-hole.
- 22 inch pipe, 8 mm wall-thickness, ERW seam, poor trim, with an OD notch.
- 8 inch pipe, 5 mm wall-thickness, ERW seam, with OD notch.

Transducers and validation of the new transducer design

For the FMC measurement reported in this section, transducers were used that are similar to the newly designed ones. Measurements have been performed with two 7.5 MHz transducers with pitch 0.43 mm, element size 0.37 mm, 60 active elements, no curvature for lateral focusing, and impedance matching for plastic (wedges). The probes have 128 physical elements. The studied indications are all artificially made and over 10 mm in length (in the lateral /scan direction, out-of-plane of the IWEX image). Therefore, the lateral focusing is not very important for these test cases while it will be for actual flaws.

The newly designed transducer is expected to give better performance, especially due to the lateral focus but also because impedance matching to water will give a better pulse signature and signal-to-noise ratio.

Thus, if good IWEX images are generated using the available probes then it is expected that the newly designed probes will provide even better IWEX images.

Results

The new algorithm is tested on these four test cases and the resulting IWEX images are shown in Figure 6-17 to 6-20. It may be seen that the weld geometry as well as the indications are very well visible in the IWEX images. Moreover, all modes are accurately aligned which is necessary for unambiguous and precise interpretation and sizing of the imaged defects.

The variety of pipe samples (flat plate, 22-inch pipe with poor trim, 8-inch pipe) could all be imaged with the same algorithm.

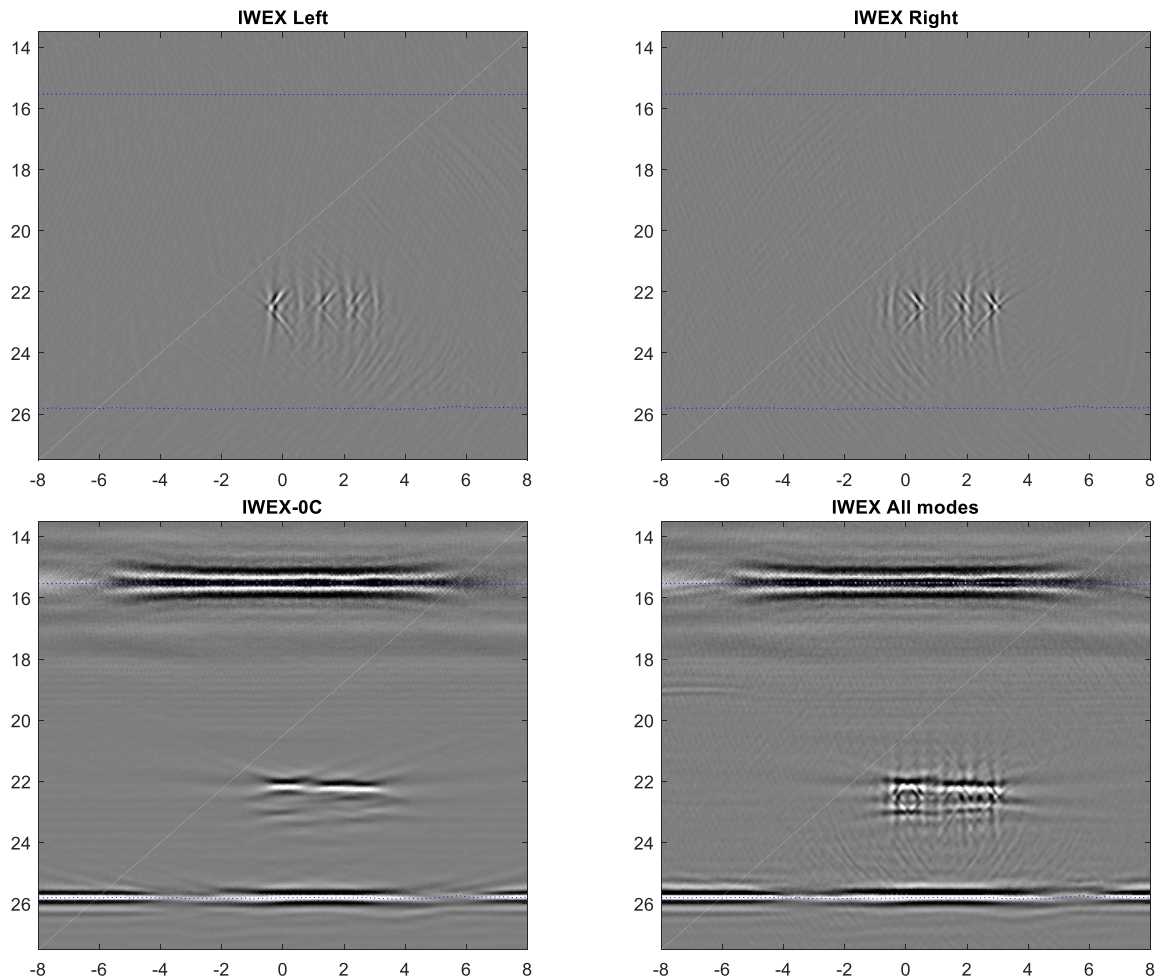


Figure 6-17, Immersion IWEX measurements of a flat plate, 10.1 mm wall-thickness, with three 0.5 mm boreholes.

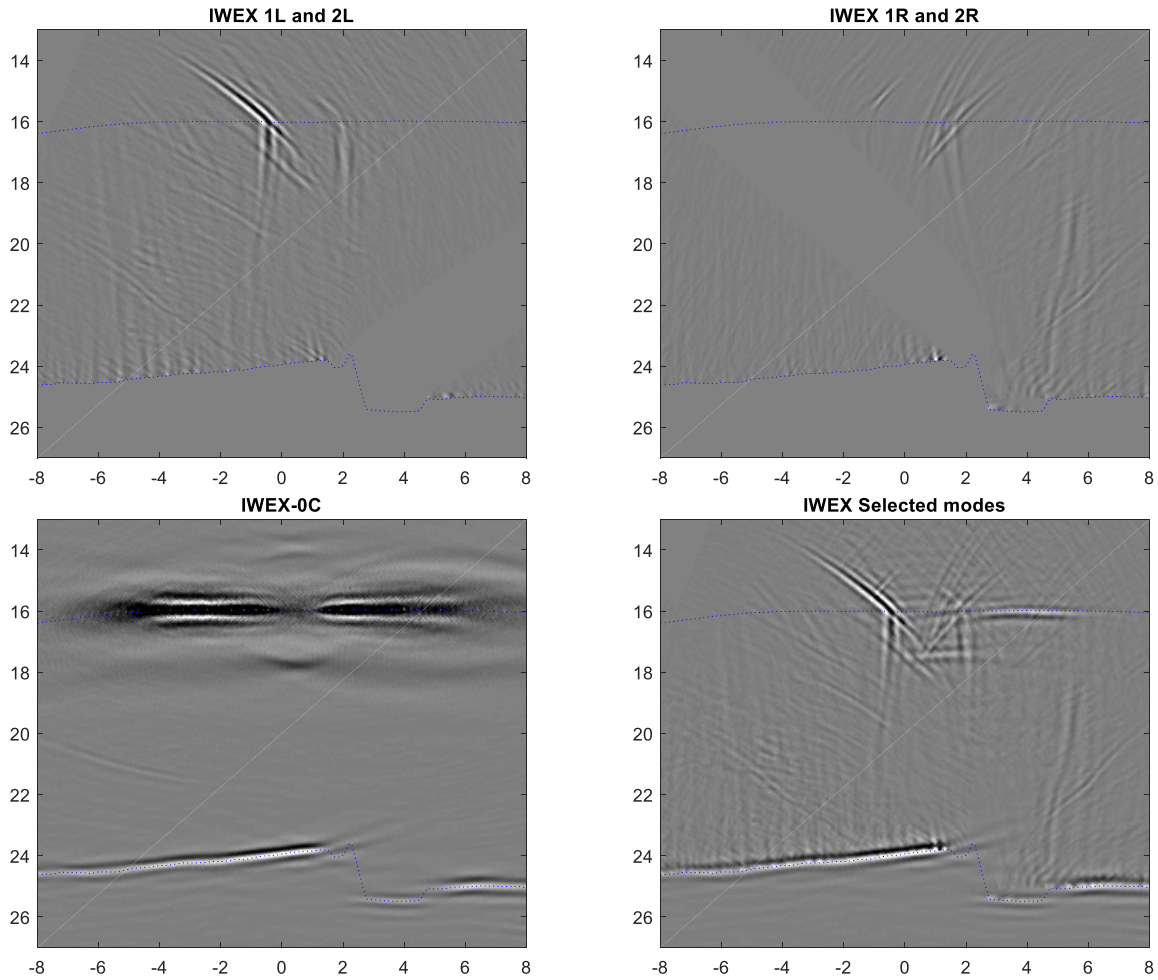


Figure 6-18, Immersion IWEX measurements of a 22" pipe, ERW weld, 8 mm wall-thickness, with an OD notch.

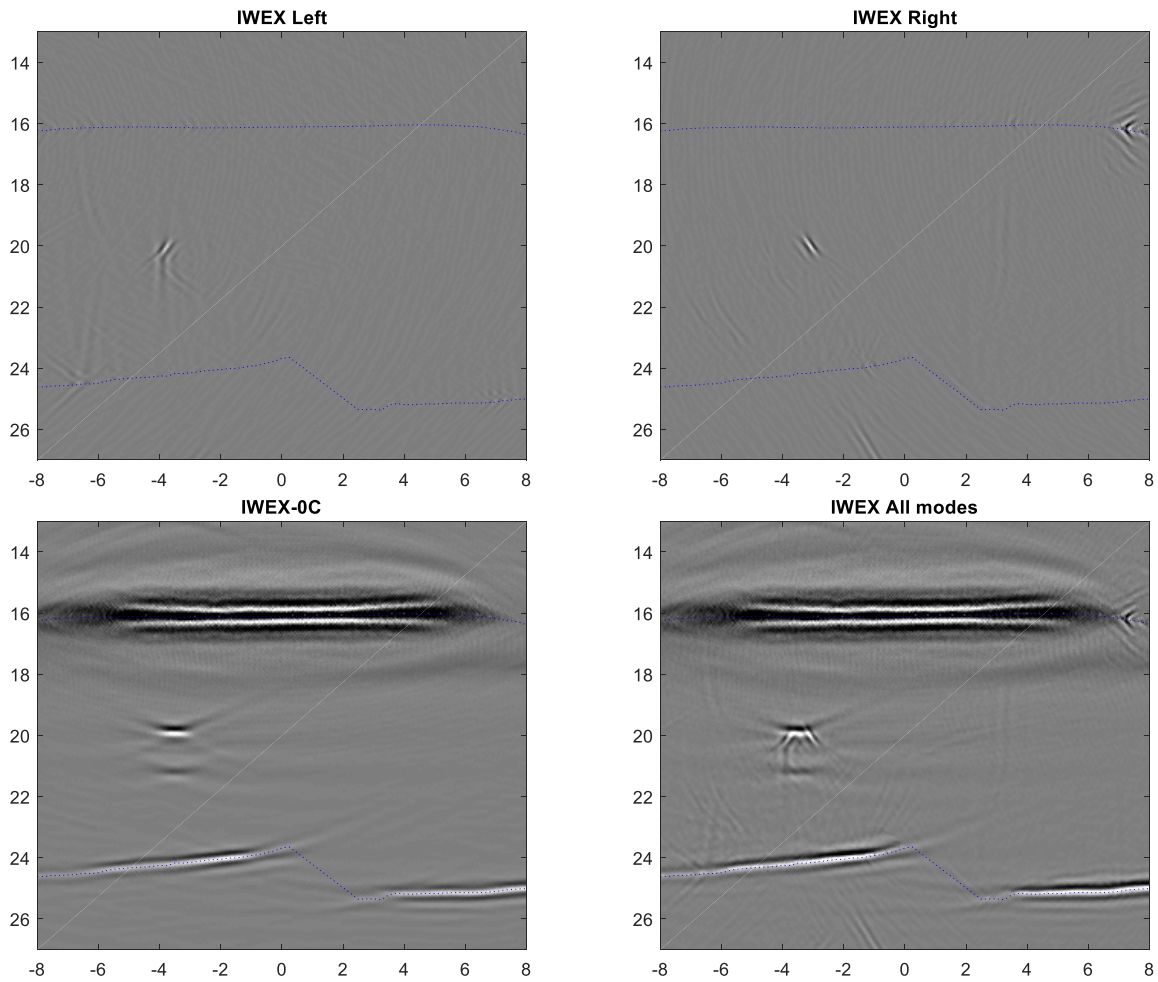


Figure 6-19, Immersion IWEX measurements of a 22" pipe, ERW weld, 8 mm wall-thickness, with a 1.1 mm side-drilled-hole.

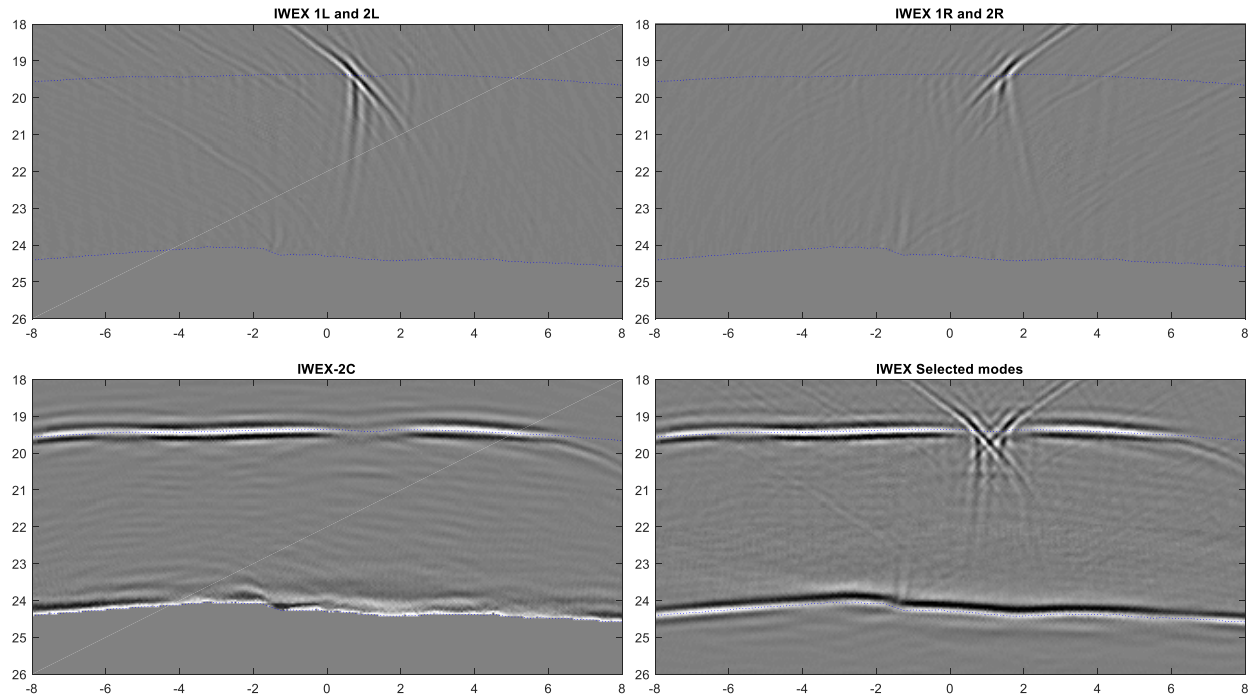


Figure 6-20, Immersion IWEX measurements of an 8" pipe, ERW weld, 8 mm wall-thickness, with an OD notch.

Automated calibration and pipe surface detection for immersion

Experiments were carried out to determine the design parameters of the array probes required. Furthermore, a calibration workflow was designed to determine unknown parameters of the setup geometry as well as material properties. The calibration routine was improved by calibrating additional parameters to increase the accuracy.

Calibration of the speed of sound in water

In the original approach presented, the sound velocity in water was estimated from a temperature measurement. Using a standard model derived from experimental data¹, the sound velocity c in fresh water can be determined from the temperature t (in °C):

$$c = 1.402385 * 10^3 + 5.038813 * t - 5.799136 * 10^{-2} * t^2 + 3.287156 * 10^{-4} * t^3 - 1.398845 * 10^{-6} * t^4 + 2.787860 * 10^{-9} * t^5$$

¹ W. Marczak: Water as a standard in the measurements of speed of sound in liquids. Journal of the Acoustical Society of America 102(5), 1997, pp. 2776-2779.

This approach requires a temperature measurement, which introduces difficulties with a closed system such as a water-filled cushion.

A method has been derived to estimate the velocity of sound in water. The calibration measurement is taken at the same position where the measurement for inspection is taken. This enables the option of monitoring and potentially correcting for the velocity of sound in water during an immersion scan, if required.

Calibration of shear velocity in the pipe material

The shear velocity in the material is one of the more critical parameters for accurate imaging. It was derived that changes of ± 20 m/s can be tolerated for a typical seam weld imaging setup. However, an experimental study shows that variations in pipeline steel may exceed this limit². From a set of 11 samples of carbon steel examined in this study, variations of the shear velocity between 3215 and 3367 m/s were found.

To overcome this problem, an additional step was added to the calibration in which the shear velocity is estimated from the measurement itself. To this end, the acoustical path shown in Figure 6-21 is used.

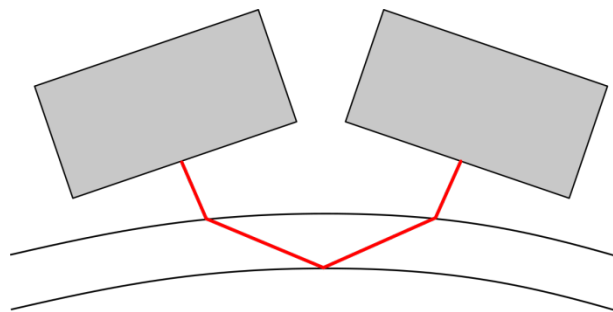


Figure 6-21: Ultrasonic path used for shear velocity estimation using the reflection at the inner pipe surface.

Instead of using individual paths between array elements, all array elements are used together to generate an image of the inner pipe surface. By varying the shear velocity of the imaging model, different images are obtained for a range of potential shear velocities. If the shear velocity of the imaging model matches the actual shear velocity of the pipe material, the image is optimally focused. This can be measured by monitoring the amplitude of the reflection off the inner pipe surface in the image.

² E.A. Ginzel, R.K. Ginzel: Study of acoustic velocity variations in line pipe steel. Materials Evaluation, May 1995, pp. 598-603.

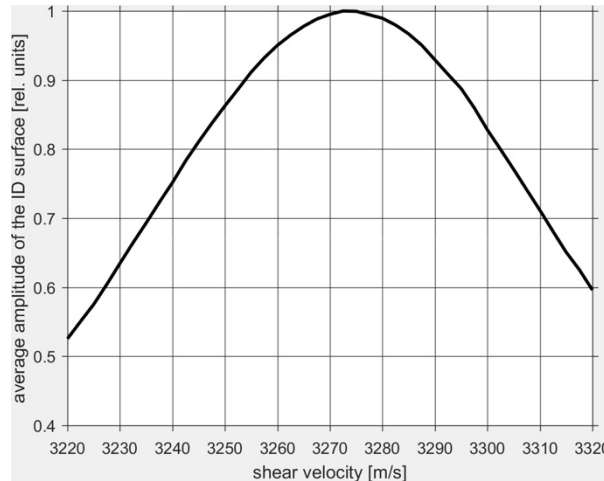


Figure 6-22: Average amplitude of an image of the inner pipe surface for different shear velocities tested.

Improvement of pipe surface detection

For the application of immersion imaging, it is important to detect the outer surface of the object accurately. In the first version of the surface detection algorithm, an image of the outer pipe surface was made, and the surface points detected in every column of the image were directly used as surface positions.

To increase the robustness of the surface detection to weak signals or false detections, additional constraints were added to the surface model. As an approximation for the curvature of the detected surface, the second-order derivative of the vertical position of the surface points can be used.

Figure 6-23 presents surface detection results for which this constraint was applied. In order to allow for changes in shape such as the kinks at horizontal positions of ± 7 mm in the image, the curvature constraint can also be relaxed locally, allowing for multiple sections within the surface profile with limited curvature within each individual section. This way, the model can be adapted to different types of pipe and surface geometries.

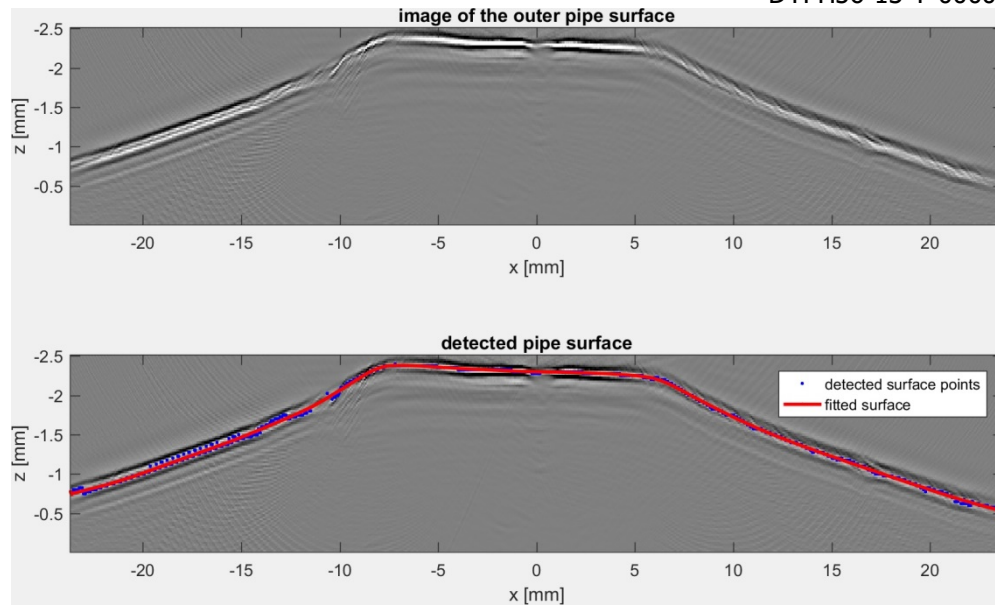


Figure 6-23: Detection of the OD surface from the image (top) using pipe curvature constraints (bottom). Note that the vertical scale is exaggerated by a factor of four to simplify plotting.

Development of software for full-matrix-capture recording of seam scans

Testing of immersion probes

Upon delivery of the array probes designed for the immersion application they were tested. Based on tests carried out using different pipe coupon samples, the applicability of the probes was verified. This confirms the decisions made during the design phase of the probes.

The images obtained with the probes tailored towards the immersion application are of similar quality to the simulated images used when designing the probe. This is also shown in the following sections.

Development of software for full-matrix-capture (FMC) recording of seam scans

In order to carry out scans in an immersion setup, it is currently required to record raw signals in the form FMC data. Subsequently, these measurements obtained for all transmitter-receiver combinations can be processed to determine the positions of the outer and inner pipe surfaces, and to generate images of the weld. The separation of the recording and the processing step is for practical consideration because of the extensive processing time required during this phase of development. It is envisioned that this time can be reduced significantly in a later stage of development.

Software was developed to enable the recording of FMC data while scanning a pipe sample. The start of each measurement cycle is triggered by the position of an axial encoder, similar to the scanning setup used for IWEX in combination with plastic wedges.

The size of the raw FMC data for a single axial scan cross-section is about 130 MB. However, this data volume can be reduced by omitting parts of the signal that are not required for the subsequent reconstruction. In addition, data compression with a reduction rate of about 50 % was implemented to cope with the large volume of raw data.

FMC scanning of laboratory samples

With the specifically designed immersion probes being available from item 120, a first round of immersion test measurements was carried out in a laboratory environment. FMC data were recorded over a scan length of approximately 10 cm (4 inches) on two pipe coupons.

For these preliminary tests, a simple probe holder made from 3D-printed parts was used. It allows for accurate adjustment of the alignment between the two array probes. The setup is shown in Figure 6-24. In addition to the pipe coupon, a flat steel reflector is present in the scanning setup. This reflector was used to calibrate the relative position of the array probes before carrying out the scan. Alignment between the calibration reflector and the pipe sample is not required. In a future implementation of the process, the calibration step may also be carried out at a different location. Re-calibration of the setup on this reflector is required only when the relative alignment between the probes has changed.

For this laboratory set-up, the probe holder is connected to a linear axis aligned with the axial direction of the pipe coupon. The arrays can be moved manually or driven by a motor at low speed, similar to the linear scanner used in the field for full sized pipe.

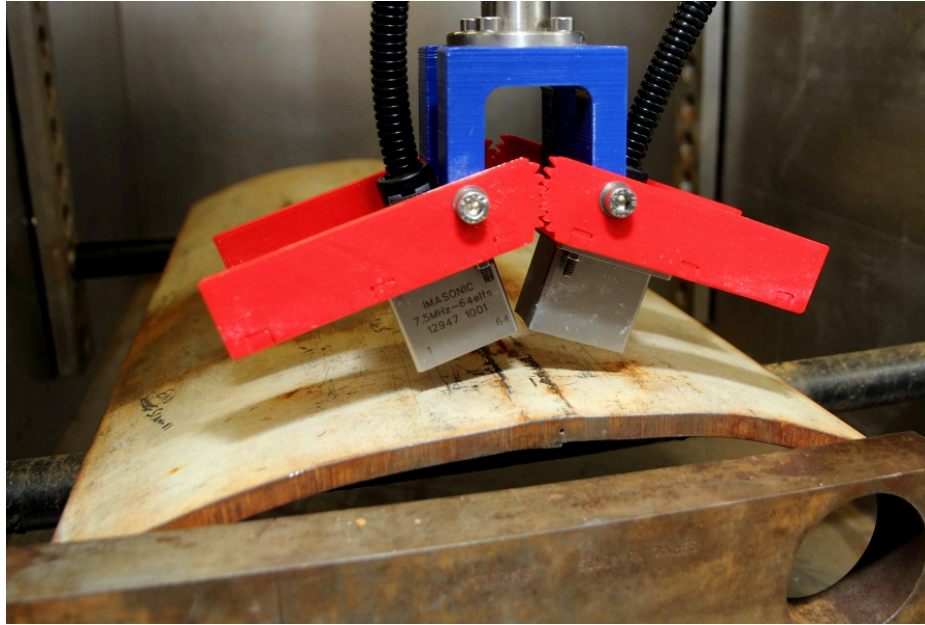


Figure 6-24: Setup for immersion scans with arrays above the pipe coupon. A flat reflector (front) is put next to the pipe coupon to facilitate calibration of the relative position of the two arrays. The setup is shown without water for better visibility of the arrangement.

For each scan, the following processing steps and measurements were carried out:

- 1) A single FMC measurement was taken with the arrays submerged in water. This measurement is used to determine the latency of the measurement system.
- 2) A single FMC was recorded with the arrays positioned above the flat reflector. From this measurement, the following information is extracted:
 - a) the velocity of sound in water,
 - b) the relative distance and angle of each array with respect to the flat reflector, and
 - c) the relative distance between the two arrays.
- 3) Another single FMC was recorded with the arrays above the actual pipe sample. The following processing is carried out:
 - a) The outer pipe surface is detected by making an IWEX image in water.
 - b) The shear velocity in the pipe sample is calibrated. To this end, a range of potential shear velocities is used to generate images of the ID surface as described in the previous quarterly report. The image with the strongest amplitude is selected, and the associated shear velocity is used for imaging the sample.
- 4) The information obtained in the above calibration steps is stored.
- 5) A full scan can then be performed, for each axial position along the pipe sample, recording a full matrix capture at each axial position.
- 6) After the scan, the full matrix captures can be processed to generate images using the calibration information.

Testing of automated calibration and pipe surface detection for immersion

The calibration and surface detection routines were tested on a few different samples. In earlier it was found that these methods worked well on single scan positions. However, the robustness of these methods was not sufficient for application to FMC scans of extended length.

The laboratory FMC scans were used to refine the approaches for surface detection and imaging in order to enable their application to scans as described below. The methods required for the detection of OD and ID, and for fitting curves through the detected points in the image were put into different sub-modules. This enabled sharing of the algorithms among different processing steps.

Subsequently, all processing steps were combined to enable the automatic batch processing of FMC axial scans into a series of images without further manual intervention. Figure 6-25 provides an overview of the processing chain on a coarse level.

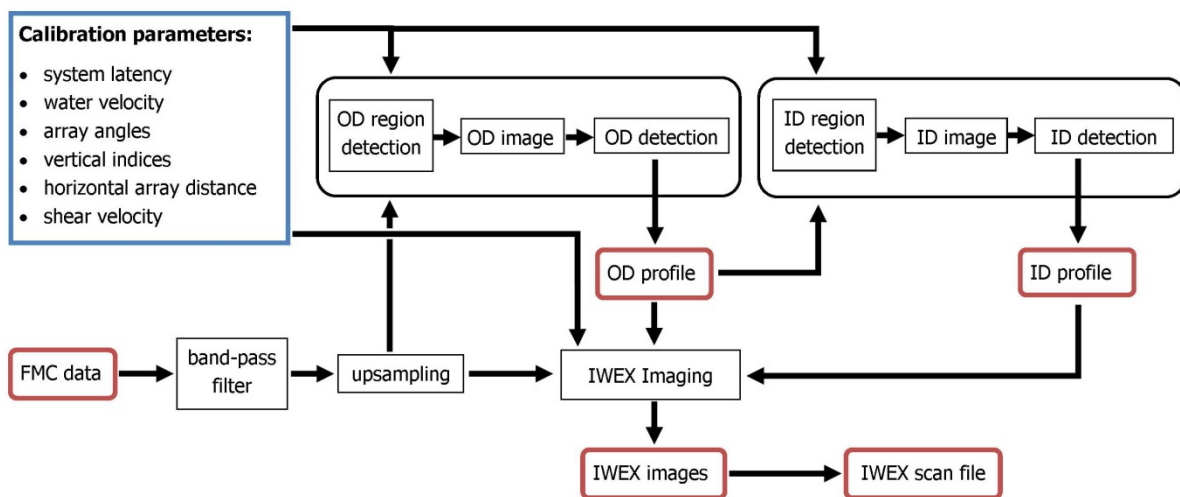


Figure 6-25: Schematic overview of the processing steps required to generate immersion images from raw full matrix capture data. In an intermediate step, OD and ID surface profiles can be obtained.

A processing step that has been added only recently, is the upsampling of A-scan data. Typically, the full matrix captures are recorded with 50 MHz sampling frequency and then processed at 100 MHz sampling frequency. The upsampled data is used as input to both the surface detection and the imaging. The upsampling step provides a slight improvement in resolution and signal-to-noise ratio due to the fact that the imaging algorithms round off to the nearest A-scan sample [TenGrotenhuis2016].

The performance of the calibration routines was verified using immersion measurements on two different pipe coupons. Without further adaptations, images obtained from the left and right

arrays were found to coincide accurately in horizontal and vertical positions as shown in Fig. 6-26.

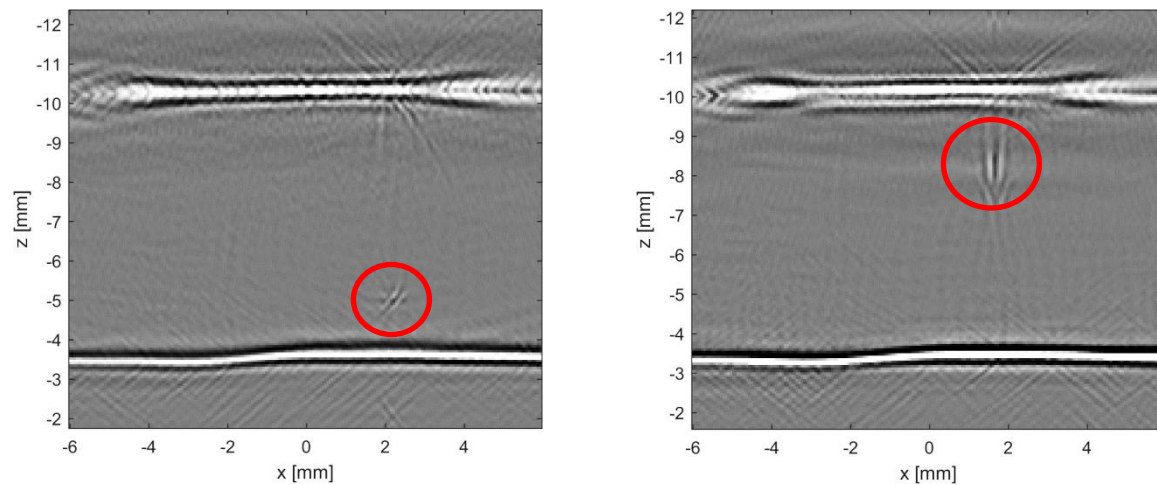


Figure 6-26: Cross-sectional images obtained by processing full matrix capture data from immersion scans taken at two different positions. Note that the different mode images obtained from the left and right side coincide with high accuracy. Left image: shallow cold weld connected to the OD surface, small inclusion (encircled). Right image: cold weld, not surface-breaking (encircled).

Adaptation of immersion IWEX algorithms and software (OD profiling, ID profiling, immersion IWEX, artifact removal) for FMC-scans

As indicated above, the processing of FMC scans provided additional insight into the requirements for the different processing modules. This led to further refinement of the methods used for detecting the outer and inner pipe surface. In the updated version of the algorithms, the following steps are taken for the detection of the outer pipe surface:

- 1) The approximate distance between the arrays and the outer pipe surface is determined from the first arrival in the pulse-echo signals, using each array element as sender and receiver.
- 2) An image of the outer pipe surface is made with coarse resolution from the FMC data.
- 3) Image points with amplitudes below 10% of the maximum amplitude are discarded.
- 4) Remaining image points with high amplitude are used as candidates for the OD surface.
- 5) A second-order polynomial is fit through these points to determine the approximate position of the OD surface.
- 6) In the determined region, an image with fine resolution is made.
- 7) The position of the outer pipe surface is determined from the image by imposing constraints on the curvature.

The following approach is used for the detection of the inner pipe surface:

- 1) Using the OD profile, an image of the inner pipe surface is made with coarse resolution. To this end, the region around the nominal wall thickness is imaged.
- 2) Image points with amplitudes below 10% of the maximum amplitude are discarded.
- 3) Remaining image points with high amplitude are used as candidates for the ID surface.
- 4) In the determined region, an image with fine resolution is made.
- 5) The position of the inner pipe surface is determined from this image by imposing constraints on the curvature.

Figure 6-27 shows the surface profiles determined for a 22" pipe coupon with offset edges on the ID at the bond line, along with the geometric arrangement of the array probes relative to the pipe surface.

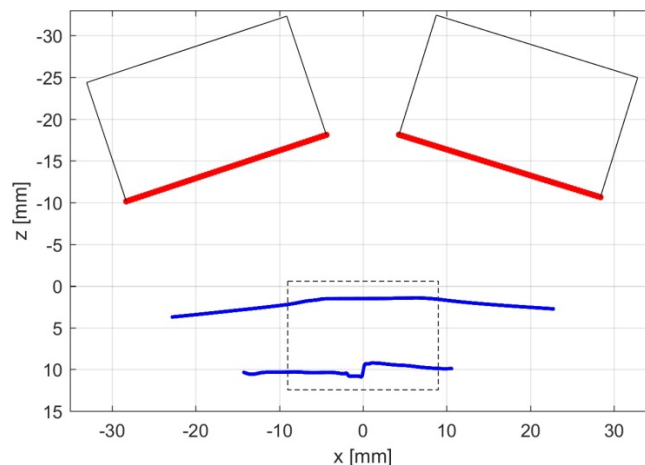


Figure 6-27: Imaging setup for immersion showing the position of the inclined arrays above a cross section of the weld. The blue lines show the surfaces detected from the measured data, the dashed rectangle represents the region of interest used for imaging.

Only acoustical paths above the first critical angle are taken into account for imaging as already suggested during previous experiments. This way, the impact of artifacts from longitudinal arrivals on the shear wave image is minimized.

Furthermore, the recommendations for the removal of imaging artifacts were extended for images from modes obtained using reflections at the ID surface:

- Only ID regions with an orientation of less than $\pm 15^\circ$ from the horizontal direction are taken into account as reflection surfaces.
- Parts of the ID surface which are only weakly imaged from the direct cross mode in the vicinity of the (assumed) bond line are not taken into account as reflection surfaces either. This is done to take into account different ID trim heights on each side of the bond line, caused by offset plate edges.

- For measurements taken with the left array, only the ID surface to the left of the (assumed) bond line is used as reflection surface for imaging the right side of the region of interest. Likewise, for measurements taken with the array on the right side, only the ID surface to the right of the weld is used as reflection surface for imaging the left side.

These restrictions were shown to work well for the experiments carried out. Figure 6-28 presents a comparison of a test image obtained during the 13th quarter and an imaging result produced with the new probes and implemented steps. The purpose of this comparison is to show that the image does not deteriorate when using the new immersion probes and applying the adapted surface detection. It is important to remember that the new arrays possess only half the number of elements (64 instead of 128 elements used in previous tests). Nevertheless, the surfaces and the artificial hole in this example are well detected and fairly well imaged.

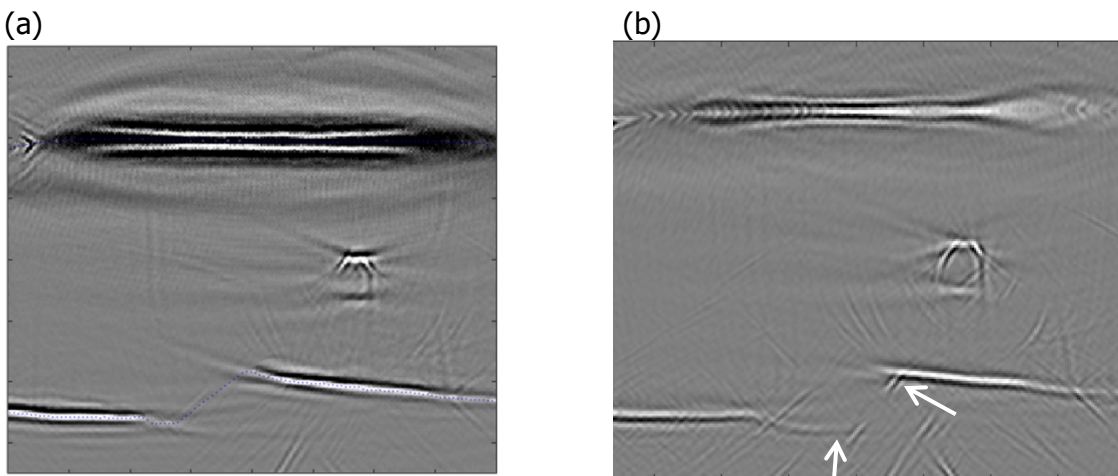


Figure 6-28: Imaging results obtained in the 13th quarter (a) and after recent adaptations (b). A photograph of the sample is shown in Fig. 6(a).

From Fig. 6-28, it should also be noted that the ID surface is imaged clearer at the plate edge offset near the bond line in comparison to the results from the 13th quarter as indicated by the white arrows in Fig. 6-28(b). Note that the shape of the ID edge cannot be recovered completely due to the fact that the lowest point at the ID surface is difficult to reach acoustically. This is caused by the shape of the ID close to the bond line with one plate overlapping the other as shown in Fig. 6-29(a).

Nevertheless, the IWEX image in Fig. 6-29(b) shows that the surface profiles and the extent of the contiguous volume of material in the vicinity of the bond line are accurately reconstructed. This enables the accurate determination of the material thickness. Likewise, the position and extent of the artificial flaw are reproduced correctly in the image.

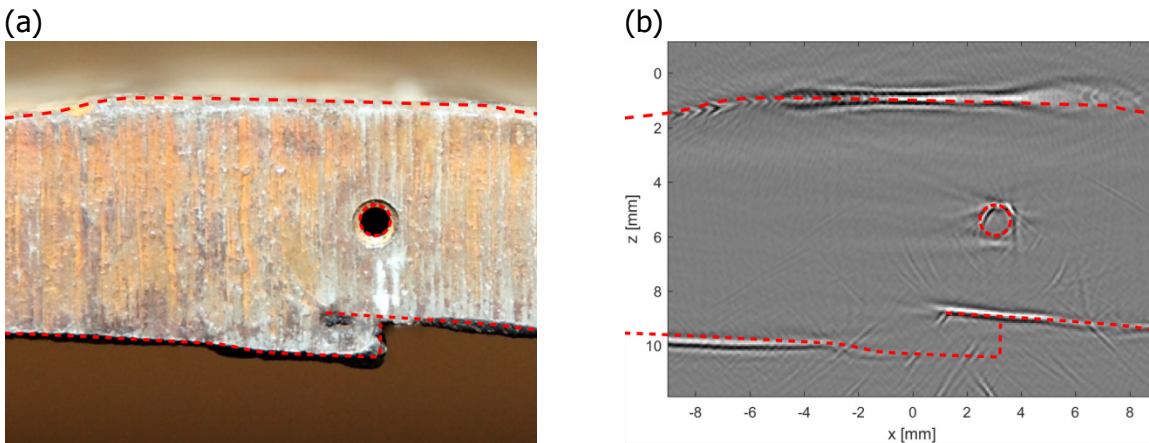


Figure 6-29: Side view of the 22" sample with offset plate edges containing a hole drilled along the axial direction, photograph (a) and IWEX image (b) with the plate contours superimposed.

On the following pages, Figs. 6-30 and 6-31 show selected positions from immersion test scans, some of which are reproductions of the above results. In contrast to the 22" sample shown in Fig. 6-30, the 16" sample presented in Fig. 6-31 has almost ideal cylindrical shape. Note that both scans can be processed with the same settings for surface detection, which emphasizes the robustness of the proposed approach.

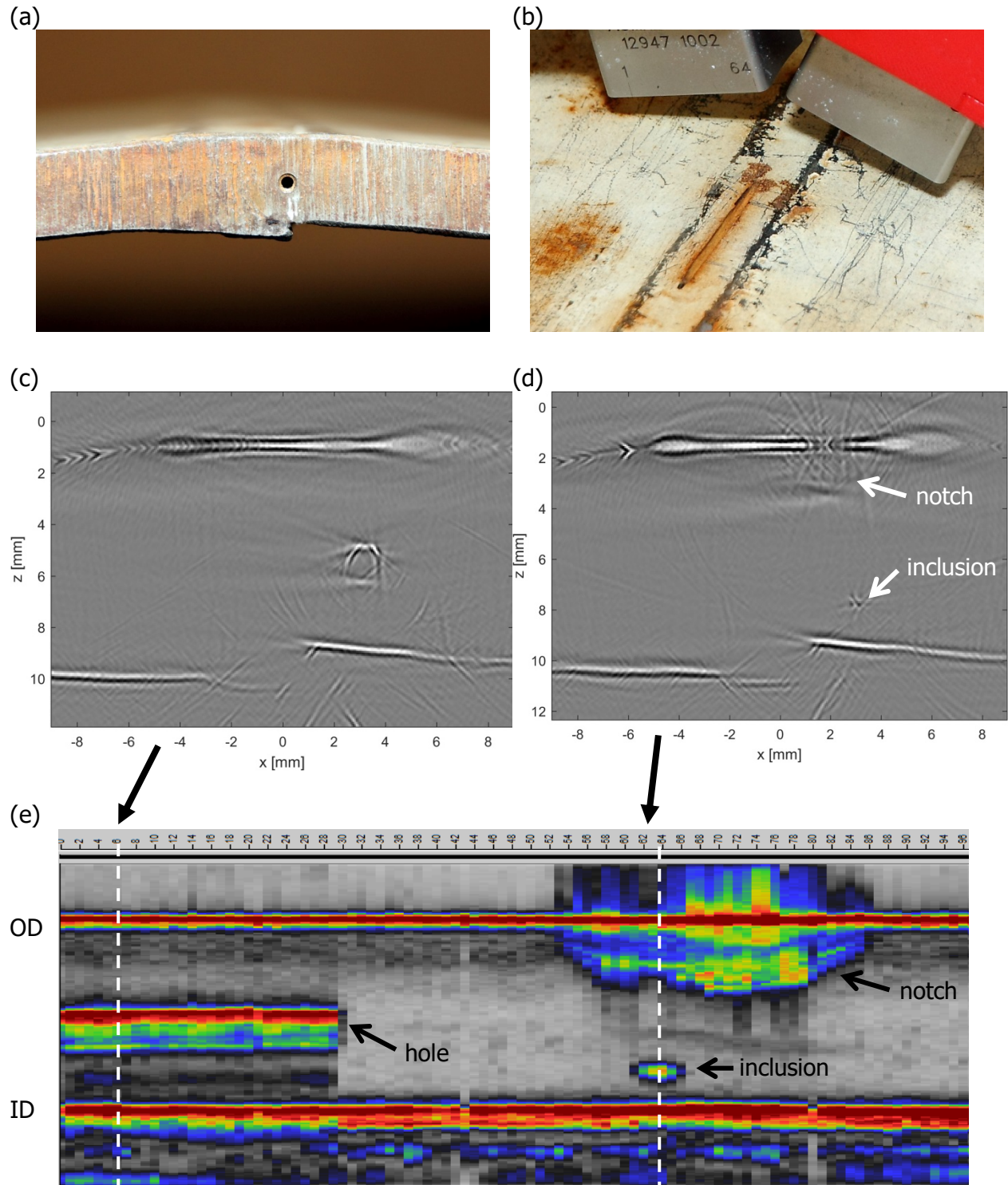


Figure 6-30: A 22" sample with offset plate edges containing a hole drilled along the axial direction (a) and a notch (b). The associated imaging results are shown in (c) and (d). The axial side view (e) shows the length and vertical positions of the indications over a scan length of 96 mm. A small, non-metallic inclusion is present below the artificial notch.

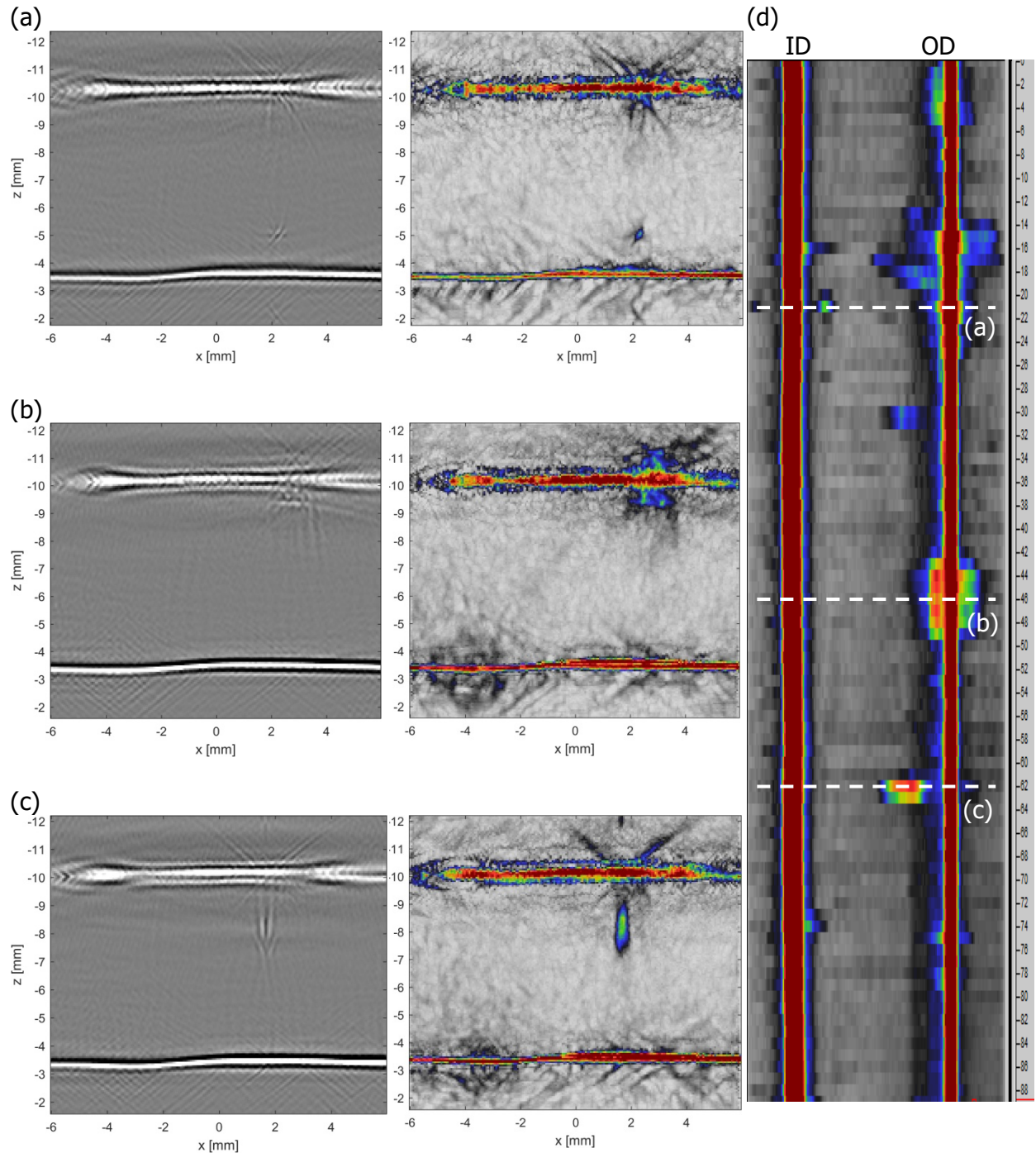


Figure 6-31: A 16" sample containing several flaws at different axial positions: shallow OD defect and small inclusion near the ID at the bond line (a), OD surface defect (b), cold weld without connection to the OD surface (c). Both unrectified (gray scale) and rectified (color) images are presented. The side view (d) with the ID on the left side and the OD on the right side provides an overview of the scanned section.

Development of software for viewing & interpretation of immersion IWEX scan files

In addition to the processing of FMC scans in Matlab, an implementation of an export function was produced to generate files that can be opened in the IWEX scan software. This way, the results obtained from immersion imaging can be evaluated with the same tools that are available for IWEX scans using plastic wedges.

Figure 6-32 presents a screen shot of the immersion scan of the 22-inch sample when viewed in the IWEX scan software showing the side-drilled hole and the notch as also shown in Figure 6-33.

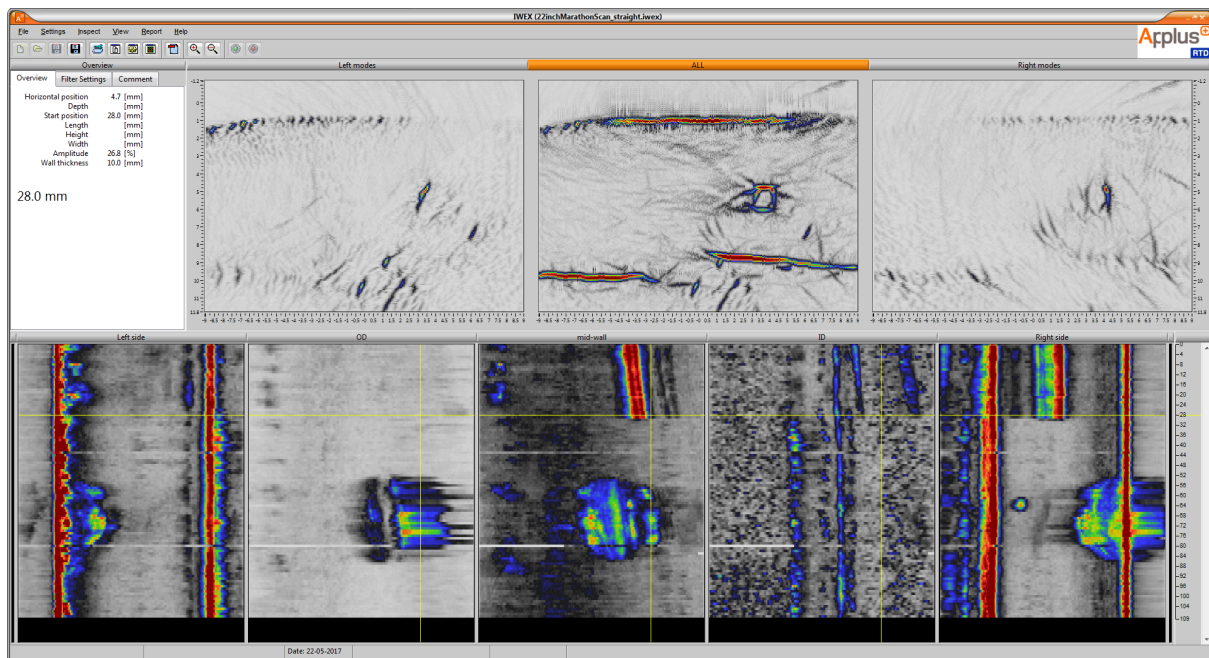


Figure 6-32: Immersion scan as shown in the scan software.

Time required for acquisition and processing

In this first implementation used to test the concept of immersion scans, the time required for scanning is currently about 15 seconds per axial section. With a typical step size of 1 mm in the axial direction of the pipe, this is equivalent to a scanning speed of only 4 millimeters per minute. Fortunately, the process can be accelerated:

- In the current test phase, the maximum length of each A-scan signal is recorded, whereas approximately only the first half is actually used for generating images.
- Currently, the full matrix capture dataset is built up by recording the signal of every source-receiver combination sequentially. This can be accelerated by transmitting with

one element, and then recording all receiver signals in parallel. The hardware system was only recently prepared to support this acquisition mode. In the long term, it should be possible to reduce the acquisition time for FMCs to a duration of about 1 to 2 seconds per scan position. After this step, further acceleration could be obtained by replacing the Gigabit Ethernet connection between hardware and computer with a connection providing higher data rate.

The processing of the raw data to generate images showing the weld with its geometry and potential flaws requires currently about one minute per axial scan position in the Matlab implementation. This is due to the various steps involved as shown in Fig. 6-36. Acceleration of the processing could be achieved by further parallelization and by reusing information from one scan position as initialization for the subsequent position. The speed of the surface detection would especially benefit from this approach.

However, the acceleration of the acquisition and processing is not part of the current project scope. It is suggested to revisit these options for implementation in a subsequent development phase.

Adaptation of immersion IWEX algorithms and software (OD profiling, ID profiling, immersion IWEX) for FMC-scans

The algorithms for the detection of the pipe surfaces were further improved. Two main changes were introduced as described in the following.

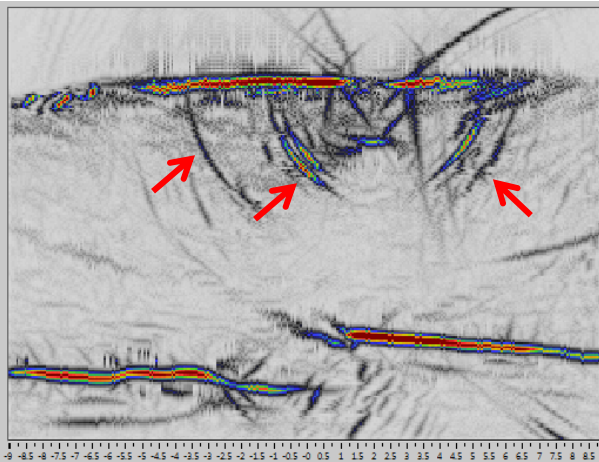
Increased robustness of OD interface detection

The correct determination of the OD surface profile is pivotal for the outcome of the immersion image. All IWEX immersion modes depend on sound paths being refracted at the outer material surface.

In the first version of the surface detection algorithm, the OD surface profile was smoothly interpolated, even in regions for which there was no clear detection result with sufficient amplitude. This can cause problems with sharp transitions at the outer pipe surface, for example in the case of selective seam corrosion.

For this reason, an updated version of the OD surface detection determines which points are to be taken into account for acoustic path calculations into the material. This leads to a significant reduction of artifacts around OD surface-breaking defects as shown in the case of an artificial notch in Fig. 6-33.

(a) Q15 result



(b) Q16 adaptation for artifact reduction

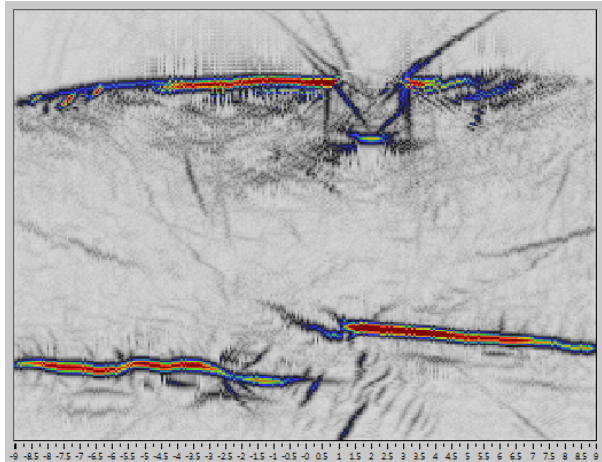


Figure 6-33: Images of an artificial notch at the OD surface created using the previous version of the IWEX immersion algorithm with artifacts indicated by the arrows appearing around the notch (a); updated version taking only valid OD points into account as described in the text (b).

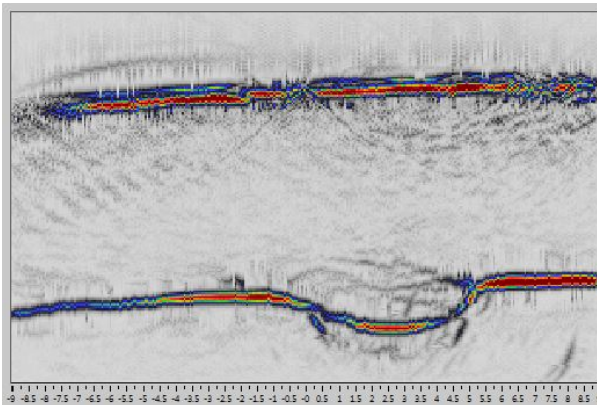
FMC scanning of lab samples

Additional samples were scanned in the Rotterdam lab. These scans were carried out to test the performance of the developed algorithms for immersion IWEX. In particular, the robustness of the method to changes in surface smoothness and ID shape were tested. For one scan, IWEX results were compared to phased array inspection.

Corroded sample

One test was carried out with an arc-welded sample exhibiting minor surface corrosion to test the performance of the immersion IWEX algorithms for rougher surfaces and regions of stronger curvature of the ID surface. The result of surface detection and defect imaging is shown in Fig. 6-34, confirming that the developed approach can tolerate surfaces with some mild corrosion that does not cover the entire surface. Furthermore, it is shown that the application of the method is not limited to ERW samples.

a) mild OD corrosion with no manufacturing flaw



b) mild OD corrosion with artificial 65% trough-wall ID surface-breaking flaw

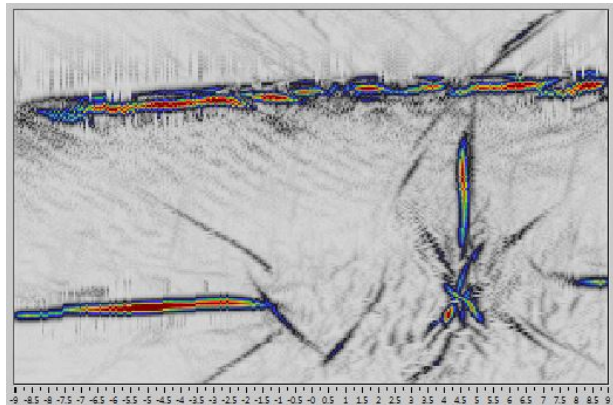


Figure 6-34: Images from a scan of an arc-welded sample with mild OD surface corrosion for two different positions on the sample.

24" sample with thick seam

Another particularly interesting sample was scanned using the immersion IWEX approach. This 24" ERW sample was described in the 12th quarterly report. It belongs to a section of about five feet length taken from a pipeline after identifying what was thought to be a possible fatigue crack. Rescanning of the sample in the lab in July 2016 showed the major anomaly that was identified in the field, but showed the anomaly was not a fatigue crack. Subsequently, 80 % of the section was used for destructive testing, confirming the major anomaly was a non-surface breaking upturned fiber with occasional small short laminations which could be described as stringers.

The misalignment of the IWEX modes that led to the misinterpretation was caused mainly by a thickened wall in the seam area apparently caused by post weld heat treatment. Figure 6-35 shows a photograph of one of the cuts, revealing the change in wall thickness around the seam area.

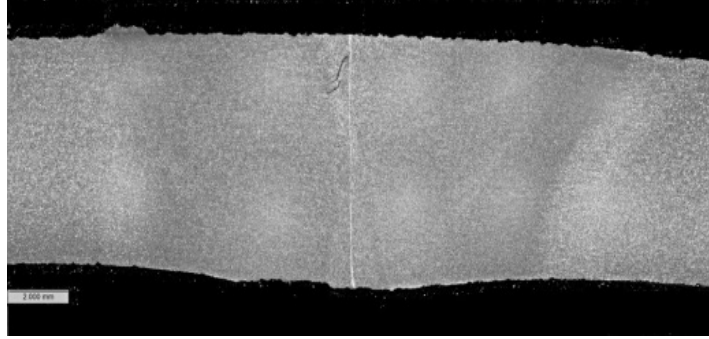


Figure 6-35: Metallographic section taken from the same joint, but at a different position than the scans shown in this report. The shape of the ERW seam with the thickened area close to the bond line is similar for the scan data presented.

The IWEX immersion was developed exactly for a case like this, as it is able to adapt to these changes in wall thickness. Therefore, the remaining sample from the same pipe was scanned using immersion IWEX.

An overview of the scan is shown in Figure 6-36. The position of the bond line can be identified in the top views. It can be seen that the arrays are slightly drifting off sideways in the course of the scan, about 2.7 mm over a scanning distance of 356 mm. This is due to the sample being scanned in the water tank without exact mechanical alignment between sample and scanner. However, it does not affect the performance of the inspection.

From the strip charts, longer indications just below the OD surface can be identified, as well as a few shorter indications at the ID. The latter can be found in the first third of the scan.

Additionally, the top views show that there are smaller, short indications to the left and right of the bond line. Most of them can be qualified as inclusions.

During testing, two independent scans were carried out on this sample. The sample was removed from the water tank between the scans and put back in a slightly different position. The images obtained after processing led to the same interpretation of the weld. The approach chosen is assumed to be robust to these minor changes in the exact geometry and alignment of the setup.

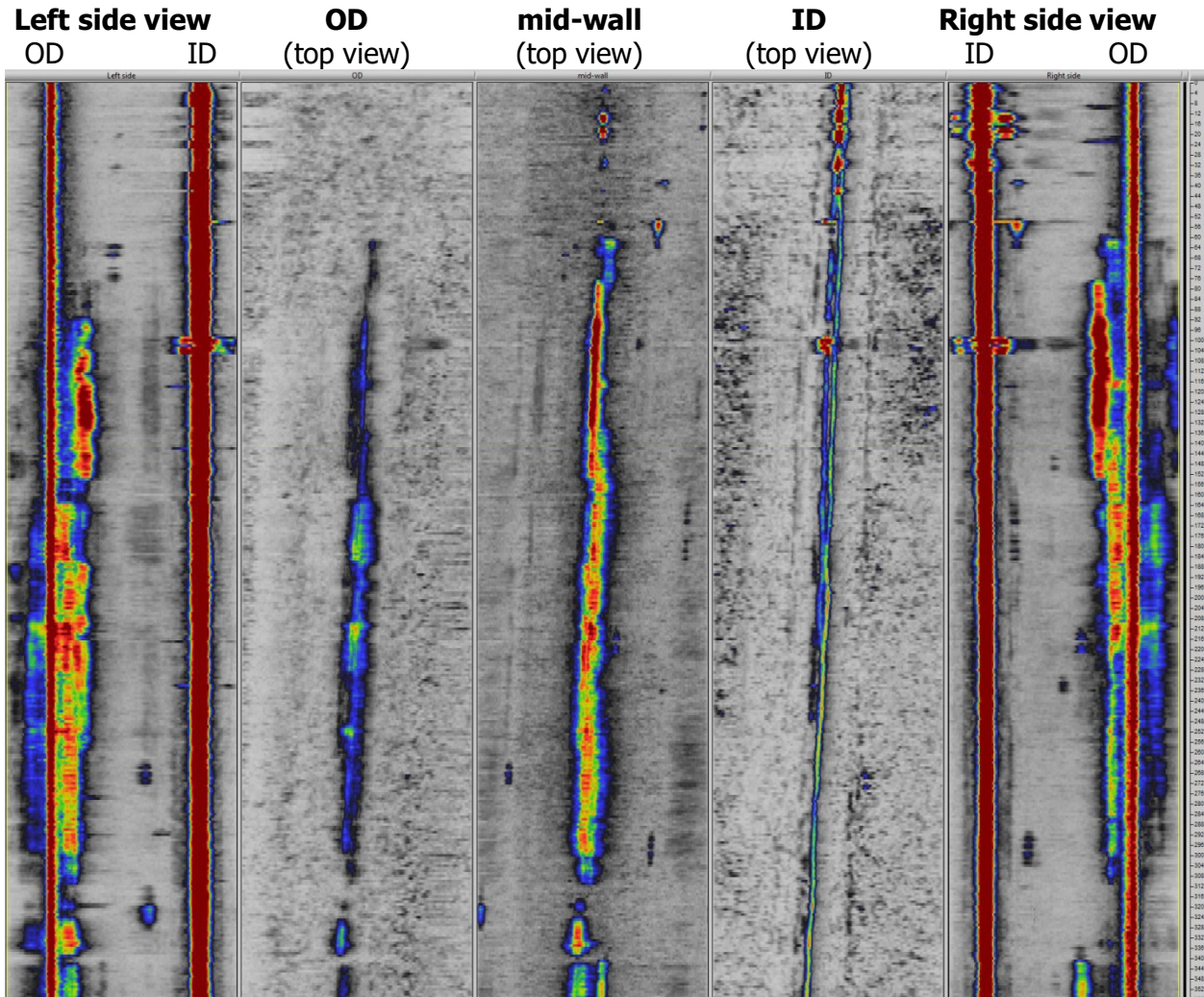


Figure 6-36: Strip charts (top and side views) of a ~14-in long IWEX immersion scan of a 24" ERW sample with increased wall thickness around the seam area.

Comparison of IWEX to phased array inspection

The 24" inch sample with thick seam was also inspected using phased array. This allows for a side-by-side comparison of strip charts as well as cross-sectional images. Several locations (A to E) were selected as shown in Fig. 6-37. Subsequently, the cross-sectional IWEX images and phased array sectorial scans are shown for each location. It can be seen that there are two indications present at each of the selected locations. For this particular sample, a combination of multiple indications at the same scan location can be seen as the rule rather than the exception.

The technician carrying out the phased array scan chose to evaluate only the ID flaws at locations A and C as relevant. However, starting from the IWEX result, it could be verified that the other indications can be detected and often sized using phased array as well.

One of the main differences in terms of evaluation is that immersion IWEX uses the actual OD and ID profiles, whereas phased array uses a nominal wall thickness of 7.2 mm.

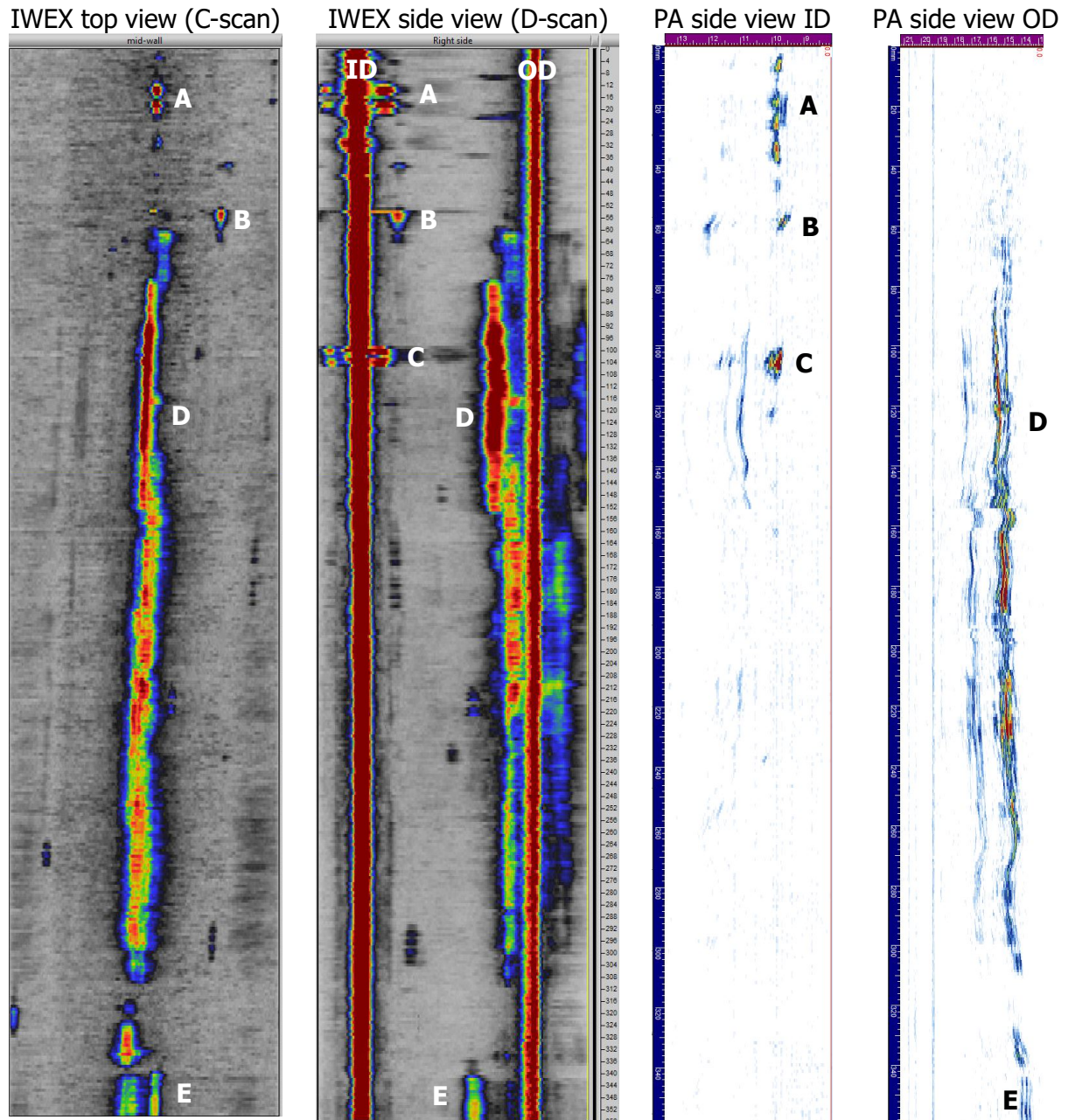
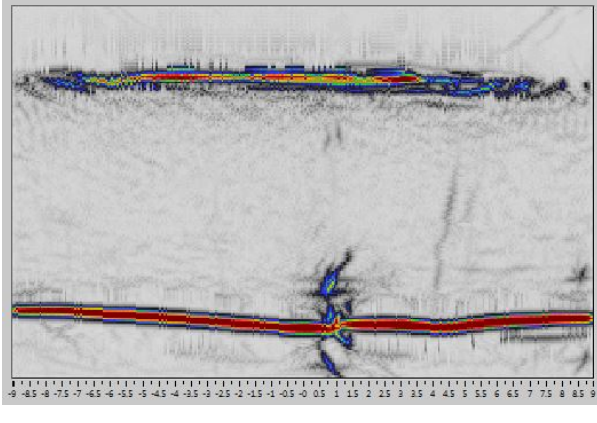
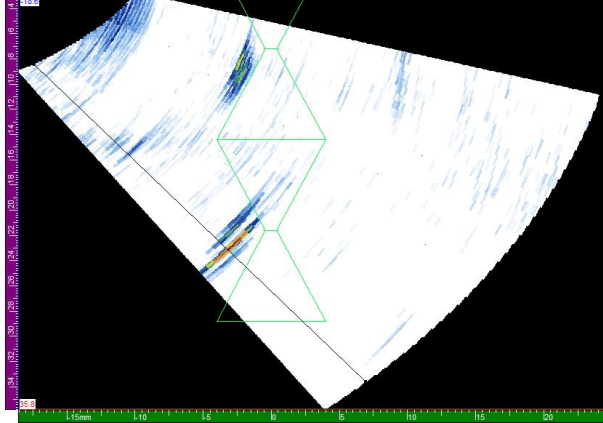


Figure 6-37: Top and side views of a 350mm long (~14-in) IWEX immersion scan of the 24" ERW sample along with phased array side views of the same sample. A few locations are marked for reference.

The following cross-sectional images allow for a side-by-side comparison of IWEX images and phased array (PA) sectorial views of the same indications. Characterization, position, and height are provided as well.

Note that the phased array inspection was set up in such a way that the indications can be found between half and full skip, and that sizing for smaller indications is in many cases simpler between 1.5 and 2 skips.

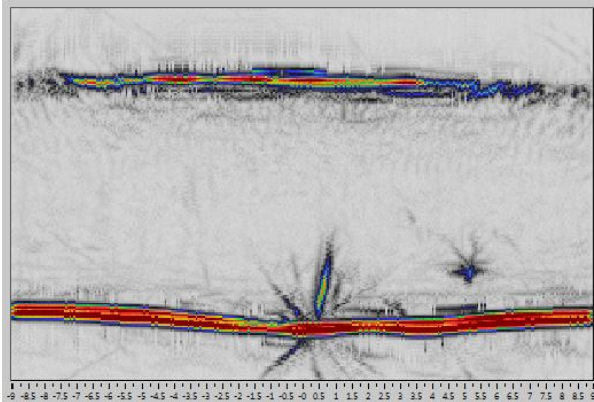
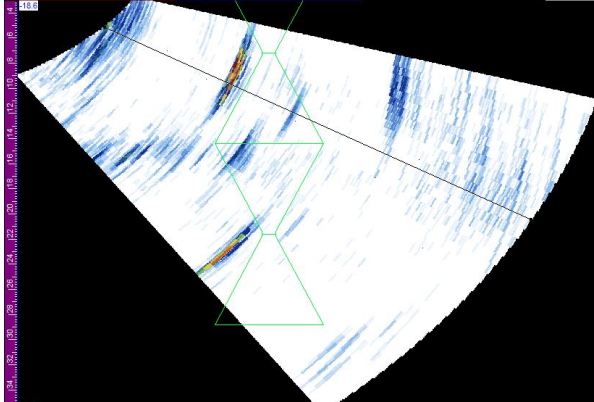
Figure 6-38. Location A

IWEX	Phased array
	
<p>Upper flaw: cold weld Height: 0.4 mm Depth from OD surface: 6.3 mm, WT: 7.7 mm Detected in IWEX-0 (direct), IWEX-1 (tandem)</p>	<p>Height: 0.5 mm Depth from OD surface: 6.6 mm Sizing: between 1.5 and 2 skips</p>
<p>Lower flaw: cold weld, surface-breaking Height: 0.4 mm Depth from OD surface: 7.3 mm, WT: 7.7 mm Detected in IWEX-0 (direct), IWEX-1 (tandem)</p>	<p>Height: 0.5 mm Depth from OD surface: 5.4 mm Sizing: between 0.5 and 1 skip</p>

Comparison:

- From the IWEX image, it can be seen that there are two separate flaws. If there was only one surface-breaking flaw, there would be an interruption of the image of the ID because of an acoustic shadow cast by the flaw. The phased array result may also be interpreted as one surface-breaking flaw.
- The vertical extent of the flaws can be determined from the IWEX image using tip diffractions. These can be seen for phased array as well, but sizing is slightly more difficult.

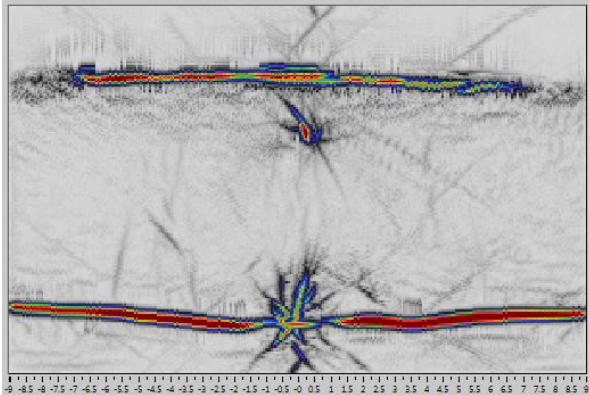
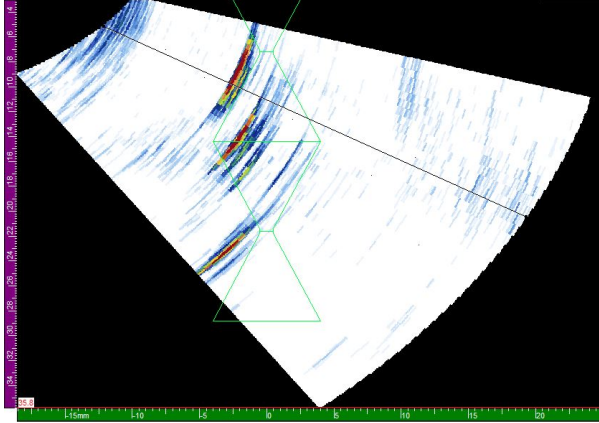
Figure 6-39. Location B

IWEX	Phased array
	
<p>Left flaw: cold weld Height: 0.4 mm Depth from OD surface: 6.3 mm, WT: 7.7 mm Detected in IWEX-1 (tandem)</p>	<p>Height: 0.9 mm Depth from OD surface: 5.3 mm Sizing: between 0.5 and 1 skip</p>
<p>Right flaw: inclusion Height: 0.2 mm Depth from OD surface: 5.6 mm, WT: 7.5 mm Detected in IWEX-0 (direct), IWEX-2 (skip)</p>	<p>Height: 0.6 mm Depth from OD surface: 4.4 mm Sizing: between 0.5 and 1 skip</p>

Comparison:

- Using phased array, the cold weld may be interpreted as surface-breaking flaw. From the IWEX image, it can be seen that there is a separation between the flaw and the ID surface.
- The sizing of the cold weld is difficult using tip diffractions. For phased array, the corner reflection at the ID surface was interpreted by the PA technician as the lower flaw tip, leading to oversizing.
- The inclusion is seen with phased array at a lateral position away from the bond line and with low amplitude. In IWEX, the position relative to the bond line and the extent of the flaw are clearly visible. Furthermore, the roundness of the shape can be derived from the fact that several IWEX modes show similar amplitudes. This means that sound is scattered similarly independent of the direction of insonification, allowing for characterization of the flaw.

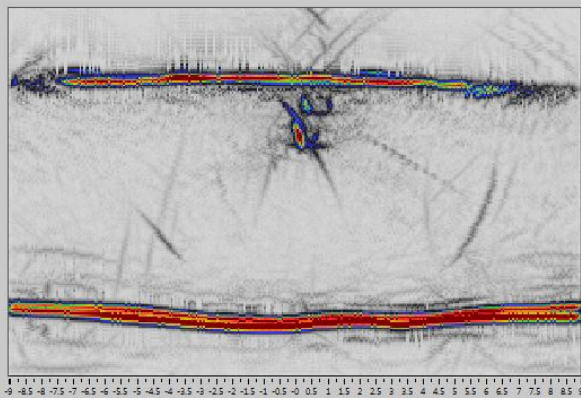
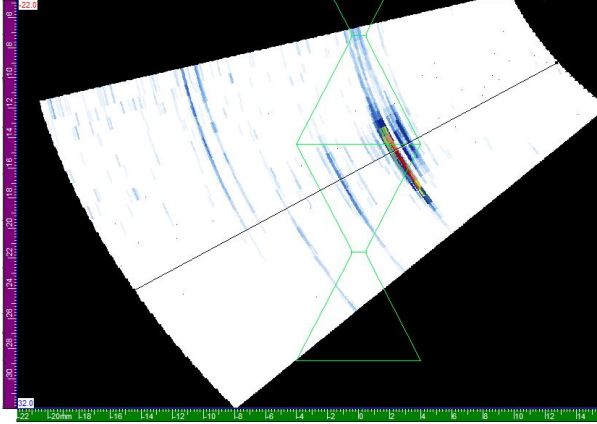
Figure 6-40. Location C

IWEX	Phased array
	
<p>Upper flaw: upturned fiber imperfection Height: 0.4 mm Depth from OD surface: 1.6 mm, WT: 7.7 mm Detected in IWEX-2 (skip)</p>	<p>Height: 1.0 mm Depth from OD surface: 0 mm Sizing: between 0.5 and 1 skip</p>
<p>Lower flaw: cold weld, surface-breaking Height: 1.0 mm Depth from OD surface: 7.3 mm, WT: 7.7 mm Detected in IWEX-0 (direct), IWEX-1 (tandem)</p>	<p>Height: 1.0 mm Depth from OD surface: 4.5 mm Sizing: between 0.5 and 1 skip</p>

Comparison:

- Both flaws can be detected using IWEX or phased array. However, characterization is more difficult with phased array. The curved shape of the upper flaw seen in the IWEX image allows this indication to be identified as upturned fiber imperfection. The lateral position with respect to the bond line supports this classification.
- The cold weld is determined to be surface-breaking. This is clearer from the IWEX image. The amplitude of the ID surface is significantly weaker at the bond line, caused by the flaw casting an acoustic shadow. Using the nominal wall thickness, phased array determines the vertical extent similarly, but does not confirm the connection to the ID surface.
- The upturned fiber imperfection is determined to be larger with phased array. This can be explained by its orientation being not normal to the pipe surface. The distance between the tip diffractions along the sound beam is greater than the actual vertical extent of the flaw. This may cause oversizing. IWEX generates an image showing the actual orientation and the vertical extent of the flaw.

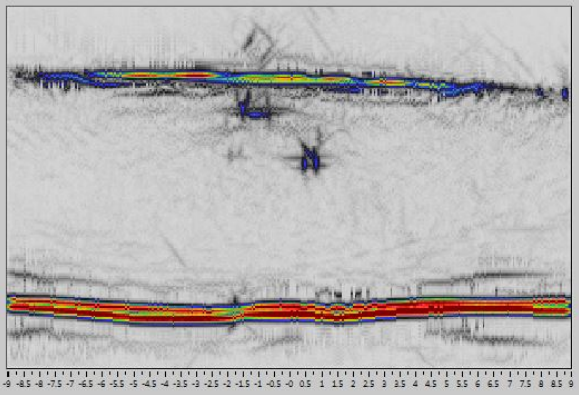
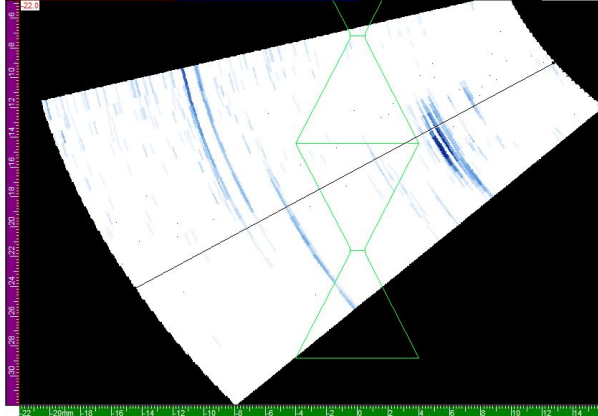
Figure 6-41. Location D

IWEX	Phased array
	
<p>Upper flaw: upturned fiber imperfection Height: 0.6 mm Depth from OD surface: 0.6 mm, WT: 7.6 mm Detected in IWEX-2 (skip)</p>	<p>Height: undetermined (<0.5 mm) Depth from OD surface: 0.1 mm Sizing: between 0.5 and 1 skip</p>
<p>Lower flaw: upturned fiber imperfection Height: 0.7 mm Depth from OD surface: 1.4 mm, WT: 7.6 mm Detected in IWEX-2 (skip)</p>	<p>Height: undetermined (<0.5 mm) Depth from OD surface: 0.4 mm Sizing: between 0.5 and 1 skip</p>

Comparison:

- Phased array shows two signals just below the cap. These may be interpreted in multiple ways:
 - as one flaw, not surface-breaking,
 - as two smaller flaws, not surface breaking, or
 - as one surface-breaking and another smaller flaw.
- IWEX shows the shape and relative alignment of two separate flaws. The shape seen in the IWEX image allows the flaws to be identified as upturned fiber imperfections. This classification of flaw type is not possible with phased array.
- The IWEX image also rules out the possibility of the indications being surface-breaking. The image of the OD surface can be seen; it is not interrupted or weakened at the location of the upturned fiber imperfections.

Figure 6-42. Location E

IWEX	Phased array
	
<p>Upper flaw: upturned fiber imperfection Height: 0.3 mm Depth from OD surface: 1.0 mm, WT: 7.6 mm Detected in IWEX-2 (skip)</p>	<p>Height: 0.7 mm Depth from OD surface: 0.1 mm Sizing: between 0.5 and 1 skip</p>
<p>Lower flaw: upturned fiber imperfection Height: 0.3 mm Depth from OD surface: 2.5 mm, WT: 7.6 mm Detected in IWEX-2 (skip)</p>	<p>Height: undetermined (<0.5 mm) Depth from OD surface: 0.6 mm Sizing: between 0.5 and 1 skip</p>

Comparison:

- The indications seen by phased array are relatively weak. This seems to be caused by a decrease in acoustic coupling as this particular scan position.
- Flaw discrimination is not possible using phased array. In the IWEX image, the shape of the flaws and the position relative to the bond line as seen at other scan positions allow for identification as upturned fiber imperfections.
- Although these two imperfections are small, the IWEX image allows for identification of the upper and lower flaw tip, whereas the phased array sectorial scan does not provide this level of detail, despite of the fact that both techniques use the same array frequency of 10 MHz.

From the comparison of the IWEX cross sections to phased array sectorial scans, the following observations can be made and conclusions can be drawn:

- Discrimination of flaw types is not possible with phased array, but achievable with IWEX. This enables distinction between benign anomalies and critical flaws.
 - Cold welds can be found with vertical orientations at the bond line.
 - Upturned fiber imperfections are characterized by the J- or L-shape seen in the IWEX image.
 - Small inclusions can be seen from different sides with similar amplitude.
- When several indications are present at the same scan position, separation and association of observed tip diffractions to different flaws is more difficult with phased array. There is an increased risk that separate flaws may be interpreted as one, which usually leads to oversizing. The alignment provided by the adaptive immersion IWEX is helpful for interpreting a combination of indications at the same scan position.
- Height sizing results are often similar between phased array and IWEX. However, greater uncertainty is expected for phased array for complex flaws, multiple flaws, or tiny flaws.
- Determination of depth and remaining ligament to surface is relatively easy with IWEX, but inaccurate with phased array when using the nominal wall thickness as a reference.
- IWEX strip charts provide a clearer overview of the weld.

Development of software for full-matrix-capture recording of seam scans

In the final quarter of the Phase II, hardware, software, and processing tools were developed for performing scans with a flexible, water-filled cushion. In order to carry out adaptive scanning, full matrix capture data must be recorded. Subsequently, this data is processed offline to generate scan files to be used for evaluation.

A first attempt of creating an application for full matrix capture (FMC) scans as described earlier was improved with the following modifications:

- While performing full matrix captures, new settings have to be sent to the hardware at regular intervals, and raw A-scan signals have to be received alternately. The robustness of the scan software was significantly increased by aligning the timing of these operations.
- The user can enter a scan start position and perform scans based on a calibrated position encoder. This way, FMC scans refer to the actual position on the sample.
- The raw acquisition signals of both array probes can be checked visually during scanning, such that the coupling condition of the water wedge can be monitored.

- The user interface provides feedback on the scanning speed. As the movement of the scanner is controlled separately, it is important to ensure that the acquisition can keep up with the movement of the wedge on the sample.

Figure6-43 presents the main scan window shown during acquisition. It enables the user to check signal quality and monitor scan progress.

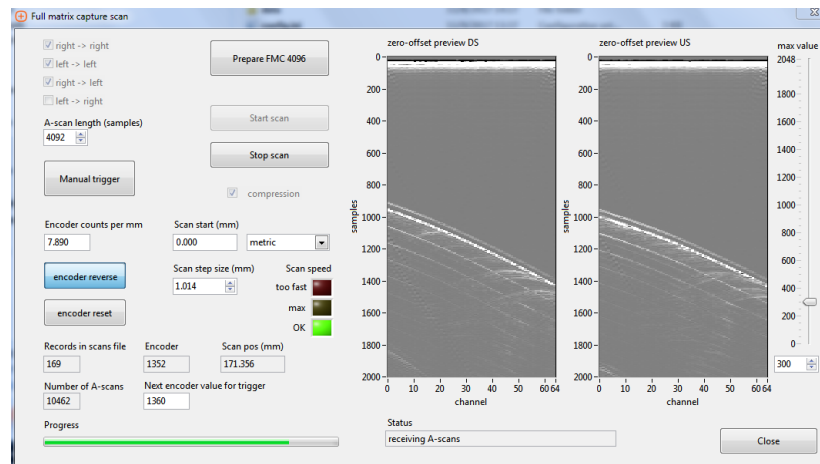


Figure 6-43: Screenshot of the acquisition software.

The current duration of an acquisition cycle is about 5.5 seconds per scan position. This limits the achievable scanning speed. In the long term, acceleration is possible either using additional software adaptations or increasing the memory bandwidth of the connection between acquisition hardware and computer.

Development of software for viewing and interpreting immersion IWEX scan files

After acquisition, the raw full matrix capture is processed to generate scan files, which can be opened using the same scan or viewer software that is used for IWEX scans with plastic wedges. With the recent updates of these programs, it was ensured that the immersion scans are still compatible and can be displayed correctly, such that evaluation can be performed in the viewer software (IWEX processor).

The calibrated scan positions used for obtaining full matrix capture data were transferred to the generated immersion scan files, such that the axial position of the flaws in the sample can be determined with high accuracy.

Delivery of immersion probes

The flexible wedge was finally delivered near the end of the project allowing testing outside of an immersion water tank. The metal housing was designed to fit the array probes previously

used for scans in the water tank. A flexible membrane is used to ensure contact with curved surfaces of various shapes. Figure 6-44 and 6-45 present photographs of the assembly and the membrane.

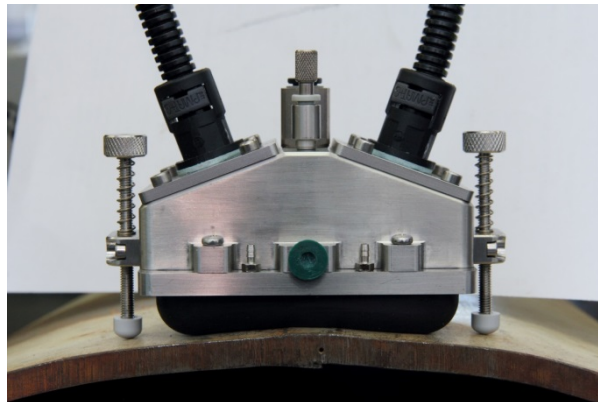


Figure 6-44: Flexible wedge as used on the pipe for scanning.



Figure 6-45: Flexibility of the water-filled wedge when pushed.

The membrane was designed to fit pipe diameters between 8.625-inch and 48-inch. In practical tests, it has already been verified that it can be used for 12.75-inch and 24-inch diameter as well as flat surfaces.

To perform scans, the flexible wedge is filled with water as shown in Figure 6-46. During tests, it has been established that only low pressure is required to obtain good acoustical coupling with the sample surface.

As with all ultrasound measurements it is important to couple the ultrasound into the pipe and prevent air bubbles and gaps which prevents efficient ultrasound transmission. Thus, it was important to remove all air bubbles inside the balloon and prevent an air gap between the membrane and steel surface.

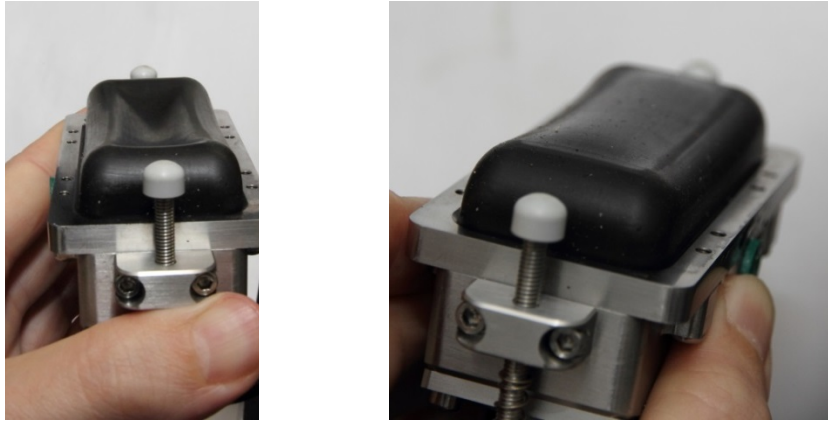


Figure 6-46: Shape of the membrane when the wedge is empty (left) and when the wedge is filled with water (right).

The filling of the wedge is a delicate procedure. Likewise, the force applied to put the wedge in contact with the pipe surface needs to be tuned to ensure correct coupling. At the same time, the force should be limited and the sample must be kept wet when the wedge is moved to reduce wear of the membrane. Examples of excessive and insufficient force are shown in Figure 6-47.

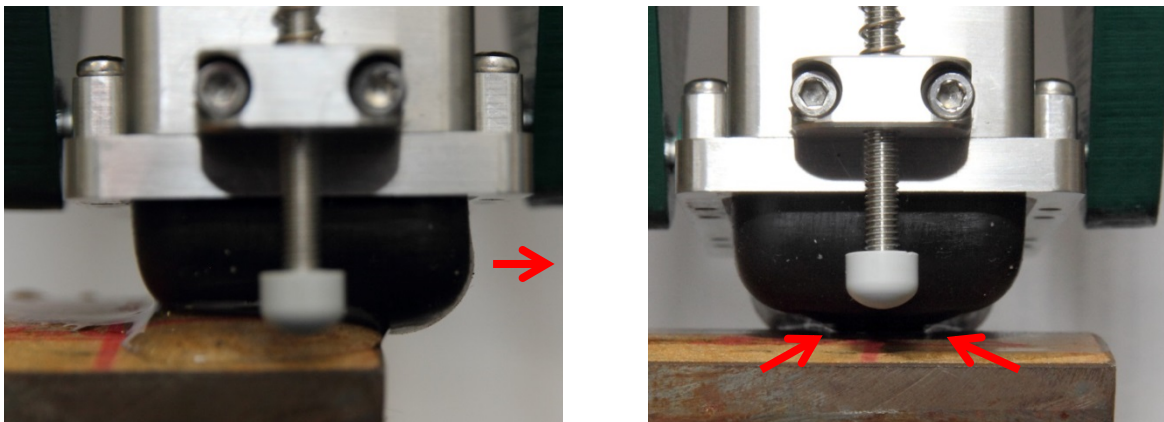


Figure 6-47: Bulging of the membrane when the applied force is too high (left) and insufficient contact when the force is too low (right).

A manual has been written to guide the complex process of immersion scans with the following steps:

- 1) Encoder calibration,
- 2) Determination of the maximum scanning speed,
- 3) Assembly and filling of the flexible wedge,
- 4) Acquisition of full matrix captures on a flat sample for calibration purposes,
- 5) Positioning of the wedge on the sample,
- 6) Steps required for performing a scan,
- 7) Preparation of files for transfer and off-line processing,

When comparing the signals acquired with the flexible wedge to scans taken in the water tank, it can be seen that the flexible membrane introduces a weak additional interface echo just before the reflection off the outer surface of the sample as shown in Figure 6-48. This additional reflection has no adverse influence on the resulting images. In the processing, the extra layer of membrane material has been neglected without perceivable impact on the scans.

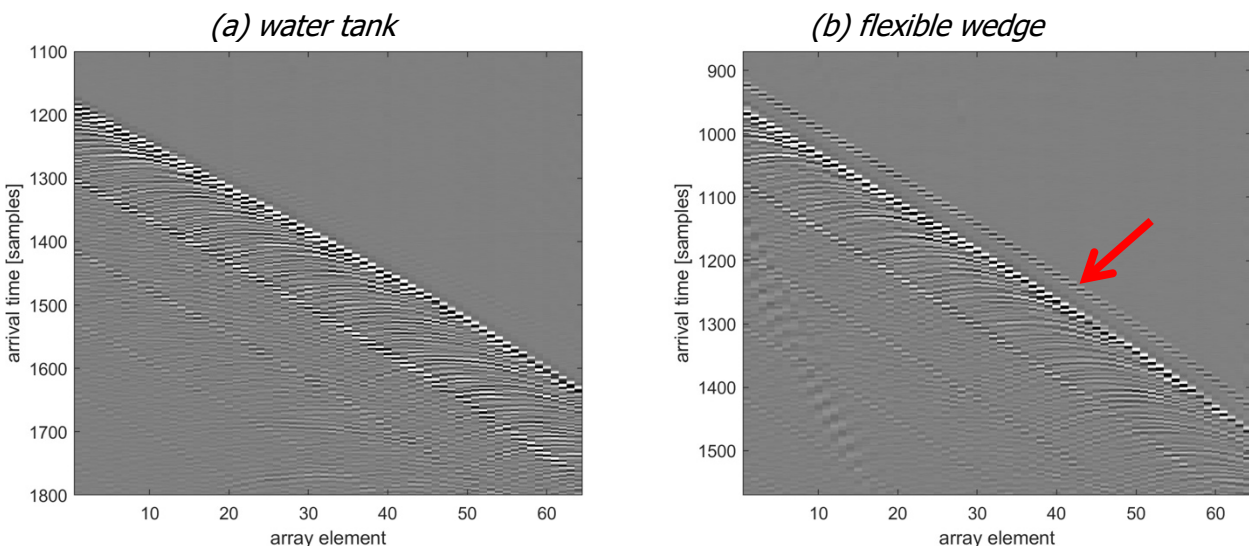


Figure 6-48: Zero-offset datasets (pulse-echo signal per array element) for signals acquired in the water tank (a) and with the flexible wedge (b). The reflection from the outer surface of the sample is followed by multiple internal reflections between the outer and inner surfaces. With the flexible wedge, an extra arrival due to the inner echo from the membrane is indicated by the arrow.

Modification of the linear scanner probe holder for water wedge measurements of seam-welds

In order to enable scanning of seam welds and stress corrosion cracking with adaptive IWEX using the flexible wedge, some adaptations of the scanning system were required.

- The linear axis controlling the movement of probes needed to be driven by a motor allowing for the slow scanning speeds currently required for adaptive IWEX.
- The probe holder developed for performing IWEX scans with plastic wedges needed to be adapted to hold the flexible wedge with the two arrays mounted at a fixed angle and distance with respect to each other. To this end, some modifications were required. The frame holding the plastic wedge is replaced by the metal housing around the immersion probes. The pressure shaft applying a force normal to the pipe surface to ensure contact between the membrane and the pipe is connected directly to the metal housing as can be seen in Figure6-49.

After these adaptations, the system was tested on a pipe sample as described in the following section. A photograph of the setup is shown in Figure6-48.

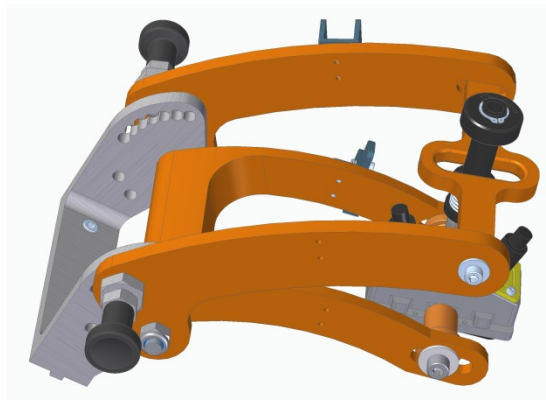


Figure 6-49: Adaptation of the probe holder for the linear scanner to accommodate the flexible wedge.

FMC scanning of lab samples

Additional scans were carried out in the 17th quarter to compare the data acquired in the water tank to signals obtained with the flexible wedge on the same samples. A photograph of the scan setup is shown in Figure6-50.

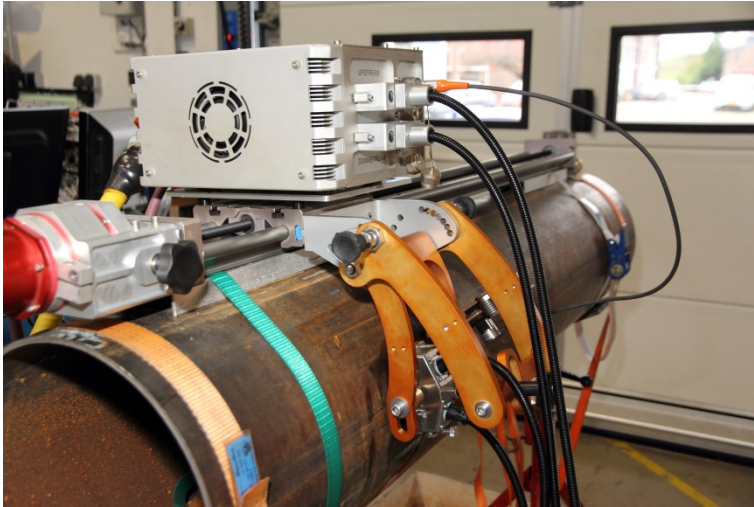


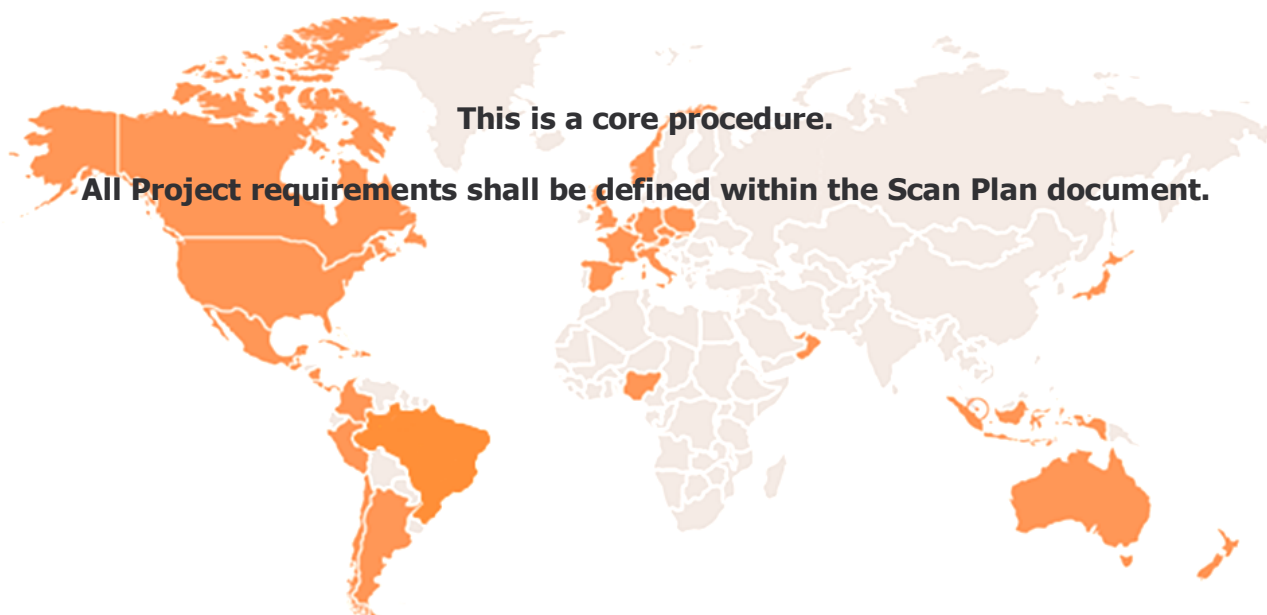
Figure 6-50: Wedge mounted in the probe holder for performing a test scan.

APPENDIX A

IWEX RTD™ WRITTEN PROCEDURE – REVISION 0

During development and trials a written procedure was developed. The procedure has evolved as experience was gained with IWEX. A copy of the RTD IWEX™ procedure is included below and should be considered representative and not necessarily the final version that will be used going forward as it is expected to evolve. For instance, as of writing of the Phase II report there is no generally accepted industry practice for producing UT images from FMC data and as one is developed it is expected this technology specific procedure will evolve with industry practice.

GENERAL PROCEDURE FOR RTD IWEX ULTRASONIC LONGSEAM AND PIPE BODY EXAMINATION



Development – Revisions					
Revision No.	Prepared By	Date	Approved By	Date	Amendment Details
00	Jeff Vinyard	January 8, 2018			Initial procedure

Prepared By:		Reviewed By:		Approved By:	
Date		Date		Date	

This publication is the intellectual property of Applus+ RTD and may not be used in whole or in part for any purpose other than the business of Applus+ RTD and may not be used for the business of the recipient and may not be passed to any other person without the permission of Applus+ RTD.

Inquiries in Canada can be directed to:	
Company	Applus+ RTD
Address	5504 – 36 Street
Place	Edmonton, Alberta T6P 3B3
Country	Canada
Phone	+1 780 440 6600
Fax	+1 780 440 2538
Internet	www.applusrtd.com

Inquiries in the USA can be directed to:	
Company	Applus+ RTD
Address	Suite 200,11801 S Sam Houston Parkway W
Place	Houston, TX 77031
Country	United States of America
Phone	+1 832 295 5000
Fax	+1 832 295 5001
Internet	www.applusrtd.com

Inquiries in Europe can be directed to:	
Company	Applus+ RTD
Address	Delftweg 144, 3046 NC Rotterdam
Place	P.O. Box 10065, 3004 AB Rotterdam
Country	The Netherlands
Phone	+31 10 716 6000
Fax	+31 10 415 8943
Internet	www.applusrtd.com

Inquiries in Asia can be directed to:	
Company	Applus+ RTD
Address	No.70 Kian Teck Road
Place	628798
Country	Singapore
Phone	+65 6430 0665
Fax	+65 6898 9704
Internet	www.applusrtd.com

Inquiries in Australia can be directed to:	
Company	Applus+ RTD
Address	94 Discovery Drive
Place	Bibra Lake
Country	Western Australia 6163
Phone	+61 8 9410 9300
Fax	+61 8 9410 9380
Internet	www.applusrtd.com

CONTENTS

1	INTRODUCTION	5
2	SCOPE	5
3	REFERENCES	5
3.1	<i>Internal Documents</i>	5
3.2	<i>Codes and Standards</i>	5
3.3	<i>COMPANY Specific Documents</i>	5
3.4	<i>Reference Documents</i>	5
3.5	<i>Abbreviations</i>	6
3.6	<i>Definitions</i>	6
4	PERSONNEL QUALIFICATIONS	7
4.1	<i>System Operator</i>	7
4.2	<i>Scanner Technicians</i>	7
5	SYSTEM EQUIPMENT DESCRIPTION	7
5.1	<i>Array and Multi-Channel Ultrasonic Equipment</i>	7
5.2	<i>System Minimum Requirements</i>	7
5.3	<i>Recording</i>	8
5.4	<i>Scanner and Umbilical</i>	9
6	SYSTEM HARDWARE SETTINGS	9
6.1	<i>IWEX Array Probes</i>	9
6.2	<i>Probe Frame Layout</i>	9
6.3	<i>Parameters of System Inspection Program</i>	10
6.4	<i>Essential Variables for IWEX Modes</i>	10
6.5	<i>Scanning Preparation & Surface Condition</i>	10
6.6	<i>Reference Line</i>	10
6.7	<i>Datum Point</i>	10
6.8	<i>Acoustic Coupling Fluid</i>	10
7	SYSTEM SOFTWARE SETTINGS	10
7.1	<i>General</i>	10
7.2	<i>IWEX Image Settings</i>	11
8	SCAN QUALITY CONTROL	12
8.1	<i>Calibration</i>	12
8.2	<i>Scanning Direction</i>	13
8.3	<i>Coupling Criteria</i>	13
8.4	<i>Step-by-Step Description of a Seam Weld or Pipe Body Examination</i>	13
9	INTERPRETATION OF RESULTS	14
9.1	<i>General</i>	14
9.2	<i>Artifacts</i>	14
9.3	<i>Imperfection Length</i>	14
9.4	<i>Imperfection Height</i>	14
9.5	<i>Imperfection Depth</i>	15
9.6	<i>OD/ID Ligament</i>	15
9.7	<i>Imperfection Horizontal Positioning (Radial, across the seamweld, or circumferential location in relation the the center of the probes and the first of a series of scans used to map SCC)</i>	15

9.8	<i>Interaction</i>	15
10	REPORTING CRITERIA	15
11	REPORTING	16
12	STORAGE OF DATA	16
Attachment 1 – Explanation of Methodology		17
Attachment 2 – Example Site Report		22
Attachment 3 – Decision Flow Chart		24

1 INTRODUCTION

Applus+ RTD provides a field-proven **In**verse **Wave** field **Ex**trapolation (IWEX) Automated Ultrasonic Testing (AUT) system, trademarked as RTD IWEX™ (hereafter referred to as System). The system was developed for the inspection of girth and longseam welds. Real time recording of inspection results utilizing array probe technology characterizes RTD IWEX.

The purpose of this procedure is to describe generic system configurations and methodology of Applus+ RTD IWEX AUT inspection process, to determine longseam and pipe body integrity.

For a more detailed description and explanation of the methodology refer to Attachment 1.

The project parameters will be documented in the Scan Plan(s) which shall accompany this document, describing as a minimum the following items:

- ⊕ Reference Specification(s);
- ⊕ Detailed project scope (DIA, WT, WPS);
- ⊕ Inspection setup configuration;
- ⊕ Probe selection;
- ⊕ Probe frame layout;
- ⊕ System parameter setup.

2 SCOPE

The System is based upon the IWEX Ultrasonic Imaging Technique.

The weld is inspected using 2D IWEX images of the weld cross-section at a sufficient number of positions of the longseam to cover the entire volume of the weld or the pipe body when not inspecting the weld. The images are constructed based on ultrasonic measurements obtained from ultrasonic arrays. The measurement at each linear position consists of a Full Matrix Capture (FMC) using all possible combinations of source–receiver elements of the array probes. The full matrix capture data is processed into IWEX images and the data is then transferred to a computer for data presentation, analysis and storage. The FMC is not stored, only the IWEX image data. A 3D presentation of the weld can be generated by the combination of 2D images along the length of the scan.

3 REFERENCES

3.1 *Internal Documents*

Relevant internal documents specific to region and application will be referenced within the Scan Plan.

3.2 *Codes and Standards*

Applicable Codes and Standards will be defined within the Scan Plan.

3.3 *COMPANY Specific Documents*

Documents as supplied and required by COMPANY will be defined within the Scan Plan.

3.4 *Reference Documents*

3.4.1 *Internal documents*

- ⊕ Applus+ RTD Written Practice, specific to the region;
- ⊕ Applicable Scan Plan(s).

3.5 Abbreviations

AUT	Automated Ultrasonic Testing	DIA	Diameter
ECA	Engineering Critical Assessment	ERW	Electric Resistance welding
FMC	Full Matrix Capture	FSW	Friction Stir Welding
HAZ	Heat Affected Zone	ID	Internal Diameter
IWEX	Inverse Wave field Extrapolation	NDT	Nondestructive Testing
OD	Outside Diameter	PCS	Probe Center Separation
PE	Pulse Echo	PRF	Pulse Repetition Frequency
SCC	Stress corrosion cracking	UT	Ultrasonic Testing
WT	Wall Thickness	WPS	Welding Procedure Specification

3.6 Definitions

- + **AUT CONTRACTOR** Applus+ RTD.
- + **System Operator or Operator** refers to the person responsible for all ultrasonic aspects of the inspection, recording and interpretation of results.
- + **COMPANY** shall mean owner and shall include their engineering agencies, inspectors and other authorized representatives. COMPANY will be defined within the Scan Plan.
- + **Cycle** is the complete set of measurements in which all sequences are consecutively run.
- + **Defect** is an imperfection of sufficient magnitude to warrant rejection based on the criteria referenced by this procedure.
- + **Depth** of the imperfection is the through-wall distance to the bottom of the imperfection as measured from the outside diameter of the pipe.
- + **Imperfection** is a discontinuity or irregularity that is caused by the welding process and is not related to geometry indications.
- + **Indication** is evidence obtained by non-destructive testing.
- + **Instruction** is a description of the steps to be followed when performing an NDT procedure.
- + **Length** of an imperfection will be defined as the length of the indication in the scan direction.
- + **May** is a verbal form used to indicate a course of action permissible within the limits of the procedure.
- + **Procedure** is a step-by-step description of the application of an NDT method.
- + **Scanner Technician** refers to the person responsible for maintaining and operating the AUT scanner.
- + **IWEX Mode** is how many sound reflections the system uses to create the image of the flaw, defining the sound path from transmitting array element to image grid point to receiving array element.
- + **Full Matrix Capture** is a specific case of Matrix Capture where the recording of coherent time domain signals is carried out using a *closed* and *complete* set of transmit and receive combinations, and the resulting dataset of such a recording..
- + **Matrix Capture** is the recording of coherent A-scan time domain signals from distributed combinations of transmitting and receiving elements, and the resulting dataset of such a recording.
- + **IWEX** is a data processing scheme, making use of FMC data, producing images of the region of inspection. Refer to Attachment 1 for a full explanation.
- + **Sequence** is a separate ultrasonic function (measurement) as executed within a cycle. Channel numbers are allocated to a sequence to associate them with a probe connection.
- + **Shall** is a mandatory term, from which no deviation is permitted.
- + **Should** indicates that among several possibilities, one is recommended as particularly suitable, without mentioning or excluding others, or that a certain course of action is preferred but not necessarily required.
- + **Through Wall Height** dimensions of the imperfection will be called the "Vertical Height" of the imperfection.

4 PERSONNEL QUALIFICATIONS

4.1 System Operator

- ⊕ Be qualified in accordance with the Applus+ RTD "Written Practice", specific to the region;
- ⊕ Only accredited personnel qualified to level II or Level III UT shall interpret the test results;
- ⊕ Be trained and passed Applus+ RTD in-house course for RTD IWEX for long seams.

4.2 Scanner Technicians

- ⊕ Be trained in using an AUT-scanner to the satisfaction of the System Operator.

5 SYSTEM EQUIPMENT DESCRIPTION

5.1 Array and Multi-Channel Ultrasonic Equipment

Array and multi-channel ultrasonic equipment shall be used, capable of measuring an adequate number of source-receiver element combinations (FMC's) and capable of processing IWEX images to ensure a complete volumetric examination of the through weld or material body thickness.

IWEX images can be constructed using different sound paths, referred to as 'IWEX modes'. The equipment shall allow that each IWEX mode can individually be selected to allow for color palette adjustment and gain added or removed to ensure imaging of all relevant reflectors.

5.2 System Minimum Requirements

The system meets the minimum requirements detailed in the following sub-sub sections:

5.2.1 Software

System software is IWEX for Seamweld Inspections version 2.0.1 or higher.

5.2.2 Global Parameters

Table 1 – Minimum requirements for the global parameters

Gain (overall gain):	-100 dB to +100 dB (0.1 dB increments)
Pulse voltage:	(1 V increments)
Pulse repetition frequency:	Up to 10 KHz
Pulse shape:	Unipolar / Bipolar
Sampling frequency:	50 / 100 MHz (as a minimum 5x center frequency)

5.2.3 Scan Parameters

Table 2 – minimum requirements for the scan parameters

Scan length:	Up to 5m, resolution 0.5-1.0 mm
⌚ Motor control speed:	0-100%
Invert scan direction:	Enable / Disable
Note: Scan length should be considered for file size	

5.2.4 Encoder Parameters

Table 3 – Minimum requirements for the encoder parameters

Trigger mode:	Auto / encoder / software
Resolution:	0.5 mm minimum or 2 (counts/mm)

Scan direction:	Forwards / Reverse
-----------------	--------------------

5.2.5 Material Parameters

Table 4 – Minimum requirements for the material parameters

Longitudinal sound wave velocity:	5950 m/sec (default)
Transversal sound wave velocity:	3250 m/sec (default)

5.2.6 Array Parameters

Table 5 – Minimum requirements for the array parameters

Number of elements:	Maximum 64 per probe
Center frequency:	1 – 15 MHz
Element pitch:	0 – 4 mm depending on probe specifications

5.2.7 Wedge Parameters

Table 6 – Minimum requirements for the wedge parameters

Sound velocity of wedge material:	1400-2500 m/sec
Wedge angle:	0 – 45° with increments of 0.5°
Horizontal and vertical index:	0 – 100 mm with increments of 0.1 mm
Distance to weld centerline:	0 – 100 mm with increments of 0.1 mm
Probe latency:	0 – 1000 ns with increments of 1 ns
Probe shift downwards (mm)	0 – 10 mm
Rotation (degr.)	0 – 10°

5.2.8 Image Area Parameters

Table 7 – Minimum requirements for the image area parameters

Image size (height and width):	0 – 50 mm with increments of 1 mm
Image positioning (relative to weld centerline and volume):	Increments of 1 mm
Masking of modes:	Enable / Disable
Masking area (height, width and position)	Increments of 1 mm

5.2.9 IWEX Mode Parameters

Table 8 - Minimum requirements for the IWEX mode parameters

Gain per IWEX mode:	-100 to +100 dB with increments of 0.1 dB
IWEX mode selection:	Enable / Disable

5.2.10 Signal to Noise

- ⊕ Electronic noise shall be lower than acoustical noise in the images from all IWEX modes.

5.3 Recording

System inspection results shall be presented real-time with a color monitor. The screen layout is configured to examine the entire region of interest by displaying and recording the following information:

- ⊕ A cross-sectional view of all (or a selection) of IWEX modes whereby the images are obtained from both the left and right probe at a single position (or a selection of positions) along the length of the scan.
- ⊕ A cross-sectional view of all (or a selection) of IWEX modes whereby the images are obtained from the right probe only at a single position (or a selection of positions) along the length of the scan.

- ⊕ A cross-sectional view of all (or a selection) of IWEX modes whereby the images are obtained from the left probe only at a single position (or a selection of positions) along the length of the scan.
- ⊕ A projected view of the maximum image amplitudes from the IWEX images to the right and left side along the length of the scan.
- ⊕ A projected view of the maximum image amplitudes from the IWEX images of the OD area along the length of the scan.
- ⊕ A projected view of the IWEX images (a selection of modes) of the ID area along the length of the scan.
- ⊕ A projected view of the maximum image amplitudes from the IWEX images of the remaining volume (Mid-Wall) area along the length of the scan.
- ⊕ See figure 4 on attachment 1 for a depiction of the various projected views.
- ⊕ Coupling check section.
- ⊕ Scan length position information.
- ⊕ Header section with possibility to present job specific information.

Other information that can be recorded:

- ⊕ Time and date of inspection;
- ⊕ Indication mark-up;
- ⊕ WT recording check (if applicable).

5.4 *Scanner and Umbilical*

The scanner/umbilical to be used should meet the following minimum requirements:

- ⊕ Automated or semi-automated operation during examination;
- ⊕ Capable of taking up 2 individually spring loaded ultrasonic probes, of which the distances to the weld centerline can be individually set;
- ⊕ 15-45 m of umbilical cable length;
- ⊕ The scanner is equipped with an encoder for accurate measurement of the scanner position along the length of the scan;
- ⊕ Encoder resolution (counts/mm): $\geq 2/\text{mm}$;
- ⊕ Scanning speed: 4-40 mm/s (depending on inspection configuration);
- ⊕ The scan speed will be set to ensure correct data collection.

6 **SYSTEM HARDWARE SETTINGS**

6.1 *IWEX Array Probes*

Array probes used for IWEX imaging for a particular inspection regime shall be taken into consideration. The probe frequency and pitch should be such that inspection volume is insonified with optimal sound energy and spatial bandwidth, to obtain an optimal signal to noise ratio and image resolution. The optimal resolution will be the best compromise between required image quality and inspection speed.

The selected probes and their parameters for each setup configuration shall be included in the Scan Plan.

All probes have a unique number for QA/QC purposes, which relate to the manufacturing process and tests conducted by either Applus+ RTD Probes department or the supplying manufacturer.

6.2 *Probe Frame Layout*

The probes used for inspection are positioned within a probe frame. The position of each probe and their inspection function is detailed into the Scan Plan.

6.3 *Parameters of System Inspection Program*

During inspection all parameter settings of the System program are stored on the computer hard drives together with all inspection data. The settings for each IWEX mode are subject to adjustments within the defined essential variables.

6.4 *Essential Variables for IWEX Modes*

- a. Probe Parameters
 - ⊕ Change in probe frequency or bandwidth;
 - ⊕ Change in crystal size and pitch;
 - ⊕ Number of elements;
- b. Material (steel all grades)
 - ⊕ Changes in nominal WT outside of the manufacturing tolerances and/or COMPANY specifications;
 - ⊕ Changes in nominal pipe diameter;
- c. Software
 - ⊕ A change of software version (unless written permission is provided by the COMPANY).

6.5 *Scanning Preparation & Surface Condition*

The scanning area shall be free of weld spatter and other irregularities, which may interfere with the inspection. The surface condition and tracking shall be monitored by the scanner technician along the scan to ensure there is no impact on the integrity of the inspection.

When the surface condition prevents or interferes with scanning, the COMPANY Representative shall be informed.

6.6 *Reference Line*

In case the bond line is not clearly visible on the pipe, prior to scanning of the longseam a reference line shall be marked along the axial direction of the scan, and the flow of the pipe marked and recorded by photograph. Nital etching of the bond line may be required.

In case the bond line is clearly visible and a weld cap is present, the weld cap can be used as reference.

When mapping SCC the area and increments for each scan offset shall be marked on the pipe with a scale and recorded by photograph.

6.7 *Datum Point*

The zero reference point and scanning direction shall be clearly marked on the surface of the pipe before commencement of scanning (data acquisition) and recorded by photograph.

6.8 *Acoustic Coupling Fluid*

The couplant, usually a liquid or semi-liquid is required between the face of the wedge and the examination surface to permit or improve the transmittance of ultrasound from the search unit into the material under examination. Typical couplants include:

- ⊕ Water based couplant;
- ⊕ Cellulose paste.

For temperatures below 0 °C (32 °F) a mixture with an anti-freeze liquid may be required.

Corrosion inhibitors or wetting agents or both may be used in conjunction with the couplants. The same couplant shall be used for both calibration and examination.

7 SYSTEM SOFTWARE SETTINGS

7.1 *General*

The ultrasonic equipment shall be electronically calibrated in accordance with the relevant valid version of Applus+ RTD control procedure for verification.

7.2 IWEX Image Settings

7.2.1 Evaluation

The IWEX image is based on a color map with a scale from 0 to 400 units (referred to as %). The color of a pixel is proportional to the image amplitude of that pixel. The contrast of the image can be adjusted by truncation of the minimum and the maximum value of the scale by using an editor, refer to for an example.

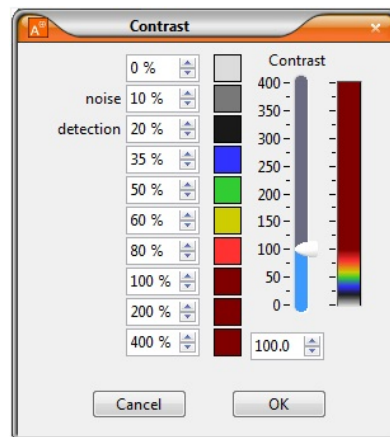


Figure 7-1 - Example of the Contrast Editor Settings.

Amplitudes lower than the minimum value of the contrast editor is displayed as a single color. This can be used to obscure noise.

7.2.2 Image Area

The image area should be large enough to cover at least the theoretical weld volume and HAZ at the left and right side. At least an extra 1 mm shall be added to all sides of the theoretical outline of this area, to ensure coverage of the OD and ID reinforcement, refer to Figure 7-2. In case the OD and/or ID reinforcement are outside the image area, the image area shall be enlarged until complete coverage is obtained.

When mapping SCC the image area should be considered to determine the number of scans that will be required with a minimum of 10% overlap over the previous scan to the left or right. For the volume of the material the area shall be set at a minimum of 1mm (0.039in) above the OD and 1mm (0.039in) below the ID.

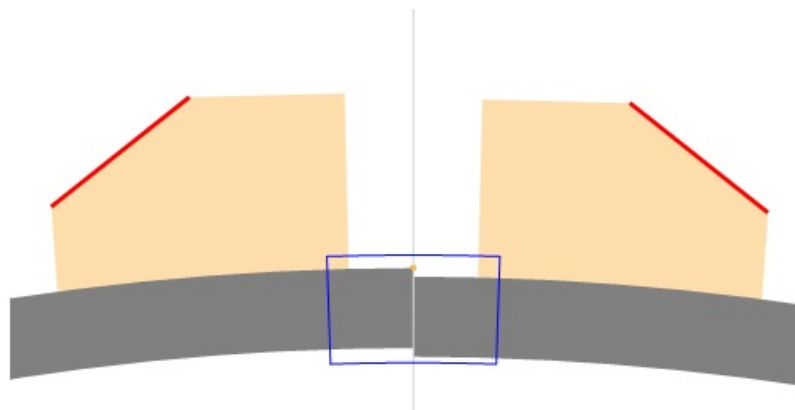


Figure 7-2 - Illustration of the image area with 1mm probe shift down (right side)

7.2.3 Image Masks

Masks can be utilised to a part in the IWEX image of each specific mode, in order to obscure noise or other non-relevant indications, for example caused by internal reflections in the wedge material. The parts that are masked shall then be covered by other IWEX modes with sufficient overlap of at least 1 mm, refer to Figure 7-3 for an illustration.

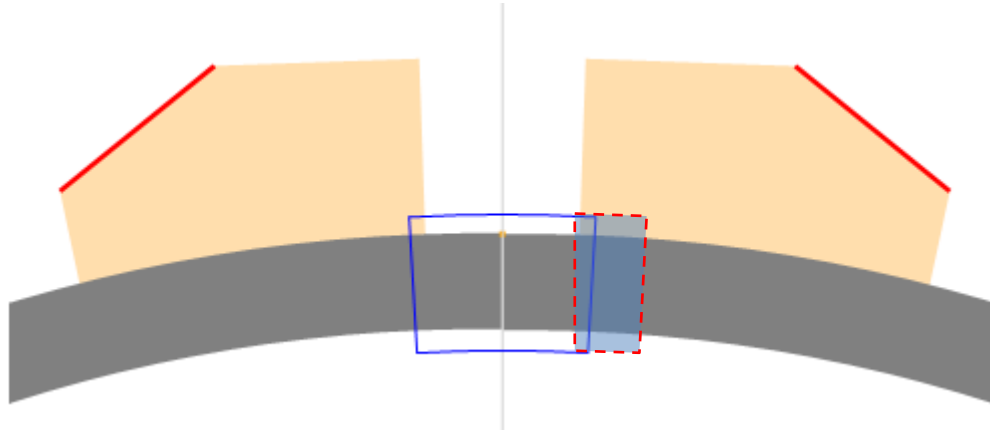


Figure 7-3 - Illustration of a masked part of the image area from the IWEX-1/3 (tandem) modes Left.

7.2.4 Advanced IWEX Settings

The IWEX images may be enhanced with the following advanced settings:

- ⊕ Thinning (default settings: maximum distance 10 and strength 3);
- ⊕ Low noise filter (default settings: filter size 10 and transition size 5);
- ⊕ Apply envelope (default setting: enabled).

Any changes to the default settings shall be specified in the Scan Plan.

7.2.5 Coupling Channels

For each IWEX mode coupling is set up using the pitch / catch technique by utilizing back wall skip at ID surface. Using both left and right probes with identical functions, the sensitivity is established and gated. The coupling sensitivity values and threshold levels shall be defined within the Scan Plan.

8 SCAN QUALITY CONTROL

8.1 Calibration

Before an examination, the system is set up on the object under examination. During setup the IWEX Calibration Tool (latest version) uses FMC's to calculate the optimal settings on the part being tested. The measurements taken during this process include the latency, wedge velocity, vertical and horizontal dimensions of the wedges being used, the wedge angle, the wall thickness of the part, the distance between the probes, and the rotation of the probes. It measures the water gap between the wedge and the part – if present –, and the velocity of the wedges to be used. These settings should not need to be adjusted under ideal circumstances, however with vintage pipe some may be adjusted to account for wall thickness and or curvature variations.

The Calibration Tool should be used in the following cases:

- ⊕ During system setup in preparation for a seam weld or pipe body examination, in order to gather relevant probe and wedge parameters;
- ⊕ When images of the ID and OD become unaligned in the cross modes 0 and 2;
- ⊕ After an equipment break down;
- ⊕ After hardware changes.

8.2 *Scanning Direction*

The scanning direction can be performed in either direction of the seamweld or SCC colony. Correlation with girth weld identification and ILI odometer needs to be considered.

The encoder accuracy is to be verified following the steps outlined below:

- ⊕ Physically measure the scan distance;
- ⊕ Enter the measured distance into the software program;
- ⊕ Perform a scan and compare the stop position of the scanner in relation to the 0 mm mark on the area scanned. The difference, if any, shall be within the specified tolerance of +/- 10 mm;
- ⊕ For inspections that require multiple scans 50mm overlap shall be used for longseam inspection from the end of one scan and the start of the next scan and 5mm circumferentially for SCC inspection. During examination, the functioning of the encoder shall be checked continuously at the end of each scan, checking the end position of the probe related to the 0 mm or start position.

8.3 *Coupling Criteria*

The coupling channels will be checked for coupling loss.

Where coupling loss is due to the surface condition (e.g. grinding, oxidation) the affected area may be improved by buffing or light sanding and the seamweld re-scanned. If the loss of coupling cannot be resolved, with COMPANY acceptance, alternative inspection solutions may be required.

The location and inspection area impacted by the loss of coupling will be recorded in the "comments" section of the System seamweld scan.

Note: Coupling criteria may be altered if dictated by the COMPANY or applicable specification.

8.4 *Step-by-Step Description of a Seam Weld or Pipe Body Examination*

Before beginning an examination, the image quality shall be reviewed by the operator by applying the settings and viewing a "live" view of all the modes used for the examination. The cross modes shall be in alignment with the cross 2 mode at the 0 depth measurement while cross 0 mode is located at the correct depth for the wall thickness of the sample under examination.

The following description outlines the step-by-step process for seam weld inspection:

1. Positioning of the scanner on the pipe:
 - a. In case of a seamweld examination: identify the centerline location of the seamweld. This may require etching.
 - b. In case of pipe body examination: position such that complete coverage of the area under examination is ensured. Multiple scans may be required to guarantee complete coverage. The overlap between multiple pipe body scans is 5mm as a minimum, and 50% as a maximum.
2. Adjust the scanner on the pipe to set distance from the bond line (seamweld centerline) and parallel to the seamweld. The accuracy of this setting should be ± 1 mm.
3. Mark a '0' datum point, illustrating scan direction on the pipe.
4. Switch on the water coupling supply and check supply pressure to both transducers.
5. Placing the transducers at the scan start point:
 - a. In case of a seamweld examination: move the transducers over the seamweld and make sure that both probes are at the start point and are in proper contact with the pipe surface.
 - b. In case of a pipe body examination: move the transducers over the area to be examined and make sure that both probes are at the start point and are in proper contact with the pipe surface.
6. Switch on the system and automatically the area under examination will be scanned in the selected direction.
7. The system will stop at the end of the scan, verify the distance scanned and the value recorded in the scan.
8. Check the data quality for encoder positions and proper coupling.

9. If lack of coupling exists that exceeds the applicable limits, a second scan of the section where coupling loss occurs will be necessary.
10. Check the inspection results for imperfection indications.
11. Remove/move the scanner from/on the pipe.

9 INTERPRETATION OF RESULTS

9.1 *General*

With information from the IWEX images visible on the result presentation, indications shall be identified and interpreted.

Indications produced by ultrasonic testing may or may not be imperfections. Changes in the weld geometry due to misalignment, OD/ID profile, internal chamfering and ultrasonic wave mode conversion may cause geometric indications similar to those caused by seam weld imperfections but that are not relevant to acceptability.

Corner trap is an indication that can be caused by reflection of the ultrasonic wave on a weld imperfection and a material boundary. In this case, corner trap may be used to detect and size surface breaking flaws.

9.2 *Artifacts*

An artifact is a misleading or confusing indication in the IWEX image.

Disregard following artifacts, but not limited to, caused by imaging algorithm:

- ⊕ Mirrored inside surface in IWEX-2;
- ⊕ Mirrored tip-diffractions (indications in IWEX-2 Left/Right close to the inside surface are mirrored below the theoretical ID due to the imaging algorithm).

Disregard following artifacts, but not limited to, caused by defects:

- ⊕ Mirrored IWEX-1 and 3 modes, indications close to the ID or OD are mirrored above the OD or below the ID. (for defects that are surface-breaking this means that the indication is twice the size of the defect);
- ⊕ Mirrored tip-diffractions (indications in IWEX-0 Left/Right close to the inside surface are mirrored below the actual ID due to the physical reflection of the ID).

9.3 *Imperfection Length*

Imperfection length shall be measured using the cross-sectional view by moving the data cursor along the scan and marking the start and stop of the imperfection using the viewer software.

9.4 *Imperfection Height*

Imperfection height sizing is performed by applying the rules as described in the Decision Flow Chart, see Attachment 3. When an indication is found in the IWEX image, it can be "boxed" for through-wall height and depth sizing. The boxing can be done by an automatic sizing tool which finds the -6 dB drop-offs in height of the indication as a default value. The maximum amplitude in the box is provided as well, but sizing is not based on the absolute value of the amplitude.

When tip diffraction signals are present, the height sizing of the defect must be determined as the vertical distance between the tip diffractions in the same IWEX mode.

When multiple IWEX modes indicate an imperfection and tip diffraction signals are absent, the height sizing of the defect must be determined on the strongest IWEX mode present indicating the imperfection.

9.5 *Imperfection Depth*

Imperfection depth from OD surface will be established using the applicable IWEX mode. Depth is the value reported after "boxing" the indication and is the distance between the IWEX assumed zero-depth line (assumed OD) and the bottom of the imperfection.

The actual OD and the IWEX assumed zero-depth line (assumed OD) may differ due to various causes. The position of the actual OD relative to the IWEX assumed OD shall be measured at the position vertically above the indication. Reported defect depth shall be corrected to the actual OD.

9.6 *OD/ID Ligament*

Ligaments from imperfections to the surfaces are described according to Figure 9-1. The remaining ligament from the top of the imperfection to the OD surface is the OD ligament. Likewise the remaining ligament from the bottom of the imperfection to the ID surface is the ID ligament.

Depth and height of the indications are reported in accordance with the following drawing:

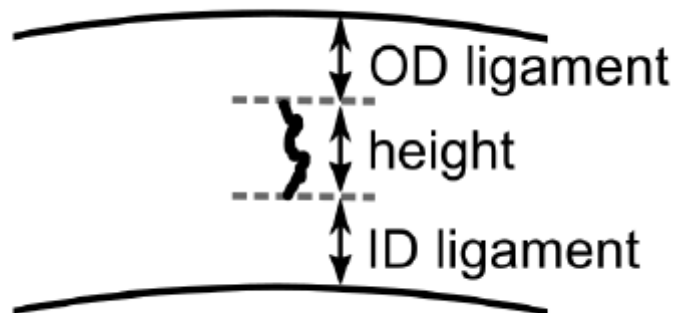


Figure 9-1 - Description of relation between OD and ID ligaments and defect height.

9.7 *Imperfection Horizontal Positioning (Radial, across the seamweld, or circumferential location in relation the the center of the probes and the first of a series of scans used to map SCC)*

Imperfection horizontal position will be established using the applicable IWEX mode. The horizontal position is the value reported after "boxing" the indication and is the distance between the IWEX assumed weld centerline and the left side of the imperfection. Positive (+) values are to the right of the IWEX assumed weld centerline, negative (-) to the left.

9.8 *Interaction*

The interaction rules within the relevant Standard / Code applicable to the Project, or specifically defined by COMPANY, shall be taken into account when determining overall imperfection length and/or height.

10 **REPORTING CRITERIA**

As the IWEX Ultrasonic Imaging technique is new and no guidelines or standards have been set by regulatory bodies (i.e. ASME) the REPORTING criteria shall be defined by the COMPANY in agreement with Applus+ RTD and issued as a separate document by the COMPANY.

For seamweld examination the minimum reporting length is ¼ inch (6 mm), unless required differently by COMPANY.

For pipe body examination the minimum reporting length shall be agreed upon between COMPANY and Applus+ RTD, and shall be detailed in the Scan Plan prior to examination.

11 REPORTING

The Applus+ RTD System Site Report, as shown in Attachment 2, shall be used for reporting of inspection results. The following information will be documented as minimum:

- ⊕ Used procedure number;
- ⊕ Used scan plan document number
- ⊕ Project name/number;
- ⊕ Weld number or Object identification number;
- ⊕ Inspection date;
- ⊕ Diameter;
- ⊕ Wall thickness;
- ⊕ Number of indications, axial location, location in depth and location in horizontal plane from centerline.

The naming and numbering system for seamweld files will be determined at project commencement in cooperation with the COMPANY.

12 STORAGE OF DATA

The IWEX images of each inspected weld/pipe, including the parameter settings, shall be stored on the main hard drive. In addition, a full back-up shall be made on a second removable hard drive.

The Date and Time function shall be used to ensure that all welds/pipes scanned are accounted for. By selecting this function the date and time of each scan made becomes part of the file name, removing the chance of overwriting any file.

Scan files should be stored in daily directories, which will be created at 24:00hrs, each day. Operators are responsible for the daily directory on the main hard drive and shall ensure that all welds are present and readable.

After completion of the inspection project, all scan data will be stored on a digital medium, and presented to COMPANY.

The official record of inspection shall be the System Site Report (or other if specified by COMPANY) and shall bear the original signature of the System Operator.

Attachment 1 – Explanation of Methodology

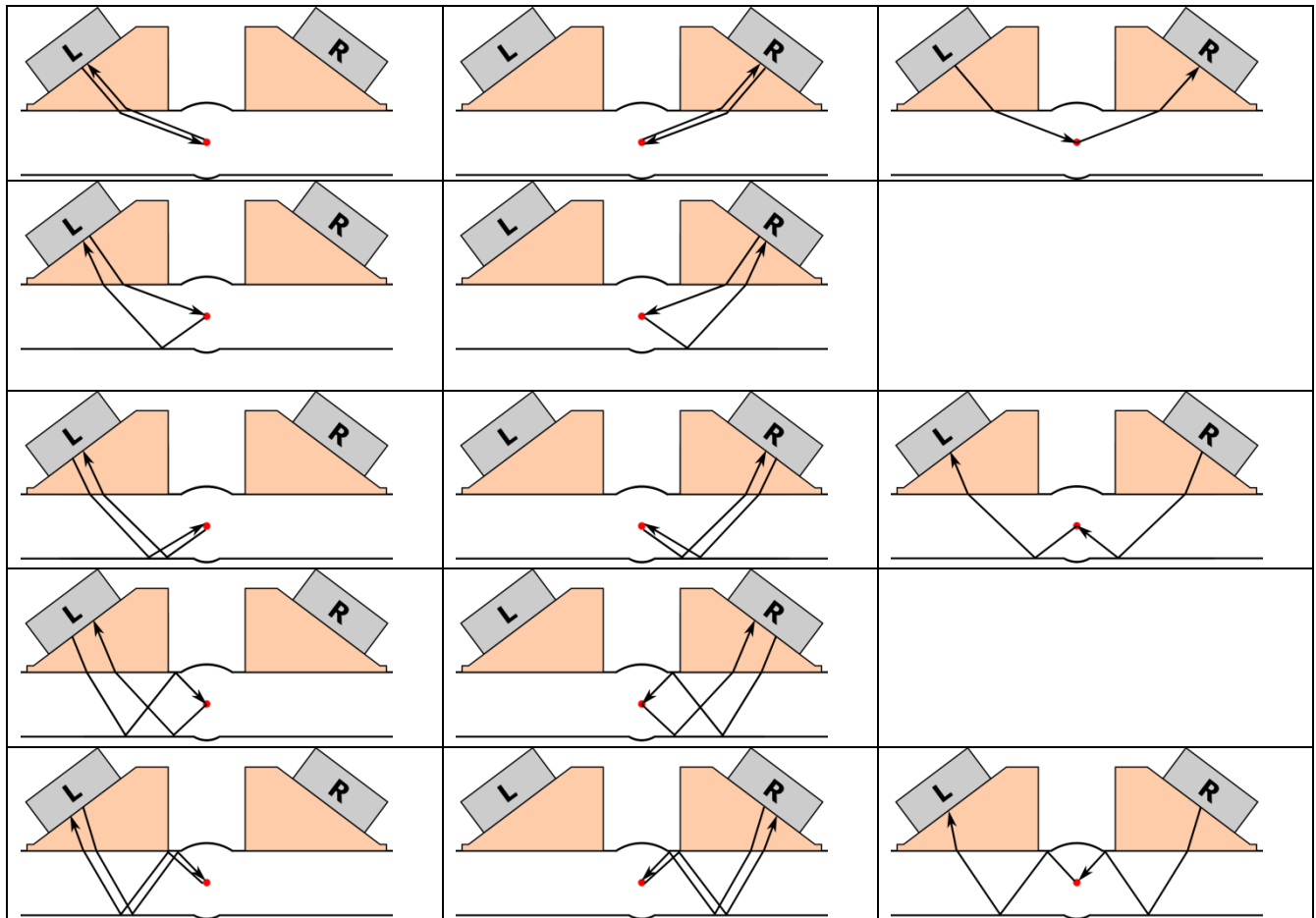
General Explanation

Inverse Wave field EXtrapolation (IWEX) method shall be used for inspection. The IWEX method is based on ultrasonic data obtained from measurements whereby combinations of source–receiver elements of ultrasonic arrays are used (Full Matrix Capture). The ultrasonic data will be processed into images.

An image can be calculated based on the transmitting and receiving paths of the ultrasonic signals, the so called IWEX modes, refer to Table 1.

IWEX-0 (Direct) mode (left/right):	Based on both direct transmitter and receiver path.
IWEX-1 (Tandem) mode (left/right):	Based on direct transmitter path and receiver path with a skip at the back wall (or vice-versa).
IWEX-2 (Half skip) mode (left/right):	Based on both transmitter and receiver path with a skip at the back wall.
IWEX-3 (Tandem skip) mode (left/right):	Based on transmitter path and receiver path with a skip at the back wall and also a skip at the back wall and front wall.
IWEX-4 (Full skip) mode (left/right):	Based on both transmitter and receiver paths having skips at both the front and back wall.
IWEX-0 Cross direct mode:	Based on direct transmitter path from the left probe and direct arrival path to the right probe.
IWEX-2 Cross half skip mode:	Based on transmitter path from the right probe with a skip at the back wall and arrival path with a skip at the back wall to the left probe.
IWEX-4 Cross full skip mode:	Based on transmitter path from the right probe with a skip at the back wall and a skip at the front wall and arrival path with skip at the front wall and skip at the back wall to the left probe.

Table 1: Overview of possible IWEX modes. Note that the modes are displayed as lines for illustration purpose only. Actual angles of incidence, reflection and actual flaws may differ, nor does it represent possibilities of tip-diffractions from these flaws.



The software of the System allows for viewing images from individual or combined IWEX modes at a single scan location or a selected area along the scan length. Furthermore, the software displays length scans of the weld whereby IWEX images are projected to the Left side, the Right side, the OD area, the volume area and the ID area. Thereby, the system provides an adequate number of inspection functions to ensure the complete volumetric coverage of the examined area.

Details of the inspection setup are documented and described in the Scan Plan.

IWEX Visualisation

During scanning – live view – or when an IWEX scan-file is opened, the data is displayed in several fields within the IWEX window, see Figure 2. The top half of the window shows three cross-sectional views of the weld. The left cross-sectional image displays data as registered by the probe on the left side of the weld, the image on the right does the same for the right probe, while the center image shows all data together: left probe, right probe, and cross-modes measured from one probe to the other.

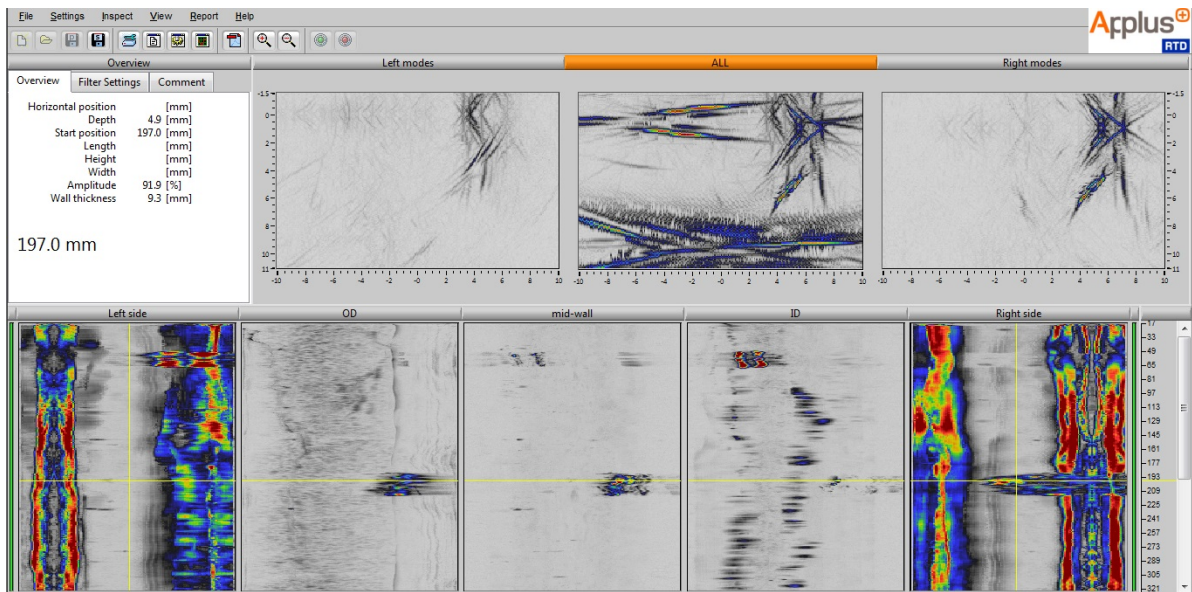


Figure 1 – Example of the IWEX cross-sectional and strip-chart views in the IWEX software

The bottom half of the IWEX window shows five strip-charts. To the far left and far right are strip-charts in D-scan view that depict the view of the weld as seen from the centerline: the left side of the weld and the right side of the weld respectively, see Figure 3. Note that this differs from the cross-sectional images in the top half, since a probe positioned e.g. on the left side can still detect the presence of indications on the right side of the weld.

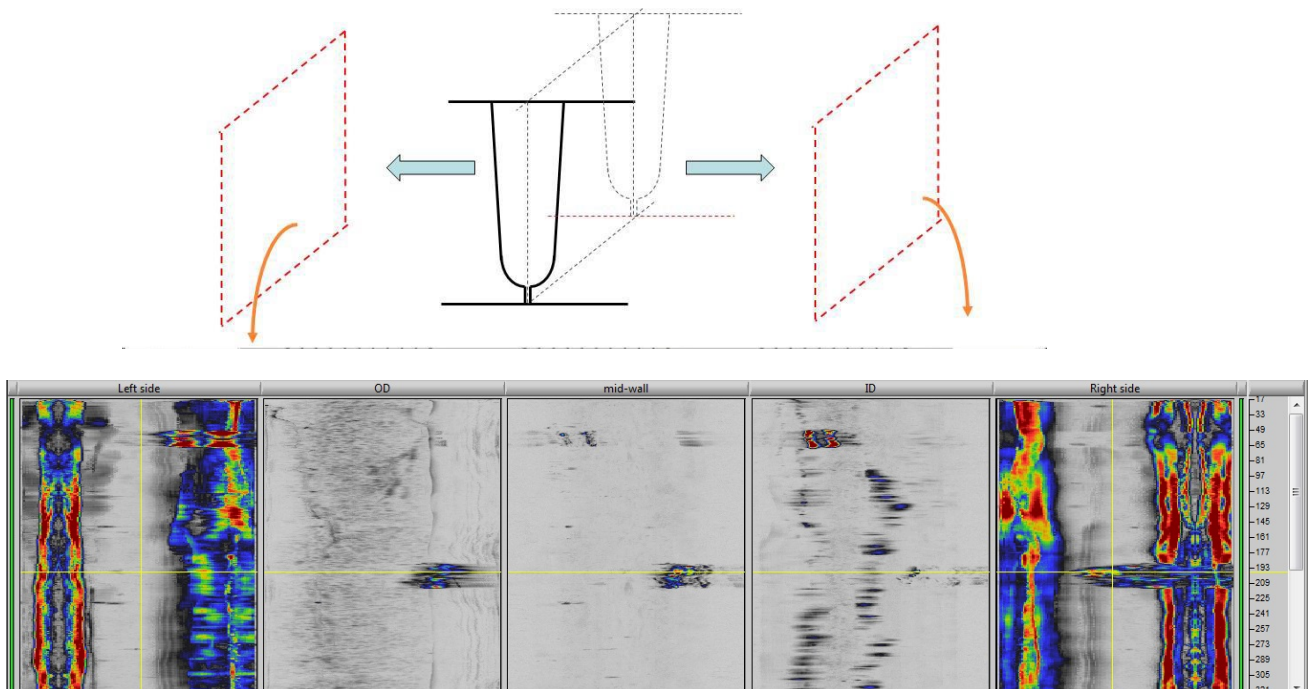


Figure 2 – D-scan views of the seamweld from the left side and the right side.

The middle three strip-charts depict a C-scan top-view of the seamweld in three parts. The three parts divide the weld in three separate layers. The 'OD' strip-chart: a layer containing the OD zone, the outside and upper part of the weld; the 'ID' strip-chart: a layer containing the inside zone and the lower part of the weld; the 'Mid-Wall' strip-chart: the remaining volume of the weld between the 'OD' and 'ID' layers, see Figure 4. The boundaries of these layers can be changed in the IWEX settings according to the layout of the weld.

In the strip chart view of the OD area, the IWEX cross mode skip is not incorporated. This mode will image strong indications caused by the upper surface and the cap geometry. On the C-scan, these indications would obscure defects in the cap that are imaged by the other modes.

In the strip chart view of the ID area, the IWEX cross mode is not incorporated. This mode will image strong indications caused by the lower surface and the inside geometry. On the C-scan, these indications would obscure defects on the ID that are imaged by the other modes.

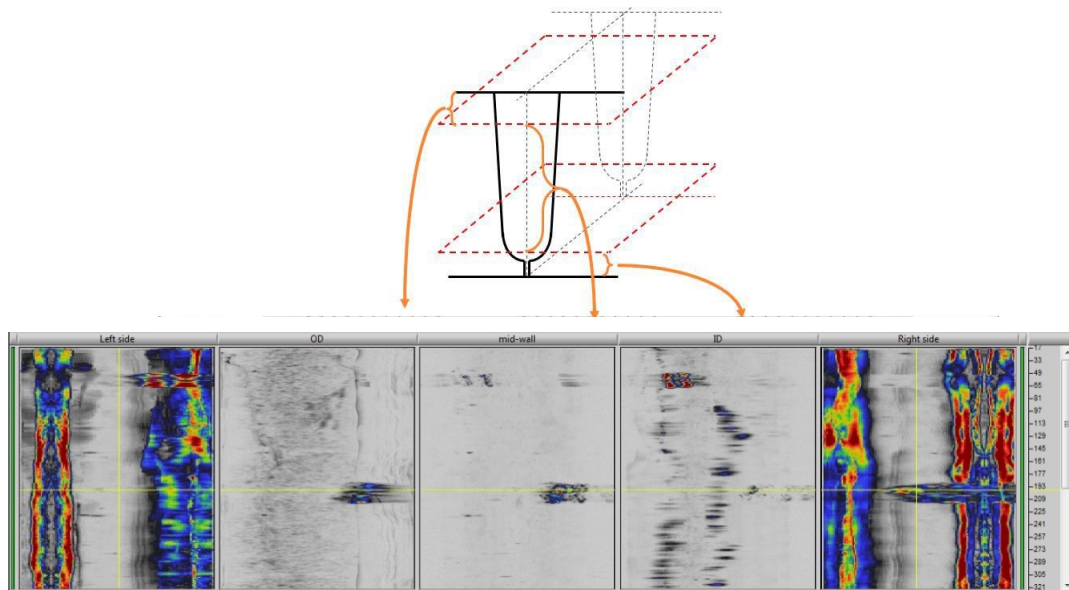


Figure 3 – Middle three strip-charts depict C-scan views of the OD, the Mid-Wall and the ID of the weld.

The IWEX software allows for 3D visualisation of a small selected area on the strip chart view. All 2D images on the selected area are cascaded and rendered into a comprehensive 3D view that can be rotated, refer to Figure 5. During scanning of a weld, the 3D visualisation can also be enabled. The 3D presentation of the weld will appear and a 3D tunnel like presentation will scroll towards the screen of a certain area of the weld.

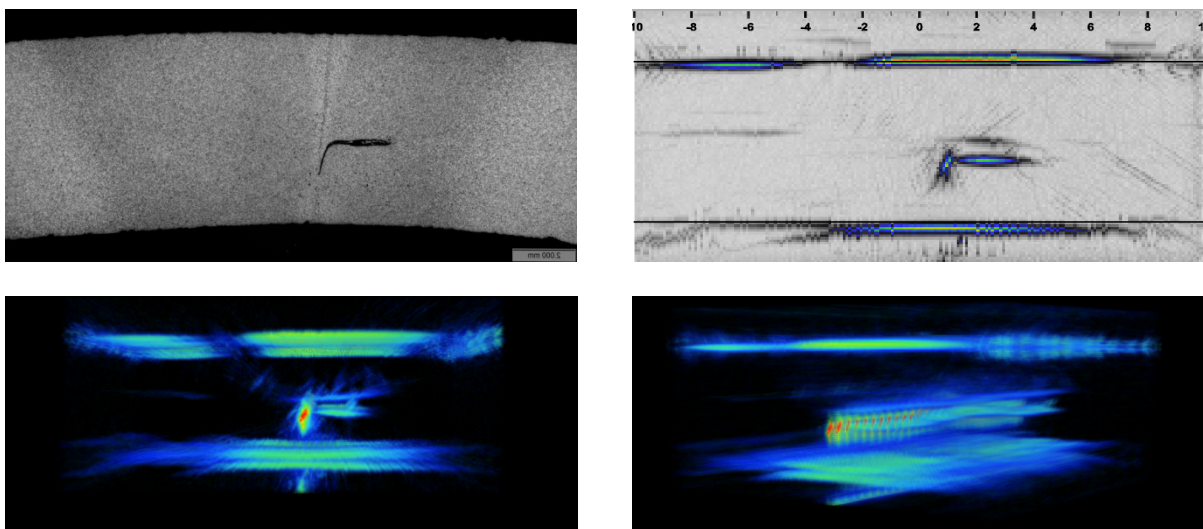


Figure 4 – Example of an inclusion defect imaged in 2D and 3D.

Masking Parts of the Image Area

The images generated from different IWEX modes can be combined into one final image. Sometimes, artifacts caused by geometry, internal reflections in the wedge or other causes, can appear somewhere in the image of a certain mode. When combining images, these artifacts may obscure areas where defects are imaged. The software allows the use of masks to remove this type of artifacts.

Three types of masks can be programmed (refer to Figure 6):

1. A mask for the OD area at the Left and Right side. This mask can be applied on the IWEX-0 (direct) mode because the main purpose of this mode is to image defects in the ID area.
2. A mask for the ID area at the Left and Right side. This mask can be applied on the IWEX-2 (indirect) mode because the main purpose of this mode is to image defects in the OD area and the body of the pipe.
3. A mask for the OD, Mid-Wall and ID areas at:
 - ⊕ The Left side. This mask can be applied on the IWEX-1 and IWEX-3 (tandem) modes of the Right side because the main purpose of these modes is to image defects at the Right side;
 - ⊕ Same for the Right side for modes from the Left side;
 - ⊕ Note that masking of the IWEX-1 and IWEX-3 modes on Left and Right sides are simultaneous and symmetrical. They cannot be set with values different for Left and Right.

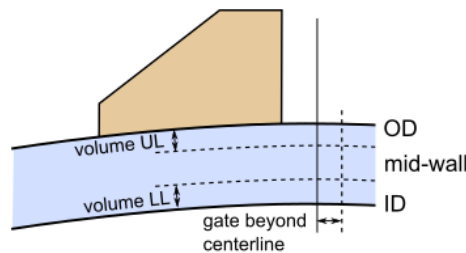


Figure 5 – Illustration of the different mask types that can be utilised to obscure noise.

Doc No. : QA-TP-UT-FINAL DRAFT
Revision : 00
Date : January 8, 2018
Title : General Procedure for RTD IWEX Ultrasonic
Longseam and Pipe Body Examination

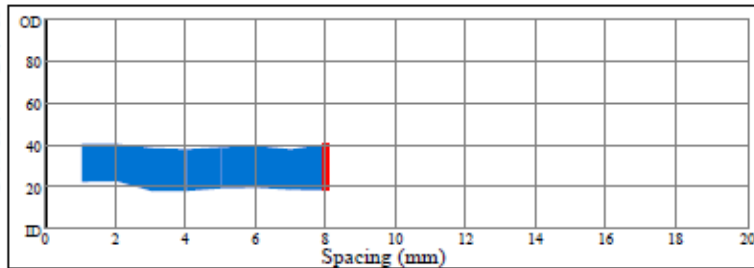
Attachment 2 – Example Site Report

Site report IWEX examination		Applus RTD USA, Inc. 11801 S Sam Houston Pkwy Houston, Texas 77031 T: +1 832 295 5001 Fax: +1 832 295 5001 Email: info.usa@applusrtd.com http://www.applusrtd.us		Applus⁺ RTD IWEX project file:				
Job number	Date of inspection							
Feature list								
ID Feature	Axial Start (ft)	Length (mm)	OD Ligament (mm)	Height (mm)	ID Ligament (mm)	H.Position (mm)	OD/Mid- Wall/ID	Type
1	4187.8	10	3.8	1.4	1.2	1.4	MW	characterize feature
2	4245.4	10	3.6	0.5	2.4	0.5	MW	characterize feature
3	4435.2	110	3.7	1.6	1.1	1.6	MW	characterize feature
Applus RTD Operator:			Contractor:			Company:		
Signature:			Signature:			Signature:		

Site report		Applus RTD USA, Inc. 11801 S Sam Houston Pkwy Houston, Texas 77031 T: +1 832 295 5001 Fax: +1 832 295 5001 Email: info.usa@applusrtd.com http://www.applusrtd.us	Applus⁺ RTD IWEX project file:
IWEX examination			
Job number	Date of inspection		

Feature: 1 - characterize feature

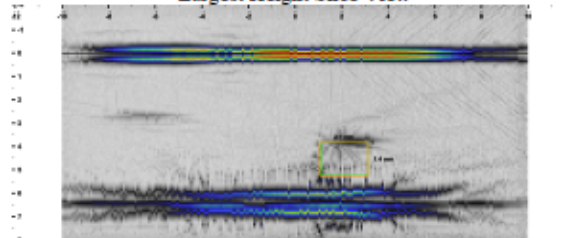
Start Chainage (mm) 4187.8
Start Circ (mm) 1.04
Length (mm) 10
Width (mm) 2.1
Height (mm) 1.4
OD Ligament (mm) 3.8
ID Ligament (mm) 1.2
Local wt (mm) 6.39
Analyst
Comments:



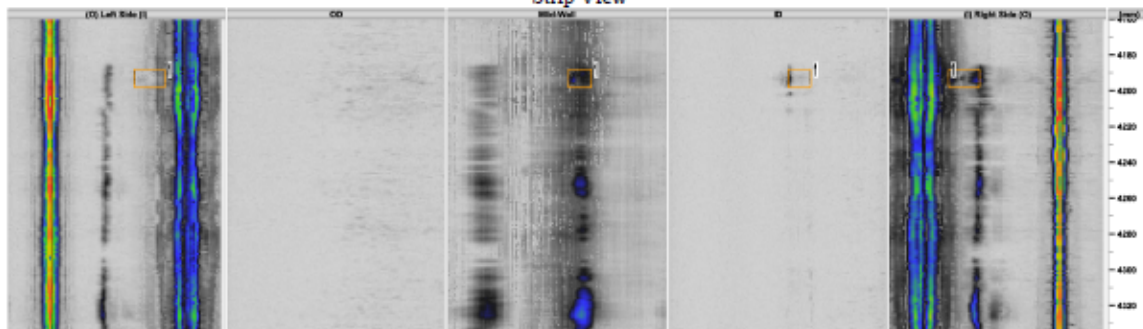
Profile box list

Scan position (mm)	Circ Start (mm)	Circ End (mm)	Depth Start (mm)	Depth End (mm)	Height (mm)
4188.82	1.04	3.01	3.81	4.96	1.15
4189.81	1.06	2.95	3.81	4.94	1.13
4190.80	1.34	3.01	3.93	5.24	1.31
4191.80	1.12	3.01	3.97	5.24	1.27
4192.79	1.06	2.91	3.91	5.16	1.25
4193.79	1.12	2.89	3.87	5.14	1.27
4194.78	1.20	2.87	3.97	5.20	1.23
4195.77	1.10	3.13	3.81	5.22	1.41

Largest Height Slice View



Strip View



Applus RTD	Contractor:	Company:
Operator:		
Signature:	Signature:	Signature:

Attachment 3 – Decision Flow Chart

